

Preface

It is well known that rheology of the blood (haemorheology) is a crucial factor in the regulation of tissue perfusion, but only in the last decades investigation on haemorheology have had a remarkable development in Clinical Medicine. Epidemiological, clinical and physiopathological researches have indeed demonstrated the role of hyperviscosity in the pathogenesis, progression and extension of many diseases like atherosclerosis, hypertension, acute and chronic cerebrovascular diseases.

This issue of Annali dell'Istituto Superiore di Sanità aims to highlight the significance of haemorheological studies in Clinical Medicine by analysing thoroughly physiopathological mechanisms and clinical aspects of the main syndromes with haemorheological alterations and by providing new methodologies of investigation.

Blood viscosity and erythrocyte deformability play a key role in maintaining and regulating microcirculation. The whole blood viscosity is a function of both the number of erythrocytes and their deformability and of the plasma proteins. Haemorheological variations due to alterations of blood cells and plasma components lead to hyperviscosity, which slows blood flow and can facilitate occlusive events through erythrocyte rouleaux formation and platelet aggregation.

Several lines of evidence have demonstrated that factors determining blood viscosity like haematocrit, plasma viscosity, red blood cell deformability and aggregation interact with many interrelated factors influencing the micro – and macro – rheology of blood: vascular factors, haemostatic factors, white blood cells,

inflammatory mediators, epistatic genes, and the environment. Although the interest of many researchers has been addressed towards the pathogenetic mechanisms of atherogenetic syndromes, the rheological properties of the blood has been investigated in many other physiopathological conditions and new and sensitive rheological techniques have been developed to evaluate rheological properties of blood in both clinical and transfusion medicine for diagnosis, therapy and monitoring purposes.

The main goal of this monograph is to give an update on research about haemorheology applied to medicine and to provide a basis for an in-depth discussion with the contribution of different research groups belonging to the main scientific societies interested in this topic: Italian Society of Clinical Haemorheology and Microcirculation (SIECM), Italian Society of Rheology (SIR), and Italian Society of Transfusion Medicine and Immunohaematology (SIMTI).

We would like to thank all the Authors and we wish this issue will be the starting point of further collaborative researches.

**Patrizia Caprari^(a), Maria Cristina Martorana^(b)
and Cesare Peschle^(a)**

^(a)Dipartimento di Ematologia, Oncologia e Medicina Molecolare, Istituto Superiore di Sanità, Rome, Italy

^(b)Centro Aziendale Produzione Emocomponenti, Azienda Ospedaliera San Camillo-Forlanini, Rome, Italy

Endothelium and haemorheology

Tommaso Gori, Saverio Dragoni, Giuseppe Di Stolfo and Sandro Forconi

Dipartimento di Medicina Interna, Cardiovascolare e Geriatrica, Università degli Studi, Siena, Italy

Summary. The vascular endothelium has been recognized to have a central importance in maintaining vascular homeostasis and in preventing cardiovascular disease. The mechanisms underlying the regulation of its function are extremely complex, and are principally determined by physical forces imposed on the endothelium by the flowing blood. In the present paper, we describe the interactions between the rheological properties of blood and the vascular endothelium. The role of shear stress, viscosity, cell-cell interactions, as well as the molecular mechanisms that are important for the transduction of these signals are discussed both in physiology and in pathology, with a particular attention to the role of reactive oxygen species. In the final conclusions, we propose an hypothesis regarding the implications of changes in blood viscosity, and particularly on the significance of secondary hyperviscosity syndromes.

Key words: endothelium, haemorheology, viscosity.

Riassunto (*Endotelio ed emoreologia*). All'endotelio vascolare è stato recentemente riconosciuto un ruolo cruciale nel mantenere l'omeostasi vascolare e nel prevenire la genesi delle patologie cardiovascolari. I meccanismi alla base della regolazione della cosiddetta funzione endoteliale sono estremamente complessi, e sono principalmente legati alla interazione tra endotelio e lo stress meccanico imposto dal flusso ematico. In questo articolo, descriviamo i meccanismi di questa interazione tra le proprietà fisiche e reologiche del sangue e l'endotelio. Il ruolo di shear stress, viscosità, interazioni cellula-cellula, ed i meccanismi molecolari di questi fenomeni sono discussi in condizioni fisiologiche e patologiche, con un'attenzione particolare al ruolo dei radicali liberi dell'ossigeno. Nelle conclusioni finali, proponiamo un'ipotesi riguardo alle implicazioni delle modificazioni nella viscosità ematica, particolarmente per quello che riguarda le sindromi da iperviscosità secondaria.

Parole chiave: endotelio, emoreologia, viscosità.

INTRODUCTION

The endothelium layer covers the inner surface of the whole vascular system. This monocellular layer separates all tissues from the circulating blood [1]. While in the past it has been considered to be an inert physical barrier, acting only as a selective sieve to facilitate bidirectional passage of macromolecules and blood gases between tissues and blood, research lines in the '80ies and '90ies have clearly demonstrated that the endothelium is a dynamic organ which holds a leading role in regulating vascular homeostasis.

Because its peculiar location allows it to sense changes in haemodynamic forces and blood-borne signals, the endothelium exerts its function in maintaining vascular homeostasis through the balanced release of a number of autocrine and paracrine substances in response to physical, biological and chemical stimuli. Substances released from the endothelium regulate thrombosis, thrombolysis, platelet adherence, vascular tone, lipid metabolism and inflammation (*Figure 1*). Given the critical role of these mechanisms, the disruption of the endothelial balance, a phenomenon called endothelial dysfunction, is a precursor of the pathogenesis of many diseases including atherosclerosis, hypertension, sepsis and some inflammatory syndromes [2].

In the following paragraphs, we will describe the relation between endothelium and hemorheology, and how a dysfunction in this relationship can interfere with the production of endothelial autacoids and vascular flow.

NOTIONS OF ANATOMY, PHYSIOLOGY AND PATHOPHYSIOLOGY OF THE VASCULAR ENDOTHELIUM

While its anatomical structure is extremely simple, composed as it is by a single layer of mesenchymal cells, the endothelium is an extremely complex tissue from the metabolic point of view. Of interest, while endothelial cells are (at rest) flat, most of the thickness of the endothelium (up to several hundred nms) is determined by a dynamic structure lying on its luminal surface. This structure, denominated the endothelial surface layer (ESL, *Figure 2*) is composed of proteins, glycolipids, glycoproteins and glycosaminoglycans. The molecular domains hosted in this glycocalyx function as receptors for adhesion molecules, components of the coagulation/fibrinolysis system, transporter for oxygen and macromolecules, and, most importantly, as mechanical transducers of the physical stress deter-

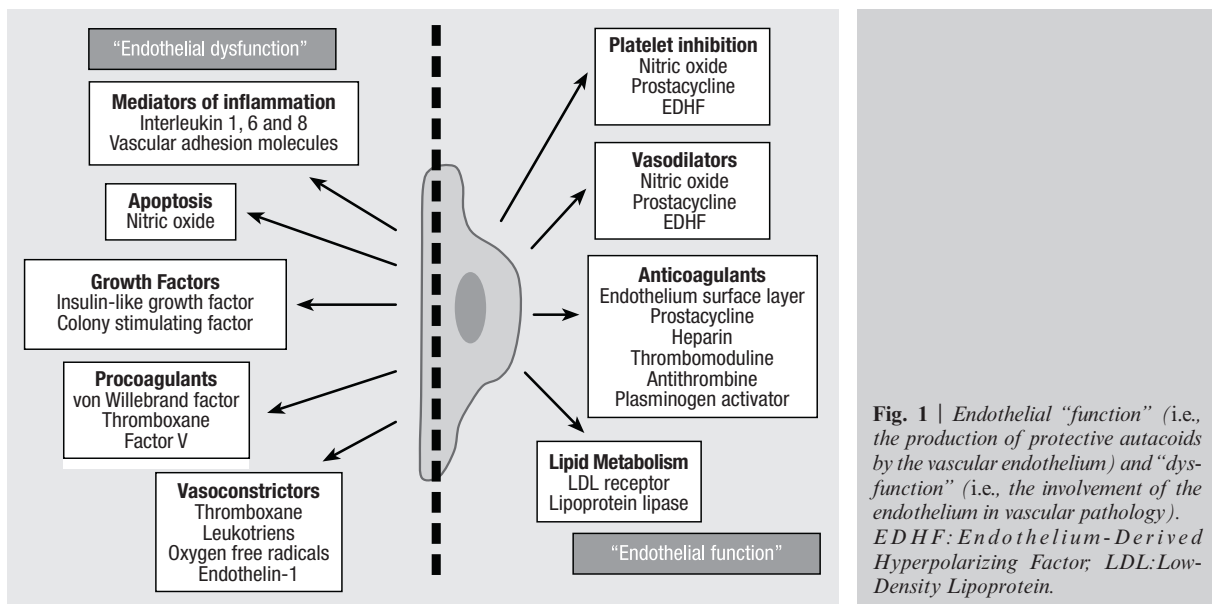


Fig. 1 | Endothelial “function” (i.e., the production of protective autacoids by the vascular endothelium) and “dys-function” (i.e., the involvement of the endothelium in vascular pathology). EDHF: Endothelium-Derived Hyperpolarizing Factor; LDL: Low-Density Lipoprotein.

mined by the flowing blood on the surface of the endothelium. With its thickness, the ESL occupies a large fraction of the lumen in capillaries and arterioles, and it has been shown that vascular resistance measured at the level of microvessels (where the ratio of ESL thickness to vascular lumen is highest) is much higher as compared to the resistance measured in glass capillaries having the same diameter [3]. This increase in vascular resistance determined by the ESL depends on: 1) physical reduction of the vascular lumen by the ESL 2) electrochemical interaction between ESL and blood components, which increases friction forces [4].

As said, the ESL functions as a transducer of mechanical forces: the modifications imposed by shear stress, i.e., the friction force determined by the flowing blood that acts tangentially on the ESL, determine mechanical modifications of the intracellular cytoskeleton, which is, on one side, structurally bound to the ESL, and, on the other, to several stretch-activated sensors, mostly protein G systems and ion channels. It seems that, in this molecular cascade, activation of MAP kinases plays a central role. Indeed, these ubiquitously expressed serine/threonine protein kinases (which are involved in the regulation of cell growth, transformation and differentiation), and in particular the extracellular signal-regulated kinases (ERK1/2)), activate several enzymes which include protein kinases (p90rsk, MAPKAP, Raf-1, MEK), transcription factors (c-myc, c-jun, c-fos, p62TCF), and cell surface proteins (EGF receptor) [5]. The cascade of molecular events that follows these reactions regulates the production of endothelial autacoids, and in particular the synthesis of nitric oxide (NO) [6], as discussed below.

Thanks to these mechanisms, early upon detection of increases in shear stress, rapid changes in ionic conductance, inositol triphosphate production and cytosolic Ca²⁺ concentrations can be observed in the

endothelial cell. Opening of K⁺ channels facilitates membrane hyperpolarization, which provides an electrochemical gradient for Ca²⁺ entry. The plasma membrane thickens and starts to form invaginations that are named caveolae [7], where the synthesis of NO occurs, stimulated by the increased Ca²⁺ availability. NO is a highly reactive free radical [8] with a number of effects, among which a potent influence on haemorrhology [9]. Indeed, NO increases red blood cell and platelet deformability, reduces platelet adhesion and aggregation [10], reduces leukocyte adhesion [11], reduces endothelial expression of adhesion molecules (which, although not being an intrinsic characteristic of blood, is an important

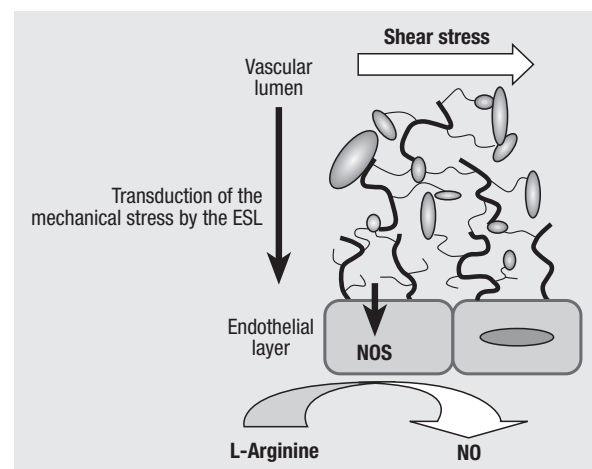


Fig. 2 | Endothelial production of nitric oxide (NO) is stimulated by oscillatory shear stress, transmitted by the endothelial surface layer to the endothelial cells. NO: Nitric Oxide; NOS: Nitrous Oxide Systems; ESL: Endothelial Surface Layer

determinant of blood-vessel interactions) [12] and, most importantly, it causes vasodilation [13].

While these changes are induced acutely by shear stress, and in particular by oscillatory shear stress [14], in cases where this physical stimulus is maintained for prolonged periods, genomic induction ensues, probably mediated by activation of the nuclear factor κ B (NF κ B) transcriptional factor. Because NF κ B binding sites are found in the promoter regions of a variety of genes, this system might have a particular importance in altering gene expression in response to sustained variations in shear stress. In particular, the increased expression of the endothelial enzymes NO synthase, one of the effects of sustained increases in shear stress, explains the parallel sustained increase in the production of this free radical [15]. Considering the beneficial effects of NO in vascular physiology, one can safely assume that the benefit associated with physical exercise (*i.e.*, chronic increase in oscillatory shear stress) in cardiovascular patients is indeed mediated by the above described mechanisms [16].

In this scenario, a particular importance has been given to other free radicals, the reactive oxygen species [17] (ROS). The ROS are free radicals normally produced in low concentrations by the mitochondrial respiratory chain and normally scavenged by multiple intra- and extracellular mechanisms, including the enzyme superoxide dismutase, glutathione and vitamin C. When produced in supranormal concentrations, ROS can overcome these scavenging mechanisms and rapidly react with NO to form the highly toxic peroxynitrite [18]. This may reduce the bioavailability of endothelium-derived NO, impairing its vasodilator activity, and, possibly, directly counteract NO-induced protective effects, as ROS cause vasoconstriction and vascular damage [19]. Therefore, these high concentrations of ROS and peroxynitrite are potent toxins for cellular structures, due to their capacity to oxidize and damage or inactivate a variety of cellular structures. Interestingly, the redox state of endothelial cells was found to be dependent on the type of the shear stress applied, an observation which provides an interesting mechanistic clue to the phenomena described until now: it has been shown that oscillatory and steady (low-grade) laminar shear stress differentially affect human endothelial redox state, the latter causing induction of ROS-producing NADH oxidase [14]. Downstream to reduced NO bioavailability and (corresponding) increased ROS bioavailability, potential mechanisms that have been proposed to explain the REDOX-dependency of vascular homeostasis include increased LDL uptake, accumulation of inflammatory cells (a process that could be emphasized by the increased expression of ligands such as ICAM and VCAM). Finally, pulsatile shear stress downregulates the expression of the gene encoding for endothelin-1, a potent vasoconstrictor and a trigger (in a feed-forward mechanism) of ROS formation [20]. In sum, steady, low-grade shear stress (and/or disruptions in the transduction mechanism of shear stress, *i.e.* the ESL) cause increased ROS production. In this appar-

ently simple mechanism lies the pathophysiology of most cardiovascular syndromes, and the importance of ROS production as the common pathway of vascular pathobiology cannot be overstated, as discussed in more detail elsewhere [17, 21].

Physiological shear stress levels have been demonstrated to induce, *in vitro*, atheroprotective endothelial gene expression patterns, while a low-grade shear stress level was associated with the expression of an atherogenic phenotype [22]. To this regard, several studies, a few decades ago, have shown that changes in the “quantity” (*i.e.*, both increases and decreases) as well as in the “quality” (from oscillatory, laminar to steady, turbulent) of shear stress are the most likely explanation for the evidence that atherosclerosis tends to develop preferentially at vascular bifurcations [23, 24]. Taken together, these phenomena provide a background rationale to why atherosclerotic lesions preferentially originate in areas of disturbed flow associated with low – non oscillatory, non laminar – shear stress [25].

WHAT DETERMINES SHEAR STRESS

The mechanical forces determined by vascular hemodynamics on the vasculature act along two gradients: a circumferential one, associated with variations in pulse pressure in the vascular lumen, and a longitudinal one, *i.e.* shear stress, which is the force that contrasts the friction applied to the blood by the vascular wall. Blood flow in arteries, arterioles and capillaries causes a degree of shear stresses in the range of 0-50 dyn/cm², according to the site and the anatomy of the vessel [26]. Obviously, important determinants of shear stress are geometrical (bifurcations, aneurysms, tortuosity of the vessel), biological (mainly NO release) and systemic (blood pressure) factors. In less plain terms, the two components of shear stress are wall shear rate and blood viscosity, where shear rate is the rate at which adjacent layers of fluid move with respect to each other. When one considers the fundamental assumption of fluid mechanics that the velocity of a fluid upon a surface nears zero, shear rate can be understood as the gradient of blood flow velocity between the vascular wall and the peak velocity located somewhere close to the middle of the vessel (in cylindrical vessels). The second component of shear rate is blood viscosity. While viscosity is normally understood as an intrinsic property of a fluid (essentially its capacity to offer resistance to flow), blood viscosity is influenced by several factors, among which of obvious importance are blood cell deformability [27], expression of adhesion molecules etc. As said above, while endothelium-derived autacoids modify both shear rate (by modulating vascular tone) and blood viscosity, in turn, the interaction between shear rate and blood viscosity is a critical modulator of endothelial function, and, consequently, of vascular homeostasis. For instance, studies employing blood substitutes have clearly shown that an elevated viscosity elicits a vasodilatory response due to increased shear stresses [28].

In sum, shear rate, (hematocrit) and viscosity concur to determine shear stress and, through the endothelial cell's biochemical apparatus, regulate vascular homeostasis. The next paragraph will discuss how changes in viscosity alter this equilibrium.

BLOOD HYPERVISCOSITY AND ITS EFFECTS ON ENDOTHELIAL FUNCTION

According to the 1970 Wells' classification, hyperviscosity syndromes are divided into three forms:

- polycytemic syndromes, which are the resultant of an increase in the number of circulating blood cells, which can be demonstrated by changes in hematocrit counts;
- sclerocytic syndromes, where an altered deformability of cellular membranes determines the decreased fluidity of the blood;
- syndromes associated with an increased serum viscosity. In these syndromes, an altered concentration and/or specific properties of an abnormally produced plasma protein (for instance, paraproteinemias) determine increased blood viscosity.

In order to make some examples, syndromes associated with "primary hyperviscosity" include polycythæmias, acute and chronic leukemias, reactive leukocytosis, thrombocytosis, thrombocythæmia and platelet hyperactivity, cryoglobulinemia as well as hyperfibrinogenæmia and myeloma.

In terms of the effects of these changes in blood viscosity on endothelial function, several lines of evidence demonstrate that hyperviscosity causes, as discussed above, a worsened endothelial function and patient prognosis. For instance, in the case of sickle cell disease, vasoocclusive crises due to enhanced adhesion of blood cells to the vascular endothelium as well as abnormal vasomotor tone regulation are a characteristic manifestation and a very common cause of morbidity and mortality. Confirming a deleterious effect of pathologically increased viscosity on endothelial function, despite the increased wall shear stress (due to the increase in flow and in viscosity), patients with sickle cell disease have normal resting brachial artery diameters and a markedly blunted flow-mediated dilation (a parameter of endothelial function) [29]. In sum, primary hyperviscosity syndromes compromise the mechanisms responsible for the transduction of the endothelium-dependent vasodilator signal, causing impaired endothelial responsiveness to changes in shear stress due to the chronically increased wall shear stress in these patients [29]. Taken together, these considerations provide a mechanistic insight for the observation that abnormal blood viscosity is associated with markers of systemic atherogenesis such as intima-media thickness [30].

THE CASE OF SECONDARY BLOOD HYPERVISCOSITY SYNDROMES – NOT SO BAD?

Along with the primary hyperviscosity syndromes, several other conditions have been shown to be associated with an increased plasma viscosity. Among

these, are cardiac, peripheral and cerebral ischemia [31], as shown in Raynaud's syndrome (in which the viscosity of the blood reflux from ischemic territories is higher than that in the contralateral arm) [32], peripheral arterial disease (where blood viscosity appears to be linearly correlated with Fontaine stage), carotid atherosclerosis [33], cardiac ischemia, where our group showed that blood viscosity increases in patients who develop ischemia during exercise testing and during atrial pacing [34]. More in general, blood viscosity is increased in the presence of cardiovascular risk factors [35]. Based on these observations, one can classify hyperviscosity in primary forms, where hyperviscosity is the mechanism of disease (Wells' classification), and secondary forms, where hyperviscosity is actually caused by (or at least associated with), ischemia. Since this subclassification was introduced [36], and based on the considerations made above, it is now known that activation of the ischemic endothelium leads to a series of molecular events that cause changes in blood viscosity [37]. In an example of the importance of endothelial function, blood viscosity was observed to be significantly increased in the morning hours (*i.e.*, when ischemic events are most likely to occur) in patients with risk factors for and/or chronic cardiovascular disease, even in the absence of ongoing ischemia [38-40].

Several lines of evidence confirm this association between ischemia and determinants of blood viscosity: for instance, patients with myocardial infarction show a decreased erythrocyte filtration and an increased blood viscosity, which are accompanied by an increased rigidity of the erythrocyte membrane [41]; in animals, these changes are associated with an increased production of ROS by membrane NADH oxidase [42]. In sum, red blood cell deformability and blood viscosity appear to be particularly REDOX sensitive [43], an observation that confirms the critical importance of ROS in vascular pathophysiology. In sum, there are conditions where hyperviscosity is a consequence (not a cause, as in the primary syndromes) of vascular disease. The significance of ischemia-induced hyperviscosity is described below.

While it is commonly accepted that sustained (primary or secondary) hyperviscosity is a source of further ischemia [44, 45], in an effort to understand the true "meaning" of ischemia-induced hyperviscosity an important consideration needs to be done. The increased viscosity observed in coronary artery disease and/or peripheral arteriopathy has been traditionally interpreted as a consequence or ROS-mediated damage to blood cells and endothelial membranes. However, one has to see the other side of the coin: an increased viscosity, might, at the beginning, act to increase shear stress in the endothelial microenvironment (*Figure 3*). As discussed above, this might increase NO release, triggering the antiatherosclerotic genotype described above (paragraphs 1 and 2). As well, a reduced deformability of red blood cells might increase their permanence within microvessels, favouring oxygen extraction and tissue perfusion. In other words, haemorheological changes of secondary syndromes might be an important com-

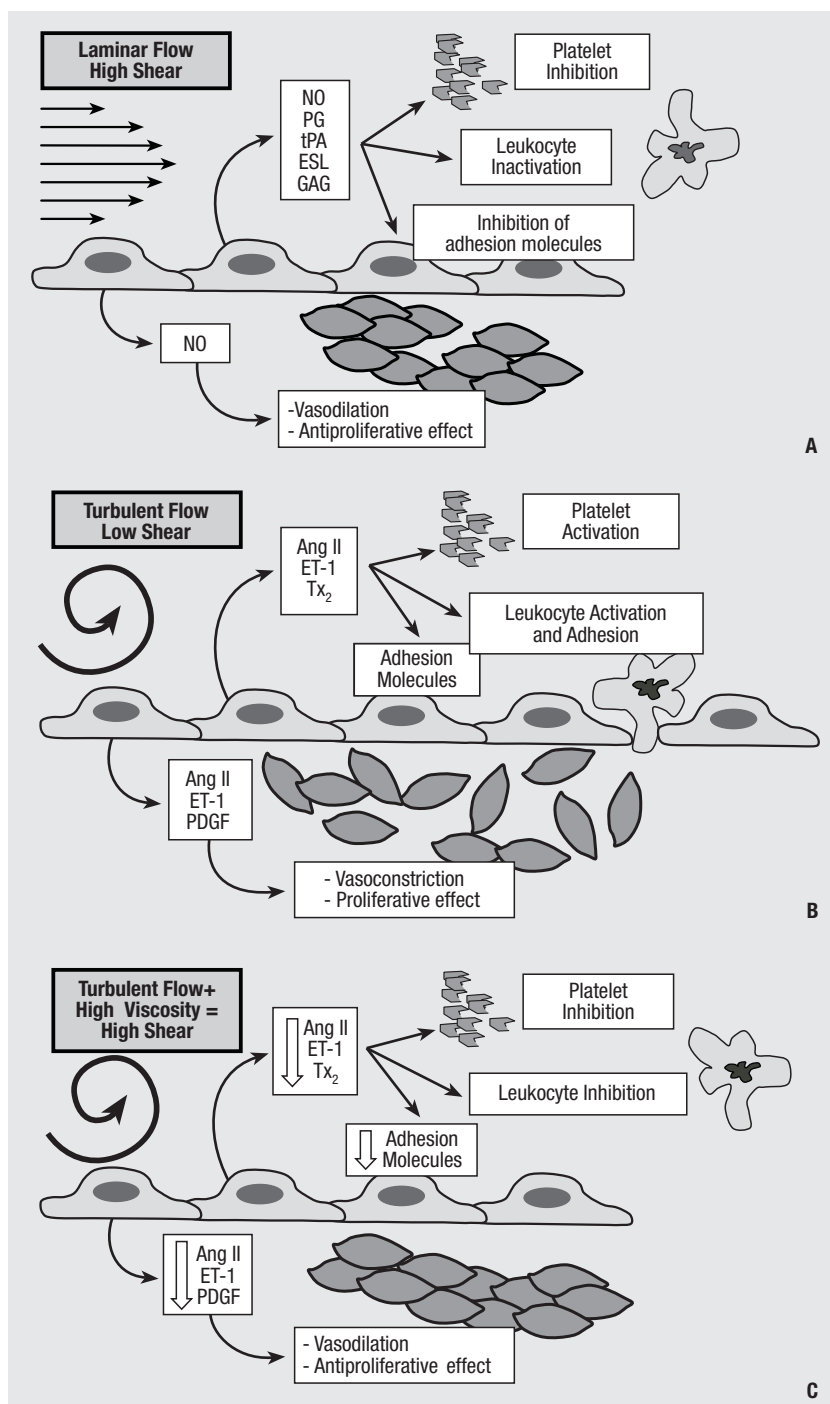


Fig. 3 | Panels A-C: In normal conditions, laminar flow determines high shear stress, which induces a protective endothelial phenotype. In conditions of turbulent flow, this shear stress is reduced, causing the endothelium to lose its protective effect. In this scenario, secondary hyperviscosity might represent a physiological counterregulatory phenomenon aimed at increasing shear stress and endothelial physiology despite non-laminar flow.

NO: nitric oxide; PG: Prostaglandin; tPA: tissue Plasminogen Activator; ESL: endothelial surface layer; GAG: glycosaminoglycan; Ang II: Angiotensin II; ET-1: Endothelin-1; PDGF: Platelet-derived growth factor; Tx₂: Thromboxane 2.

pensatory mechanisms aimed at normalizing vascular homeostasis. An excess of this compensatory mechanism might produce the opposite effects, as persistent hyperviscosity will lead to impaired perfusion and fur-

ther ischemia. In conclusion, secondary hyperviscosity might be one of the many (e.g., immunity) compensatory systems which, when gone awry, actually become source of disease.

References

- Galley HF, Webster NR. Physiology of the endothelium. *Br J Anaesth* 2004;93:105-13.
- Verma S, Buchanan MR, Anderson TJ. Endothelial function testing as a biomarker of vascular disease. *Circulation* 2003;108:2054-59.
- Pries AR, Secomb TW. Microvascular blood viscosity in vivo and the endothelial surface layer. *Am J Physiol Heart Circ Physiol* 2005;289:H2657-64.
- Pries AR, Secomb TW, Gaehtgens P. The endothelial surface layer. *Pflugers Arch* 2000;440:653-66.

5. Traub O, Berk BC. Laminar shear stress: mechanisms by which endothelial cells transduce an atheroprotective force. *Arterioscler Thromb Vasc Biol* 1998;18:677-85.
6. Weinbaum S, Zhang X, Han Y, Vink H, Cowin SC. Mechanotransduction and flow across the endothelial glycocalyx. *Proc Natl Acad Sci USA* 2003;100:7988-95.
7. Masuda H, Kawamura K, Nanjo H, Sho E, Komatsu M, Sugiyama T, Sugita A, Asari Y, Kobayashi M, Ebina T, Hoshi N, Singh TM, Xu C, Zarins CK. Ultrastructure of endothelial cells under flow alteration. *Microsc Res Tech* 2003; 60:2-12.
8. Alderton WK, Cooper CE, Knowles RG. Nitric oxide synthases: structure, function and inhibition. *Biochem J* 2001;357:593-615.
9. Celermajer DS. Endothelial dysfunction: does it matter? Is it reversible? *J Am Coll Cardiol* 1997;30:325-33.
10. Radoski MW, Vallance P, Whitley G, Foxwell N, Moncada S. Platelet adhesion to human vascular endothelium is modulated by constitutive and cytokine induced nitric oxide. *Cardiovasc Res* 1993;27:1380-2.
11. Godin C, Caprani A, Dufaux J, Flaud P. Interactions between neutrophils and endothelial cells. *J Cell Sci* 1993;106 (Pt 2):441-51.
12. Naseem KM. The role of nitric oxide in cardiovascular diseases. *Mol Aspects Med* 2005;26:33-65.
13. Furchgott RF, Carvalho MH, Khan MT, Matsunaga K. Evidence for endothelium-dependent vasodilation of resistance vessels by acetylcholine. *Blood Vessels* 1987;24:145-9.
14. De Keulenaer GW, Chappell DC, Ishizaka N, Nerem RM, Alexander RW, Griendling KK. Oscillatory and steady laminar shear stress differentially affect human endothelial redox state: role of a superoxide-producing NADH oxidase. *Circ Res* 1998;82:1094-101.
15. Uematsu M, Ohara Y, Navas JP, Nishida K, Murphy TJ, Alexander RW, Nerem RM, Harrison DG. Regulation of endothelial cell nitric oxide synthase mRNA expression by shear stress. *Am J Physiol* 1995;269:C1371-8.
16. Hambrecht R, Wolf A, Gielen S, Linke A, Hofer J, Erbs S., Schoene N, Schuler G. Effect of exercise on coronary endothelial function in patients with coronary artery disease. *N Engl J Med* 2000;342:454-60.
17. Kojda G, Harrison D. Interactions between NO and reactive oxygen species: pathophysiological importance in atherosclerosis, hypertension, diabetes and heart failure. *Cardiovasc Res* 1999;43:562-71.
18. Huie RE, Padmaja S. The reaction of NO with superoxide. *Free Radic Res Commun* 1993;18:195-9.
19. Elliott SJ, Lacey DJ, Chilian WM, Brzezinska AK. Peroxynitrite is a contractile agonist of cerebral artery smooth muscle cells. *Am J Physiol* 1998;275:H1585-91.
20. Malek AM, Greene AL, Izumo S. Regulation of endothelin 1 gene by fluid shear stress is transcriptionally mediated and independent of protein kinase C and cAMP. *Proc Natl Acad Sci USA* 1993;90:5999-6003.
21. Gori T, Forconi S. The role of reactive free radicals in ischemic preconditioning-clinical and evolutionary implications. *Clin Hemorheol Microcirc* 2005;33:19-28.
22. Malek AM, Alper SL, Izumo S. Hemodynamic shear stress and its role in atherosclerosis. *JAMA* 1999;282:2035-42.
23. Gnasso A, Irace C, Carallo C, De Franceschi MS, Motti C, Mattioli PI, Pujia A. In vivo association between low wall shear stress and plaque in subjects with asymmetrical carotid atherosclerosis. *Stroke*. 1997;28:993-8.
24. Giddens DP, Zarins CK, Glagov S. The role of fluid mechanics in the localization and detection of atherosclerosis. *J Biomech Eng*. 1993;115:588-94.
25. Friedman MH, Barger CB, Deters OJ, Hutchins GM, Mark FF. Correlation between wall shear and intimal thickness at a coronary artery branch. *Atherosclerosis*. 1987;68:27-33.
26. Ku DN, Giddens DP. Pulsatile flow in a model carotid bifurcation. *Arteriosclerosis* 1983;3:31-9.
27. Lipowsky HH. Microvascular rheology and hemodynamics. *Microcirculation* 2005;12:5-15.
28. Tsai AG, Cabrales P, Intaglietta M. Oxygen-carrying blood substitutes: a microvascular perspective. *Expert Opin Biol Ther*. 2004;4:1147-57.
29. Belhassen L, Pelle G, Sediame S, bachir D, Carville C, Bucherer C, Lacombe C, Galacteros F, Adnot S. Endothelial dysfunction in patients with sickle cell disease is related to selective impairment of shear stress-mediated vasodilation. *Blood* 2001;97:1584-9.
30. Lee AJ, Mowbray PI, Lowe GD, Rumley A, Fowkes FG, Allan PL. Blood viscosity and elevated carotid intima-media thickness in men and women: the Edinburgh Artery Study. *Circulation* 1998;97:1467-73.
31. Di Perri T, Guerrini M, Pasini FL, Acciabatti A, Piergalli D, Galigani C, Capecchi PL, Orrico A, Franchi M, Bardi P. Hemorheological factors in the pathophysiology of acute and chronic cerebrovascular disease. *Cephalalgia* 1985;5 Suppl 2:71-7.
32. Forconi S, Guerrini M, Agnusdei D, Pasini FL, di Perri T. Letter: Abnormal blood viscosity in Raynaud's phenomenon. *Lancet* 1976;2:586.
33. Carallo C, Pujia A, Irace C, De Franceschi MS, Motti C, Gnasso A. Whole blood viscosity and haematocrit are associated with internal carotid atherosclerosis in men. *Coron Artery Dis* 1998;9:113-17.
34. Forconi S, Guerrini M, Piergalli D, Acciabatti A, Del Bigo C, Galigani C, Di Perri T. [Hemorheological changes in ischemic heart disease]. *Ric Clin Lab* 1983;13 Suppl 3:195-208.
35. Caimi G, Hoffmann E, Montana M, Canino B, Dispensa F, Catania A, Lo Presti R. Haemorheological pattern in young adults with acute myocardial infarction. *Clin Hemorheol Microcirc* 2003;29:11-8.
36. Forconi S, Piergalli D, Guerrini M, Galigani C, Cappelli R. Primary and secondary blood hyperviscosity syndromes, and syndromes associated with blood hyperviscosity. *Drugs* 1987;33 Suppl 2:19-26.
37. Gori T, Lisi M, Forconi S. Ischemia and reperfusion: the endothelial perspective. *Clin Hemorheol Microcirc* 2006;35:31-4.
38. Nobili L, Schiavi G, Bozano E, de Carli F, Ferrillo F, Nonili F. Morning increase of whole blood viscosity in obstructive sleep apnea syndrome. *Clin Hemorheol Microcirc* 2000;22:21-7.
39. Antonova N, Velcheva I. Hemorheological disturbances and characteristic parameters in patients with cerebrovascular disease. *Clin Hemorheol Microcirc* 1999;21:405-8.
40. Mares M, Bertolo C, Terribile V, Girolami A. Hemorheological study in patients with coronary artery disease. *Cardiology* 1991;78:111-6.
41. Tozzi-Ciancarelli MG, Di Massimo C, Mascioli A, Tozzi E, Gallo P, Fedele F, Dagianti A. Rheological features of erythrocytes in acute myocardial infarction. *Cardioscience* 1993;4:231-4.
42. Nemeth N, Lesznyak T, Szokoly M, Furka I, Miko I. Allopurinol prevents erythrocyte deformability impairing but not the hematological alterations after limb ischemia-reperfusion in rats. *J Invest Surg* 2006;19:47-56.
43. Baskurt OK, Temiz A, Meiselman HJ. Effect of superoxide anions on red blood cell rheologic properties. *Free Radic Biol Med* 1998;24:102-10.
44. Engler RL, Schmid-Schonbein GW, Pavelec RS. Leukocyte capillary plugging in myocardial ischemia and reperfusion in the dog. *Am J Pathol* 1983;111:98-111.
45. Dormandy J, Ernst E, Bennett D. Erythrocyte deformability in the pathophysiology of the microcirculation. *Ric Clin Lab* 1981;11 Suppl 1:35-8.

Flow dynamics and haemostasis

Mario Mazzucato^(a), Andrea Santomaso^(b), Paolo Canu^(b), Zaverio M. Ruggeri^(c)
and Luigi De Marco^(d)

^(a)Unità di Raccolta e Manipolazione Cellule Staminali Emopoietiche, IRCCS-CRO Aviano, Pordenone, Italy

^(b)DIPIC, Ingegneria Chimica, Università di Padova, Italy

^(c)Roon Research Center for Arteriosclerosis and Thrombosis, Division of Experimental Thrombosis and Hemostasis, The Scripps Research Institute, La Jolla, CA, USA

^(d)Servizio Immunotrasfusionale Analisi Cliniche e Laboratorio d'Urgenza, IRCCS-CRO Aviano, Pordenone, Italy

Summary. Fluid-dynamic conditions that are compatible with tensile stress on the bonds between platelet glycoprotein Iba and immobilized von Willebrand factor A1 domain (VWF-A1) led to Ca⁺⁺ release from intracellular stores (type α/β peaks), which preceded stationary platelet adhesion. Raised levels of cyclic adenosine monophosphate (cAMP) and cyclic guanosine monophosphate inhibited these [Ca⁺⁺]i oscillations and prevented stable adhesion. Once adhesion was established through the integrin $\alpha_{IIb}\beta_3$, new [Ca⁺⁺]i oscillations (type γ) of greater amplitude and duration, and involving a transmembrane ion flux, developed in association with the recruitment of additional platelets into aggregates. We have defined the distinct roles that the two ADP receptors, P2Y₁ and P2Y₁₂, play in the early events that follow the initial platelet interaction with immobilized VWF-A1 under high flow conditions. We have examined the consequences of specific pharmacologic inhibition of P2 receptors and our findings demonstrate a differential role of P2Y₁ and P2Y₁₂, respectively, in platelet adhesion and aggregation onto immobilized VWF under elevated shear stress, and highlight the distinct contribution of signaling pathways dependent on Src family kinases, PLC, and phosphoinositide 3-kinase (PI 3-K) to these processes. Results have been achieved through original experiments under flow, thoroughly characterized by *ad hoc* image analysis techniques and quantitative kinetic analysis.

Key words: platelets, ADP receptors, signaling, von Willebrand factor, adhesion equilibrium constant, image analysis.

Riassunto (Fluidodinamica ed emostasi). Le condizioni fluidodinamiche in grado di determinare adeguata tensione al legame tra la glicoproteina piastrinica GPIba e il dominio A1 del fattore di von Willebrand immobilizzato sulla superficie adesiva portano al rilascio di Ca⁺⁺ dai depositi intracellulari (picchi α/β), fenomeno che precede l'adesione piastrinica stabile. Elevati livelli di adenosina monofosfato ciclico (cAMP) e guanosina monofosfato ciclico (cGMP) inibiscono il rilascio di Ca⁺⁺ dai depositi intracellulari e prevengono l'adesione piastrinica stabile. Stabilita l'adesione piastrinica attraverso l'azione dell'integrina $\alpha_{IIb}\beta_3$, si evidenziano nuove oscillazioni di [Ca⁺⁺]i (type γ), più durature e di maggiore entità, che coinvolgono anche un flusso ionico transmembrana, e che sono associate ad un reclutamento di nuove piastrine nel formare l'aggregato. Abbiamo definito i ruoli distinti dei due recettori piastrinici per l'ADP, il P2Y₁ e il P2Y₁₂, nelle prime fasi dei fenomeni adesivi che seguono immediatamente l'interazione tra la piastrina e il dominio A1 del VWF immobilizzato sulla superficie di contatto in condizioni di flusso ad alte forze di scorrimento. Abbiamo esaminato le conseguenze dell'inibizione dei due recettori P2 mediante l'uso di inibitori specifici e abbiamo dimostrato un ruolo differente, per quanto riguarda il P2Y₁ e il P2Y₁₂, nell'adesione e aggregazione piastrinica sul VWF immobilizzato in condizioni di elevato *shear rate*. Abbiamo infine dato rilievo al contributo specifico delle vie di trasmissione del segnale dipendente dalle Src kinasi, PLC e fosfoinositide 3-kinasi (PI 3-K). Questi risultati sono stati ottenuti mediante specifici esperimenti in condizioni di flusso, estensivamente caratterizzati mediante tecniche di analisi di immagine *ad hoc* e analisi cinetiche quantitative.

Parole chiave: piastrine, recettori per ADP, trasmissione del segnale, fattore von Willebrand, costanti di equilibrio di adesione, analisi d'immagine.

INTRODUCTION

Blood circulates with greater velocity at the centerline of a vessel than near the wall, and this difference creates a shearing effect between adjacent layers of

fluid that is greatest at the wall. The shear rate (s⁻¹) is directly proportional to the shear stress (N/m²) and inversely proportional to the viscosity of the fluid (N/m² · s). Quiescent platelets circulate in the blood-

stream whereas the activation of platelets at sites of vascular injury plays a key role in haemostasis. At high shear rates, equivalent to those generated by blood flow in arterioles or stenotic arteries, adhesion requires von Willebrand factor (VWF) endogenously present in the subendothelial matrix or absorbed onto injured tissue components exposed to plasma. The drag that opposes platelet adhesion and aggregation increases with the flow rate, which in turn increases the wall shear stress; consequently, its effects on platelet thrombus formation are more relevant in arteries than in veins and, particularly, in arterioles. The highest shear rate values in the normal circulation may range from 500 to 5000 s^{-1} with a median value of 1700 s^{-1} . The binding of glycoprotein (GP) Ib α to the A1 domain of VWF is the main adhesive interaction capable of tethering platelets to a surface even when the flow velocity is elevated, but cannot mediate irreversible adhesion by itself [1]. Rather, the interaction maintains platelets in close contact with the surface, albeit with continuous translocation in the direction of flow (*rolling*), until other receptors and ligands mediate a stable attachment after activation. When VWF is bound to collagen, the transition from rolling to stable adhesion occurs in seconds indicating a rapid activation that may be aided by signals originating from the mechanical stimulation of VWF-GP Ib α bonds under tensile stress [2]. At this stage of the process, plasma VWF binds to the surface of adherent and activated platelets, through an interaction that involves engagement of the integrin $\alpha_{IIb}\beta_3$ with the Arg-Gly-Asp sequence in the VWF C1 domain. Membrane-bound VWF is the substrate to which, in a high shear rate environment, flowing platelets attach through their GP Ib α to maintain thrombus growth in a process that repeats itself in successive layers. Like in the initial adhesion to the vessel wall, the binding of other ligands to activated $\alpha_{IIb}\beta_3$ is also required to support stable platelet aggregation [3].

MATERIALS AND METHODS

Blood preparation

Venous blood from medication-free healthy volunteers, who gave their informed consent according to the declaration of Helsinki, was mixed with 1/6 final volume of citric acid/citrate/dextrose, pH 4.5, or a specific α -thrombin inhibitor, either hirudin (Iketon, Milan, Italy) at the final concentration of 400 units/ml or PPACK (Calbiochem, La Jolla, CA) at the final concentration of 50 μ M. Fifty ml of ACD-containing blood was centrifuged at 1000 g for 50 s at 22–25 $^{\circ}$ C, and the supernatant platelet-rich plasma (PRP) was collected. The platelets were incubated for 20 min at 37 $^{\circ}$ C with the fluorescent calcium probe Fluo-3AM (Molecular Probes, Eugene, OR) at the final concentration of 8 μ M. Erythrocytes separated from the same blood were washed three times in a divalent cation-free Hepes-Tyrode buffer pH 6.5 and finally resuspended in the same buffer and with the addition of 1.75 mM Probenecid (Sigma, St. Louis,

MO), used to prevent leakage of Fluo-3AM from the platelets. An adequate volume of PRP containing $2\text{--}8 \times 10^8$ FLUO 3-AM loaded platelets/ml was mixed with an aliquot of the erythrocyte suspension (50% hematocrit) and apyrase (grade III; Sigma) at the final concentration of 5 ATPase U/ml. The mixture was centrifuged at 1000 g for 15 min, the supernatant was discarded and the cell pellet was suspended in autologous plasma (prepared from the blood collected in hirudin or PPACK by centrifugation at 1650 g for 15 min at 22–25 $^{\circ}$ C) or Hepes-Tyrode buffer pH 7.4 and 1.75 mM Probenecid in a proportion such that the hematocrit was 42–45%. The labeling procedure did not significantly alter the function of platelets as evidenced by the response to agonists and the expression of surface activation markers [2].

Flow experiments

Human plasma VWF was diluted in phosphate-buffered saline, pH 7.4. Different concentrations of protein were used to coat the glass coverslips (24 x 50 mm) that represented the lower surface of a parallel plate flow chamber. A silicon rubber gasket determined the flow path height (125 μ m) between the glass coverslip and the upper plate. The chamber was assembled and filled with PBS, pH 7.4. A syringe pump (Harvard Apparatus Inc., Boston, MA) and silicone tubing connections were used to aspirate blood through the chamber at the desired flow rate. The perfusion system was mounted onto an inverted microscope equipped with epifluorescent illumination (Diaphot-TMD; Nikon Instech, Kanagawa, Japan) and intensified CCD video camera (C-2400-87; Hamamatsu Photonics, Shizuoka, Japan). All these experiments were recorded at a video rate of 25 fps on S-VHS videotape. Recorded images were captured and digitized from videotape. Image analysis was then performed off-line.

Image analysis technique

Image analysis is crucial for the following theoretical discussion. It must provide reliable identification and tracking of cells on long image sequences, rapidly (*i.e.*, without manual operations on individual images) and consistently (no subjective criteria, operator dependent). For that purpose we developed our own algorithms and programs [4], based on the MATLAB Image Tool (The MathWorks, Inc.). The method includes original options for automatic thresholding grey-scale images, and dedicated tracking algorithms, able to account for the physics of the flow experiment. Object identification between subsequent frames is obtained with a time-varying, two dimensional probability density function build around each single identified object [5] and oriented with the flow.

Adhesion data analysis

Thanks to the automatic particle tracking algorithm that we developed, details on each particle feature can be collected over time, providing information on the

establishment and breakage of adhesive bonds between a platelet moving in shear flow and the substrate, as well as the path traveled by the cell on the surface and cytoplasmic Fluo-3AM/ Ca^{2+} concentration in the cells, as a function of time.

The platelet stays on the surface for a certain time, then rolls on the surface, stops, starts rolling again, many times before final detachment, and the duration of each step may vary. The actual history of platelet displacements is decisive in understanding and quantifying the strength of adhesion, as well as characterizing the surface density of ligands. After a transient, deposition and reentrainment of platelet equilibrates, reaching an adhesion equilibrium and the average number of surface events remains constant. The length of the initial transient indicates the minimum interval of observation required to collect statistically significant data. Often, quite a long observation period (approximately from 125 to 1500 frames with a temporal resolution of 25 fps) must be allowed to reliably identify the average surface concentration (equilibrium between the on and off process). On the other hand, the asymptotic value changes according to the experimental conditions such as wall shear stress, platelet count, hematocrit, and surface concentration of active sites. Varying a certain condition, like the wall shear stress (through different flow rates imposed by the pump), often requires adjusting the observation time to have a significant value for the deposition/removal rates. All our experiments were recorded up to steady-state conditions on the surface are achieved. Secondary data, directly determined from observables, can then be derived such as the distribution of lifetimes for all the interacting platelets.

Of specific interest for a kinetic and thermodynamic study is the direct measurement of on- and off-rates. The cumulated number of platelets that tethered and detached in the field of view up to a given time are determined and reported into diagram. The slope of the curve represents the rate of attachment (R_{on}) and detachment (R_{off}) [5].

HOW SHEARING AFFECTS PLATELET ADHESION AND ACTIVATION ONTO VON WILLEBRAND FACTOR SURFACE

Platelet GP $\text{Ib}\alpha$ may function as an adhesion receptor and signaling receptor when platelets are adhering onto VWF surface at high shear rate conditions. We identified 2 types of effects, based on the intracellular Ca^{2+} concentration, its variation rate and relation with platelet motion on the surface. One type appears while platelets translocate on the VWF surface and it is characterized by a rapid increase of intracellular Ca^{2+} concentration. This peak was named α when the $[\text{Ca}^{2+}]_i$ rises above 400 nM or β when lower. In experiments performed with a wall-shear rate of 3000 s^{-1} , approximately 20% of the translocating platelets exhibit at least one α or β Ca^{2+} peak, and 9% established stationary adhesion

within the observation period. Approximately 30% of the firmly adherent platelets had a distinct type of Ca^{2+} increase, named γ , which reached levels higher than 2000 nM, and even 3000 nM in many cases, can last several seconds, pulsing the Ca^{2+} concentration (Figure 1). After a Ca^{2+} increase of type γ , platelets were observed to promote the arrest of other platelets translocating in their vicinity, and these in turn showed pronounced cytosolic Ca^{2+} elevations and started to form aggregates. Once established, these aggregates could grow quickly, displaying periodical and synchronous $[\text{Ca}^{2+}]_i$ pulsations.

Our observations demonstrate that the interaction of platelet $\text{GPIb}\alpha$ with VWF leads to 2 distinct types of $[\text{Ca}^{2+}]_i$ elevations linked to sequential stages of integrin $\alpha_{\text{IIb}}\beta_3$ activation. The first Ca^{2+} increase appears to be initiated by a mechanical stimulation, their frequency increasing with wall shear stress above 2 Pa. Within this group, the distinction between type α and β peaks was based solely on Ca^{2+} concentration and the fact that α peaks have a reproducible shape that facilitates the analysis of their relation to platelet motion. Indeed, type α peaks reached a maximum while platelets were transiently arrested but at a predictably short time before detachment from the surface, when the tensile stress on the $\text{GPIb}\alpha$ -VWF bonds is larger. These findings support the hypothesis that $\text{GPIb}\alpha$ has a mechanoreceptor function, although the proximal events

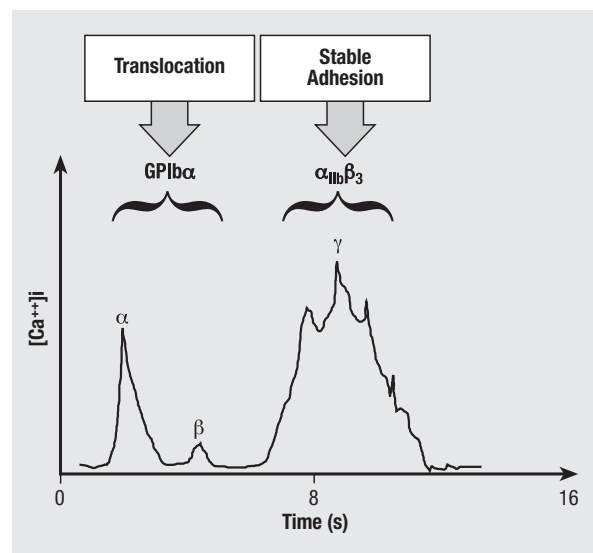


Fig. 1 | Real-time analysis of $[\text{Ca}^{2+}]_i$ during platelet translocation and aggregate formation on immobilized VWF. Platelets loaded with Fluo-3 AM were suspended with washed erythrocytes in homologous plasma and perfused over immobilized VWF for 3 minutes at a shear rate of $1500 \text{ seconds}^{-1}$. Platelet appears in the optical field and moved in the direction of flow. The translocation of platelet occurs mostly during a few seconds of relatively rapid movement, coincident with the appearance of transient $[\text{Ca}^{2+}]_i$ peaks (α/β); a higher and longer lasting increase in $[\text{Ca}^{2+}]_i$ (γ) develops while the platelet is stationary.

responsible for transducing forces into a biochemical signal remain to be fully explained. Binding of the GPIIb α cytoplasmic tail to the membrane skeleton through filamin-a [6] and to the ζ isoform of 14.3.3, [7], a regulatory molecule in cellular signaling, may be relevant. Neither association is needed for the GPIIb α -dependent induction of $\alpha_{IIb}\beta_3$ activation in heterologous cells, but a role in flowing platelets is likely. Notwithstanding these uncertainties, it is clear that type α/β peaks are the consequence of rapid Ca^{2+} release from intracellular stores. Such cytoplasmic Ca^{2+} elevations are likely mediated by inositol-1,4,5-trisphosphate generated with diacylglycerol through the action of phosphatidylinositol-specific phospholipase C.

The first level of $\alpha_{IIb}\beta_3$ activation induced by platelet interaction with VWF under shear stress leads from transient to stable adhesion and is regulated by the cellular levels of cAMP and cGMP that control type α/β Ca^{2+} signals. However, thrombus formation cannot progress at this stage, possibly because $\alpha_{IIb}\beta_3$ molecules are activated only in the vicinity of stimulated GPIIb α and they can bind immobilized VWF but not soluble VWF and fibrinogen as required for aggregation. A second level of $\alpha_{IIb}\beta_3$ activation must be reached for aggregation to occur, and this appears to require signal amplification associated with Ca^{2+} elevations of type γ , induced by ADP released in response to the initial GPIIb α stimulation [2].

Then, it was established that secreted adenosine diphosphate (ADP) is necessary for the shear-induced platelet aggregation initiated by the interaction of soluble VWF with GPIIb α . ADP binds to different G protein-linked P2 receptors, two of which (P2Y₁ and P2Y₁₂) are present on platelets [8]. Ligation of P2Y₁, linked to Gq, activates phospholipase C (PLC) and mobilizes Ca^{2+} from intracellular stores, leading to the activation of protein kinase C and subsequent platelet aggregation. Ligation of P2Y₁₂, linked to Gi, inhibits adenylyl cyclase, lowers cAMP levels, and potentiates ADP-induced platelet aggregation [9]. The function of both P2Y₁ and P2Y₁₂ is required for platelet aggregation after adhesion to collagen-bound VWF under flow conditions [10]. Distinct roles of two ADP receptors in the activation of platelets interacting with immobilized VWF in a flow field were described. We identified two sequential Ca^{2+} signals associated with the activation of flowing platelets interacting with immobilized VWF (*Figure 1*). The earlier α/β peaks, linked to the engagement of GP Ib α by VWF-A1, involved Ca^{2+} release from intracellular stores and anticipated stationary adhesion. The results now obtained with selective antagonists of the two platelet ADP receptors modify earlier concepts reported in the literature, demonstrating a previously unrecognized role of P2Y₁ in generating the early signals associated with a first level of $\alpha_{IIb}\beta_3$ activation required for stable adhesion to VWF. Such a conclusion rests on the observation that platelets

with blocked P2Y₁ exhibited the relatively rapid translocation velocity and short transient arrest times sustained by GP Ib α binding to VWF-A1 without $\alpha_{IIb}\beta_3$ engagement, as seen with PGE1-treated platelets. Blocking P2Y₁ function decreased by approximately 30% the proportion of platelets that exhibited type α oscillations while translocating on VWF, and reduced by approximately 500 nM the $[Ca^{2+}]_i$ of a type α peak. The reduction in activation mirrors the proportion of platelets that show a γ peak after an α peak, indicating that signaling from P2Y₁ following GP Ib α -dependent ADP release may be crucial for the increase of $[Ca^{2+}]_i$ to the levels needed for $\alpha_{IIb}\beta_3$ activation. This hypothesis is supported by the observation that inhibition of PLC β , which acts downstream of P2Y₁ and generates an effector of Ca^{2+} release from intracellular stores (*Figure 2*) inhibits platelet adhesion to VWF and related Ca^{2+} oscillations as effectively as the P2Y₁ antagonist. PLC γ_2 , which is also inhibited by U73122,29 may contribute to GP Ib-dependent signaling as previously inferred from studies on platelet adhesion to VWF under static conditions [11]. Thus, as also suggested elsewhere, intracytoplasmic Ca^{2+} levels may be related to the degree of activation of platelets interacting with VWF under high shear stress conditions: less than 200 nM equals resting; 400 nM equals β peak, subactivation; 1000 nM equals α peak induced by GP Ib α signaling, leading to ADP release; 1500 nM equals α peak+P2Y₁ signal, first level of $\alpha_{IIb}\beta_3$ activation and stable adhesion; more than 1500 nM equals γ peak, full $\alpha_{IIb}\beta_3$ activation with platelet aggregation modulated by P2Y₁₂ function (*Figure 2*). The contribution of P2Y₁ to GP Ib α -initiated $\alpha_{IIb}\beta_3$ activation, therefore, may have different functional relevance in relation to hemodynamic parameters of the blood circulation. Src family kinase-dependent pathway is initially involved in the transduction of the signal originated by VWF-A1 binding to GP Ib α , as shown by the abrogation of all Ca^{2+} peaks caused by the Src inhibitors PP1 and PP2. Similar conclusions have been reached by others using different experimental conditions [12, 13].

In contrast to the early role of P2Y₁ in promoting stable platelet adhesion to immobilized VWF, which is an absolute requirement for subsequent aggregation, we found that P2Y₁₂ is not involved in generating any of the Ca^{2+} transients initially associated with platelet activation.

On the other hand, we found that P2Y₁₂ function is critical for the full development of platelet aggregates on immobilized VWF, in agreement with its reported role in shear-induced platelet aggregation initiated by soluble VWF binding to GP Ib α and in thrombus formation on collagen-bound VWF. Others have reported that P2Y₁₂ is involved in maintaining elevated Ca^{2+} levels in aggregating platelets [14] a function that is likely to be important for thrombus growth, as we confirm here, but appears to be distinct from earlier signaling events that initiate aggregation.

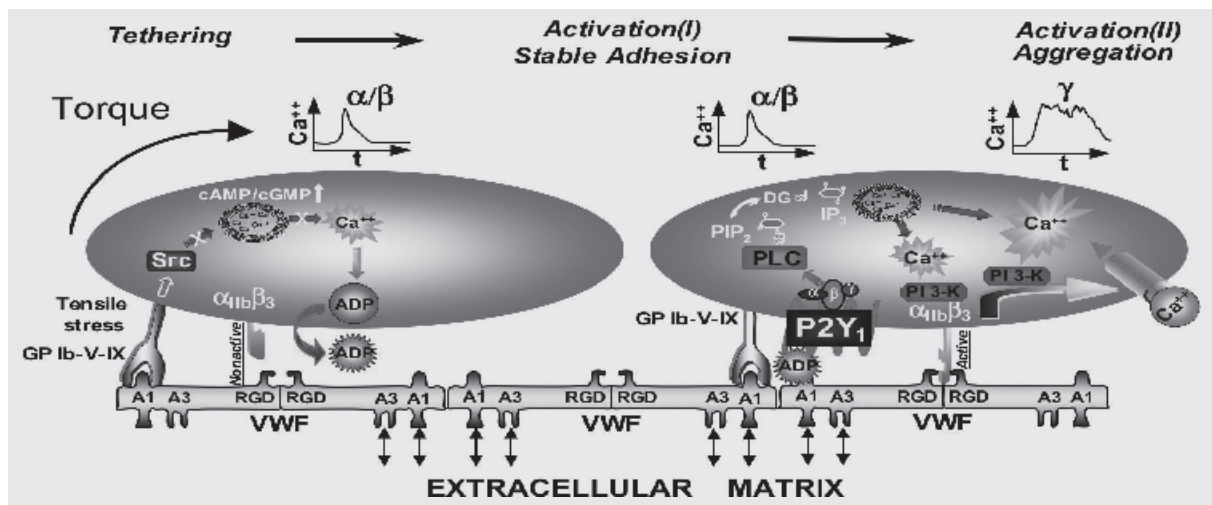


Fig. 2 | Schematic representation of the sequential signaling events induced by the interaction of platelets with immobilized VWF under high shear stress. On the left, a platelet is shown during the initial tethering to the A1 domain of immobilized VWF mediated by the GP Ib-IX-V complex. An $\alpha\beta$ [Ca^{2+}] elevation is elicited as a consequence of this interaction and leads to the release of ADP from intracellular storage granules. Src family kinases may be involved at this stage, (13) and cAMP/cGMP levels modulate this and other downstream responses. Subsequent events are shown in the platelet on the right. The released ADP binds to the Gq-coupled P2Y₁ receptor, which leads to PLC activation and enhances Ca^{2+} release from internal stores during $\alpha\text{Ib}\beta_3$ oscillations. At this stage, a first level of localized $\alpha_{\text{IIb}}\beta_3$ activation is reached that supports a more prolonged platelet adhesion mediated by the RGD sequence in the VWF C1 domain. Initial PI 3-K activation may enhance this response. Subsequently, further PI 3-K activation and possibly the involvement of Src family kinases contribute to a more generalized $\alpha_{\text{IIb}}\beta_3$ activation that permits soluble ligand binding (exemplified here by fibrinogen and VWF) and supports the formation of platelet-platelet aggregates. This second level of $\alpha_{\text{IIb}}\beta_3$ activation is concurrent with or subsequent to a type γ [Ca^{2+}] elevation dependent on a transmembrane ion flux. The second ADP receptor, P2Y₁₂, supports the formation of larger platelet aggregates through mechanisms that occur after the measured Ca^{2+} oscillations. The thromboxane A₂ pathway inhibited by aspirin appears to have a very limited role in the successive stages of platelet adhesion, activation, and aggregation induced by the interaction with immobilized VWF. IP₃ indicates inositol-1,4,5-trisphosphate; Src, Src family tyrosine kinases; PLC, phospholipase C; PKC, protein kinase C; PI 3-K, phosphatidylinositol 3-kinase; PIP₂, phosphatidylinositol bisphosphate; DG, diacylglycerol.

HOW SHEARING AFFECTS PLATELET AGGREGATION MEDIATED BY VON WILLEBRAND FACTOR

A unique feature of the binding of soluble VWF to platelet GP Ib α is the positive regulation by high shear forces. Shear-induced platelet aggregation is initiated by the binding of soluble VWF, through its A1 domain, to platelet GP Ib α . This interaction, which occurs above a threshold shear, triggers platelet signaling events that lead to platelet activation and the modulation of $\alpha_{\text{IIb}}\beta_3$ to form a high affinity receptor capable of binding soluble adhesive ligands such as VWF or fibrinogen [3, 15]. Physiologically relevant shear stress alone is capable of inducing this dual-step platelet aggregation without the addition of an exogenous agonist [16, 17]. Although initiated by the VWF/GP Ib α interaction, irreversible platelet aggregation induced by shear requires concomitant binding of VWF to both GP Ib α and $\alpha_{\text{IIb}}\beta_3$ complexes [18, 19]. Despite the many advances in our understanding of shear-induced VWF/GP Ib α interactions [20], the underlying mechanisms regulating signaling through GP Ib α remain poorly defined. Binding of soluble VWF to GP Ib α under stationary conditions, can be artificially induced by modulators like ristocetin and botrocetin, which bind to the VWF A1 do-

main [21]. However, distinct regions of both the ligand and receptor are involved in addition to regions common to both modulators. A panel of anti-VWF, and anti-GP Ib α antibodies have been characterized for their effects on ristocetin- and botrocetin-induced VWF/GP Ib α interactions, in addition to their effect on shear-induced platelet aggregation. Based on these studies, it now appears that ristocetin-, rather than botrocetin-dependent binding of VWF to platelet GP Ib α under stationary conditions more closely simulates the shear-dependent binding of VWF to GP Ib α [22]. Thus, ristocetin-dependent binding of VWF to GP Ib α may provide a useful means of simulating signaling mechanisms relevant to shear-dependent VWF/GP Ib α interactions. In this context, ristocetin-mediated interaction of VWF with platelet GP Ib α evokes a transient Ca^{2+} signal in the absence of extracellular Ca^{2+} [23], indicating activation of the PLC / IP₃ pathway leading to elevated cytoplasmic Ca^{2+} levels, mobilized from intracellular stores. An important role of the platelet cytoskeleton in regulating the VWF/GP Ib α interaction has recently been demonstrated [24]. In these studies, pre-treating platelets with inhibitors of actin polymerization enhanced the rate and extent of shear-induced platelet aggregation, and also lowered the shear threshold

required to induce aggregation. Similar treatment also enhanced the rate and extent of platelet aggregation induced by VWF in the presence of ristocetin. These observations raise the intriguing possibility that regulation of the VWF/GP Ib α interaction by the cytoskeleton is key in preventing shear-induced platelet aggregation in the normal circulation.

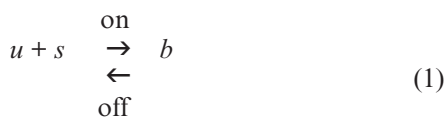
KINETICS OF BOND FORMATION AND RUPTURE

By perfusing blood through a flow chamber and analyzing surface events using a tailored image processing and particle tracking algorithms, we can quantify deposition and removal rates, and attempt to correlate fluxes with actual shear rate. Statistical reasoning allow formulating single-event observations into mean-field behaviour, suitable for a macroscopic, clinical scale application.

Cell adhesion, mediated by the interaction of dedicated receptor and ligand molecules bound to interacting surfaces, requires suitable, unambiguous criteria for predicting whether a cell-to-cell encounter results in durable adhesion. Rates of adhesion and detachment are generally accepted as key determinants for the purpose, especially in a dynamic flow environment [25]. Critical to the role of the initial bonds platelets-VWF is the balance of their on- and off-binding rates which must be tuned to support platelet tethering and transient arrests without the need to establish stable bonds [26]. While an impressive amount of information has been gathered on the rate of bond dissociation [27, 28], little attention has been given to the frequency of formation of molecular interactions, mainly because variables involved in adhesion rate cannot be easily determined. Progress in this direction has been made [29], however a methodological framework for quantitative investigation of the parameters involved in cell-surface interaction (kinetics of the on- and off- process and characterization of the adhesion equilibrium) with specific attention to blood platelets is lacking.

Adhesion kinetics

According to early formulations (Bell's model [30]) the variation with time of the number of cells bound to the surface, N_b , is given by analogy with a reversible bimolecular chemical reaction between unbound cells (u) and surface sites (s):



so that the rate of change of the number of bound cells is given by:

$$\frac{dN_b}{dt} = R_{on} - R_{off} = k_{on} N_s N_u - k_{off} N_b \quad (2)$$

where R are the arrival/removal rates, k the kinetics constants, N_u is the number of unbound receptors on flowing platelets that can interact with the surface, and N_s is the number of sites of deposited substrate available for the platelets to bind. R 's can be directly measured from image analysis, but the identification of the intrinsic parameters (k 's) requires specifications on the quantities involved in equation (eqn) (2). The instantaneous and average N_b are also experimentally measurable through continuous image analysis; together with R_{off} measurements k_{off} can be easily calculated. Different experiments can reveal the dependence of k_{off} on experimental factors, and specifically the wall shear rate. Variables involved in the adhesion rate (R_{on}) are not as easily determined. The number of sites on the surface available for the platelets to bind can be expressed as the difference between total number of sites available on the surface, N_s^o , and those already drawn in binding platelets

$$N_s = N_s^o - \alpha N_b \quad N_s^o = K_{VWF} C_{VWF} \quad (3)$$

N_s^o can be related to the concentration of substrate (often von Willebrand factor in our studies), C_{VWF} , used to coat the surface. The complete adsorption curve (Figure 3a), which can be determined by binding assays experiments, at low substrate concentration, before surface saturation, reduces to a simple proportionality through the adsorption equilibrium constant, K_{VWF} . The coefficient α is the number of bonds a single platelet can establish with the surface ligands. It is frequently assumed $\alpha = 1$, the minimum for platelet-surface interaction, although evidences of multiple bonds formation, like rolling on the surface, have been observed. A procedure to estimate α can be devised, to check whether multiple bonds are likely, synergistically opposing tensile stress. N_u , the platelet number close to the surface, is the most critical piece of information. They can be quite different from the blood platelet count, N_p , because of radial segregation of cells in blood [31]. We can assume

$$N_u = \beta \delta N_p \quad (4)$$

i.e. the number of platelets in the marginal layer is δ (>1)-times the average platelet count. β is the number of receptors per platelet. Assembling all the above developments in eqn (2), we can express the adhesion rate in term of measurable variables:

$$\begin{aligned}
 R_{on} &= k_{on} (K_{VWF} C_{VWF} - \alpha N_b) \cdot \beta \delta N_p \\
 &= k'_{on} (K_{VWF} C_{VWF} - \alpha N_b) N_p
 \end{aligned} \quad (5)$$

Platelet count N_p and substrate concentration C_{VWF} are normally known, substrate adhesion

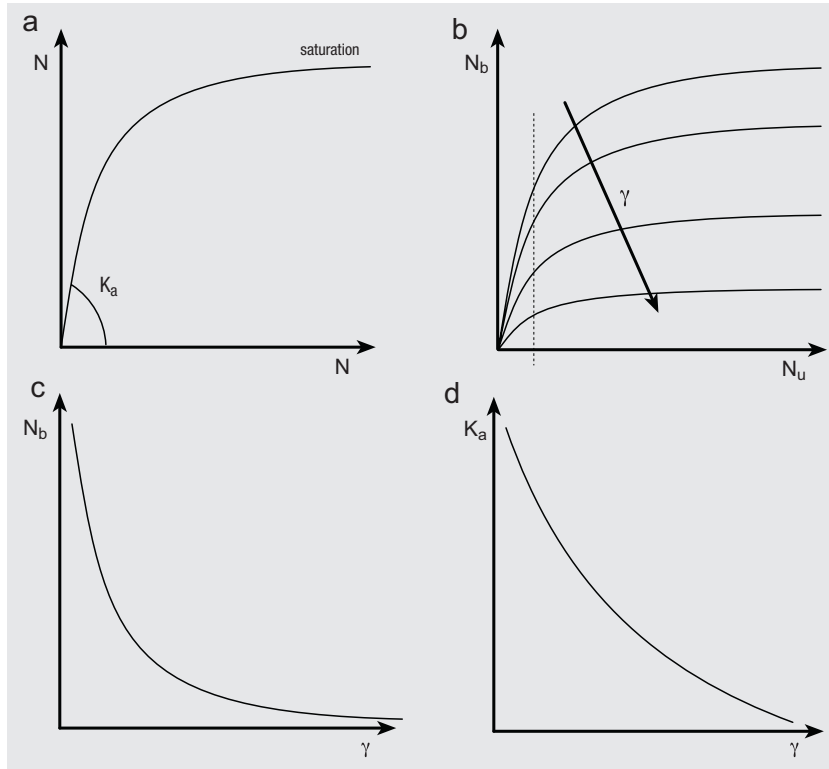


Fig. 3 | Thermodynamics of adhesion: a) bound versus unbound platelets at equilibrium; b) effect of wall shear rate on the equilibrium curves; non-saturation, constant platelet count conditions are marked by a vertical dotted line; c) effect of wall shear rate on the equilibrium surface concentration of platelets, and d) on the equilibrium constant.

constant K_{VWF} can be determined through binding assays, while α , β , and δ factors are unknown. According to eqn (5), R_{on} measurements can be used to assess α , the number of bonds truly formed on the surface, from at least two experiments with a different platelet count and/or substrate concentration, being k'_{on} the same. On the contrary, β and δ factors remains undistinguishable from k_{on} within an apparent adhesion kinetic constant, $k'_{on} = \beta \delta k_{on}$. Unless techniques are identified to independently measure the actual platelet concentration in the marginal layer (i.e., δ) and the number of receptors per platelet (i.e., β), we will not be able to estimate the intrinsic adhesion rate constant k_{on} by measurements of the adhesion rate R_{on} . Uncertainties are mostly in the determination of the platelet concentration at the surface which is heavily dependent on the fluid flow mechanics in specified vessel geometry, and the blood characteristics that can affect it, such as hematocrit and other blood composition variables that can influence its viscosity. We are not aware of any predictive model for radial platelet concentration at the present, so that estimation of pure k_{on} remains an open issue.

Adhesion thermodynamics

Thermodynamics aims at characterizing and predicting the equilibrium in a process. The adhesion-desorption of cells on a surface is said to be macroscopically in an equilibrium state when the rate of surface arrival is equal to the rate of departure from the surface:

$$R_{on} = R_{off} \quad \text{or} \quad \frac{dN_b}{dt} = 0 \quad (6)$$

Under such circumstances we can build up the expression of the equilibrium surface concentration of cells by developing the expressions of the rates:

$$R_{on} = k_{on} N_s N_u = k_{off} N_b = R_{off} \quad (7)$$

Combining eqns and we obtain the equilibrium concentration of bound cells:

$$N_b = \frac{K_a N_u N_s^o}{1 + \alpha K_a N_u} \quad K_a \equiv \frac{k_{on}}{k_{off}} \quad (8)$$

defining the adhesion equilibrium constant K_a , eqn has the typical Langmuir adsorption form, as shown in Figure 3a.

Figure 3a is similar to results observed in binding assay techniques, in static conditions, that provide the adhesion equilibrium constant (K_{VWF}) used above. Flow experiments give a unique opportunity to investigate the strength of the adhesive bond. Increasing the flow rate, and then the wall shear stress, the amount of platelets bound to the surface as a function of unbound platelet concentrations is expected to decrease, as schematically shown in Figure 3b. Experiments at different platelet count can be planned to identify

the whole equilibrium curve, but it is more practical to perform experiments always at the same approximately platelet count. The effect of the wall shear stress on the equilibrium constant can be assessed anyway. For that purpose, non-saturation conditions (see *Figure 3b*) are preferred since K_a variations can be directly measured. In such a case, the number of binding cells is expected to vary with wall shear rate, as shown in *Figure 3c* and consequently the equilibrium constant similarly, as in *Figure 3d*. Note that a lower average concentration of platelets on the surface or a smaller equilibrium constant does not imply lower on- and off-rates. On the contrary they are expected to increase, with the wall shear rate, while the equilibrium surface concentration decreases anyway. The function $K_a(\gamma)$, once experimentally measured, can be used to determine the dependence on wall shear rate of the individual kinetics constants, according to

$$K_a(\gamma) = \frac{k_{on}^0}{k_{off}^0} e^{(B_{on} - B_{off})\gamma} \quad (9)$$

where B 's are the compliance factors explaining the sensitivity of each individual constant to the shear rate. Unfortunately, the assumption of pure removal (neglect of arrival rate) is often used to determine k_{off}^0 , so that the observed exponential dependence of the kinetic constants on the applied force (*i.e.*, γ), can be misleading.

CONCLUSIONS

Our results support the definition of a mechanism that links shear-induced stimulation of GPIIb/3 to 2 sequential and distinct stages of platelet activation characterized by specific cytosolic Ca^{++} elevations. These findings provide the basis for a detailed definition of the signaling pathways initiated by the VWF-GPIIb/3 interaction under flow conditions

that may regulate platelet participation in hemostasis and thrombosis. The functional importance of these signals in relation to those generated by other thrombogenic substrates, such as collagen, remains to be established. In this regard, the nature of the vascular lesion evoking a platelet response and fluid dynamic conditions may be important in determining which pathway of platelet activation will be followed. For example, injured endothelial cells release VWF that, while bound to their surface, may initiate platelet adhesion and activation in the absence of subendothelial denudation. Clarification of this issue is one of the goals of future studies.

A method of adhesion data analysis, combining tailored image processing techniques, statistical analysis, kinetic and thermodynamics modeling has been proposed. The study is motivated by and has been applied to the initial interaction of platelets with surface-immobilized von Willebrand factor in flow experiments. Results indicate the key role of a reliable automatic image processing procedure to provide information critical in explaining how biomechanical properties of tether bonds ultimately control the process of platelet adhesion. Non-conventional information, such as deposition and removal rates could be obtained in a number of experimental conditions, supporting kinetics and thermodynamics speculations. The effort to develop an appropriate interpretation of adhesion data is a valuable contribution to help elucidating the adhesive properties of platelets that determine their participation in atherogenesis and ultimately the formation of occlusive thrombi.

By understanding the multifaceted mechanism involved in platelet interactions with vascular surfaces, new approaches can be tailored to selectively inhibit the pathways most relevant to the pathological aspects of atherothrombosis.

Submitted on invitation.

Accepted on 3 April 2007.

References

1. Savage B, Saldivar E, Ruggeri ZM. Initiation of platelet adhesion by arrest onto fibrinogen or translocation on von Willebrand factor. *Cell* 1996;84:289-97.
2. Mazzucato M, Pradella P, Cozzi MR, De Marco L, Ruggeri ZM. Sequential cytoplasmic calcium signals in a two-stage platelet activation process induced by the glycoprotein Ib α mechanoreceptor. *Blood* 2002;100:2793-800.
3. Ruggeri ZM, Dent JA, Saldivar E. Contribution of distinct adhesive interactions to platelet aggregation in flowing blood. *Blood* 1999;94:172-8.
4. Machin M, Santomaso A, Cozzi MR, Battiston M, Mazzucato M, De Marco L, Canu P. Characterization of platelet adhesion under flow using microscopic image sequence analysis. *Int J Artif Org* 2005;28:678-85.
5. Machin M, Santomaso A, Mazzucato M, Cozzi MR, Battiston M, De Marco L, Canu P. Single particle tracking across sequences of microscopical images: application to platelet adhesion under flow. *Ann Biomed Eng* 2006;34:833-46.
6. Cunningham JG, Meyer SC, Fox JEB. The cytoplasmic domain of the α -subunit of glycoprotein (GP) Ib mediates attachment of the entire GP Ib-IX complex to the cytoskeleton and regulates von Willebrand factor-induced changes in cell morphology. *J Biol Chem* 1996;271:11581-7.
7. Du X, Fox JE, Pei S. Identification of a binding sequence for the 14-3-3 protein within the cytoplasmic domain of the adhesion receptor, platelet glycoprotein Ib α . *J Biol Chem* 1996;271:7362-7.
8. Usami S, Chen HH, Zhao Y, Chien S, Skalak R. Design and construction of a linear shear stress flow chamber. *Ann Biomed Eng* 1993;21:77-83.
9. Remijn JA, Wu YP, Jeninga EH, Ijsseldijk MJW, van Willigen G, de Groot PG, Sixma JJ, Nurden AT, Nurden P. Role of ADP receptor P2Y(12) in platelet adhesion and thrombus formation in flowing blood. *Arterioscler Thromb Vasc Biol* 2002;22:686-91.
10. Niiya K, Hodson E, Bader R, Byers-Ward V, Koziol JA, Plow EF, Ruggeri ZM. Increased surface expression of the membrane

- glycoprotein IIb/IIIa complex induced by platelet activation. Relationship to the binding of fibrinogen and platelet aggregation. *Blood* 1987;70:475-83.
11. Mangin P, Yuan Y, Goncalves I, Eckly A, Freund M, Cazenave JP, Gachet S, Jackson P, Lanza F. Signaling role for phospholipase C gamma 2 in platelet glycoprotein Ib alpha calcium flux and cytoskeletal reorganization. Involvement of a pathway distinct from FcR gamma chain and Fc gamma RIIIA. *J Biol Chem* 2003;278:32880-91.
 12. Marshall SJ, Senis YA, Auger JM, Feil R, Hofmann F, Salmon G, Peterson JT, Burslem F, Watson SP. GPIIb-dependent platelet activation is dependent on Src kinases but not MAP kinase or cGMP-dependent kinase. *Blood* 2004;103:2601-9.
 13. Kasirer-Friede A, Cozzi MR, Mazzucato M, De Marco L, Ruggeri ZM, Shattil SJ. Signaling through GP Ib-IX-V activates $\alpha_{IIb}\beta_3$ independently of other receptors. *Blood* 2004;103:2003-10.
 14. Nesbitt WS, Giuliano S, Kulkarni S, Dopheide SM, Harper IS, Jackson SP. Intercellular calcium communication regulates platelet aggregation and thrombus growth. *J Cell Biol* 2003;160:1151-61.
 15. Gralnick HR, Williams SB, McKeown LP, Rick ME, Maisonneuve P, Jenneau C, Sultan Y. Von Willebrand's disease with spontaneous platelet aggregation induced by an abnormal plasma von Willebrand factor. *J Clin Invest* 1985;76:1522-9.
 16. Moake JL, Turner NA, Stathopoulos NA, Nolasco LH, Hellums JD. Involvement of large plasma von Willebrand factor (vWF) multimers and unusually large vWF forms derived from endothelial cells in shear stress-induced platelet aggregation. *J Clin Invest* 1986;78:1456-61.
 17. Kroll MH, Hellums JD, McIntire LV, Schafer AI, Moake JL. Platelets and shear stress. *Blood* 1996;88:1525-41.
 18. Goto S, Salomon DR, Ikeda Y, Ruggeri ZM. Characterization of the unique mechanism mediating the shear-dependent binding of soluble von Willebrand factor to platelets. *J Biol Chem* 1995;270:23352-61.
 19. Goto S, Ikeda Y, Saldivar E, Ruggeri ZM. Distinct mechanisms of platelet aggregation as a consequence of different shearing flow conditions. *J Clin Invest* 1998;101:479-86.
 20. Vasudevan S, Roberts JR, McClintock RA, Dent JA, Celikel R, Ware J, Varughese KI, Ruggeri ZM. Modeling and functional analysis of the interaction between von Willebrand factor A1 domain and glycoprotein Iba. *J Biol Chem* 2000;275:12763-8.
 21. Berndt MC, Ward CM, Booth WJ, Castaldi PA, Mazurov AV, Andrews RK. Identification of aspartic acid 514 through glutamic acid 542 as a glycoprotein Ib-IX complex receptor recognition sequence in von Willebrand factor. Mechanisms of modulation of von Willebrand factor by ristocetin and botrocetin. *Biochemistry* 1992;31:11144-51.
 22. Dong J-F, Berndt MC, Schade A, McIntire LV, Andrews RK, López JA. Ristocetin-dependent, but not botrocetin-dependent, binding of von Willebrand factor to the platelet glycoprotein Ib-IX-V complex correlates with shear-dependent interactions. *Blood* 2001;97:162-8.
 23. Milner EP, Zheng Q, Kermod JC. Ristocetin-mediated interaction of human von Willebrand factor with platelet glycoprotein Ib evokes a transient calcium signal: observations with Fura-PE3. *J Lab Clin Med* 1998;131:49-62.
 24. Mistry N, Cranmer SL, Yuan Y, Mangin P, Dopheide SM, Harper I, Giuliano S, Dunstan DE, Lanza F, Salem HH, Jackson SP. Cytoskeletal regulation of the platelet glycoprotein Ib/V/IX-von Willebrand factor interaction. *Blood* 2000;96:3480-9.
 25. Zhu, C. Kinetics and mechanics of cell adhesion. *J Biomech* 2000;33:23-33.
 26. Savage B, Almus-Jacobs F, Ruggeri ZM. Specific synergy of multiple substrate-receptor interactions in platelet thrombus formation under flow. *Cell* 1998;94:657-66.
 27. Doggett TA, Girdhar G, Lawshe A, Schmidtke DW, Laurenzi II, Diamond SL, Diacovo TG. Selectin-like kinetics and biomechanics promote rapid platelet adhesion in flow: the GP Iba-vWF tether bond. *Biophys J* 2002;83:194-205.
 28. Kumar RA, Dong J, Thaggard JA, Cruz MA, Lopez JA, McIntire LV. Kinetics of GPIIb-vWF-A1 tether bond under flow: effect of GPIIb mutations on the association and dissociation rates. *Biophys J* 2003;85:4099-109.
 29. Pierres A, Benoliel A M, Bongrand P. Use of a laminar flow chamber to study the rate of bond formation and dissociation between surface-bound adhesion molecules: effect of applied force and distance between surfaces. *Faraday Discuss* 1998;111:321-30.
 30. Bell GI. Models for the specific adhesion of cells to cells. *Science* 1978;200:618-27.
 31. Aarts PAMM, van den Broek SAT, Prins GW, Kuiken GDC, Sixma JJ, Heethaar RM. Blood platelets are concentrated near the wall and red blood cells, in the center of flowing blood. *Arterioscler* 1988;8:819-24.

Acute myocardial infarction in young adults: evaluation of the haemorheological pattern at the initial stage, after 3 and 12 months

Gregorio Caimi, Amelia Valenti and Rosalia Lo Presti

Dipartimento di Medicina Interna, Malattie Cardiovascolari e Nefrourologiche, Università degli Studi, Palermo, Italy

Summary. Acute myocardial infarction (AMI) in young adults is considered by some authors as an autonomous disease, characterized by peculiar risk factor pattern, clinical course and prognosis. We studied, in a group of 96 patients aged < 46 years with recent AMI, the haemorheological parameters (whole-blood, plasma and serum viscosity, haematocrit, whole-blood filterability and erythrocyte deformability), and the influence of risk factors and coronary lesion extent on them. We re-examined 41 of the AMI patients after 3 and 12 months. At the initial stage, AMI subjects showed a hyperviscosity syndrome, not influenced by the number of risk factors and only slightly more evident in patients with more extensive coronary damage. In the AMI patients re-examined after 3 and 12 months, no significant variation in the haemorheological pattern emerged in comparison with basal values. The persisting alteration demonstrated that the hyperviscosity syndrome observed at the initial stage was not simply an acute reaction to AMI, and that it was not influenced by intervention on modifiable risk factors.

Key words: juvenile acute myocardial infarction, blood rheology, erythrocyte deformability.

Riassunto (*Infarto miocardico giovanile: valutazione emoreologica in fase iniziale, dopo 3 e 12 mesi*). L'infarto miocardico acuto (IMA) che insorge in età relativamente precoce è talvolta considerato un'entità nosologica autonoma, poiché presenta peculiarità nella prevalenza dei fattori di rischio, nel decorso clinico e nella prognosi. In 96 pazienti di età inferiore a 46 anni e con recente IMA, abbiamo valutato l'assetto emoreologico (viscosità ematica, plasmatica e sierica, ematocrito, filtrabilità ematica e deformabilità eritrocitaria) e la possibile influenza esercitata su di esso dal numero dei principali fattori di rischio e dall'estensione del danno coronarico. La valutazione è stata ripetuta in 41 pazienti anche dopo 3 e 12 mesi. In fase iniziale era presente una sindrome da iperviscosità, non influenzata dal numero dei fattori di rischio e solo lievemente più marcata, limitatamente ad alcuni parametri, nei pazienti con lesioni coronariche più estese. Nei pazienti riesaminati a distanza di tempo non abbiamo osservato modificazioni significative dei parametri emoreologici nei confronti dei valori basali. La persistenza nel tempo delle anomalie reologiche indica che esse non sono semplicemente una conseguenza dell'evento ischemico acuto, e che non sono influenzabili dall'intervento terapeutico sui fattori di rischio modificabili.

Parole chiave: infarto miocardico acuto giovanile, emoreologia, deformabilità eritrocitaria.

INTRODUCTION

Acute myocardial infarction (AMI) has a low incidence in young adults. The percentage of patients under 40 is between 2 and 8% of all AMI subjects [1, 2] and it increases to 10% for people under 46 [3]. Until now it is not certain if AMI in young adults may be considered as an early expression of coronary artery disease (CAD) or an autonomous disease.

AMI in young adults is typical as regards risk factors, clinical, angiographic and prognostic characteristics. In young people the risk factor pattern is different from older people. Cigarette smoking is the most common factor [4], followed by family history for

CAD [5]. The latter observation has induced many authors to investigate genic polymorphisms as risk or protective factors for CAD [6].

AMI in young women has been associated with the use of oral contraceptives [7, 8]. Some studies demonstrate a link between AMI in young adults and cocaine abuse, for its harmful acute and chronic action on myocardial perfusion, oxygen demand and its direct toxicity on myocardium [9]. Congenital coronary artery abnormalities without atherosclerotic lesions are not sporadic in young people [10, 11].

AMI in young adults is also typical as regards the clinical picture. Young patients reach hospital

earlier than other patients [2], helping efficacy of revascularization and complication treatment. Only a small percentage of young patients with AMI, unlike the older ones, had a previous myocardial infarction and this is relevant for both prognosis and progression to heart failure. As regards electrocardiographic and echocardiographic onset, data are conflicting. In young people with AMI often there is not CAD or just one coronary vessel is affected by significant narrowing; three-vessel disease is infrequent. Consequently, the reperfusion with percutaneous intervention is more frequent than coronary artery bypass graft and this has a favourable influence on prognosis. In young people AMI has a lower incidence of complications such as early and late heart failure, angina, re-infarct and atrio-ventricular block. Death during hospitalization and after six months are both significantly reduced [2].

Our aim was the examination of the main haemorheological determinants in young adults with AMI and in particular the influence of cardiovascular risk factors and the extent of CAD on the haemorheological profile. The same subjects were re-examined after 3 and 12 months. This study is part of the scientific project identified as the "Sicilian study on juvenile myocardial infarction".

Subjects

We studied 96 subjects (89 men and 7 women) aged < 46 years, with recent AMI. The mean age was 39.0 ± 6.0 years (range 19-45). The time interval between AMI onset and first examination was 13 ± 7 days. Regarding risk factors (RF), 47% had family history of CAD, 78% were cigarette smokers or ex-smokers; hypercholesterolemia was present in 36%, diabetes mellitus in 11% and essential hypertension in 18%. Cocaine use was admitted in 5%. Four of the 7 women were taking oral contraceptives.

Regarding electrocardiographic localization, AMI was inferior in 41.8%, anterior and lateral in 53.1%. Coronary angiography was performed in 76 patients and showed no lesions considered significant in 19 subjects, one-vessel disease in 32, two- or three-vessel disease in 25.

We subdivided AMI subjects according to the number of RF, taking into account the following: family history, cigarette smoking, hypercholesterolemia, diabetes mellitus and essential hypertension. Thirty-seven patients had < 2 RF, 32 had 2 RF and 27 patients had > 2 RF.

Forty-one AMI subjects (39 men and 2 women) were re-examined 3 months and 12 months after the first evaluation. Their mean age was 41.0 ± 4.0 years and their baseline rheological pattern was not significantly different from that observed in the whole AMI group.

The control group included 62 subjects (52 men and 10 women, mean age 38.3 ± 9.7 years, 36 smokers, 12 ex-smokers). In this group 39% had family history of CAD, 58% were cigarette smokers and 19% ex-smokers; hypercholesterolemia was present in 26%, diabe-

tes mellitus in 12% and essential hypertension in 15%. No subjects in this group had history or clinical signs of atherosclerotic disease in any vascular area.

Methods

On fasting venous blood we evaluated the following major haemorheological determinants:

- whole-blood viscosity at high (450, 225 and 90 s^{-1}) shear rates, using the cone-on-plate viscosimeter Wells-Brookfield $\frac{1}{2}$ LVT and at low (2.37 and 0.51 s^{-1}) shear rates using a Contraves LS30; blood viscosity was evaluated at native hematocrit;
- plasma and serum viscosity at the shear rate of 450 s^{-1} (viscosimeter Wells-Brookfield $\frac{1}{2}$ LVT);
- haematocrit (Ht), obtained by using a micromethod technique;
- whole-blood filterability (VBC - mL/min), obtained by filtering whole blood through $5 \mu\text{m}$ polycarbonate sieves, under negative pressure of 20 cm of water and at a temperature of 37°C , according to the Reid method [12];
- erythrocyte deformability using the diffractometer Rheodyn SSD of Myrenne [13, 14]. This instrument measures the diffraction pattern of a laser beam passing through erythrocytes suspended in a viscous medium and deformed by a force with defined shear stresses. A measure of erythrocyte deformation is the elongation index (EI) = $(L-W)/(L+W) \times 100$, where L = length and W = width of the erythrocytes. We considered EI at the shear stresses of 30 and 60 Pascal.

Statistical analysis

All the data were expressed as means \pm SD; the statistical differences between control subjects and the whole group of young adults with AMI, or subgroups

Table 1 | Means \pm SD of the haemorheological determinants in 62 control subjects and in 96 AMI subjects at the baseline evaluation (T1)

	Control Subjects	AMI T1
BV 450 s^{-1} (mPa · s)	3.62 ± 0.44	$4.34 \pm 0.46^*$
BV 225 s^{-1} (mPa · s)	3.90 ± 0.47	$4.72 \pm 0.59^*$
BV 90 s^{-1} (mPa · s)	4.66 ± 0.63	$5.48 \pm 0.69^*$
BV 2.37 s^{-1} (mPa · s)	10.36 ± 4.60	$15.55 \pm 4.09^*$
BV 0.51 s^{-1} (mPa · s)	23.66 ± 10.50	$31.30 \pm 8.10^*$
PV 450 s^{-1} (mPa · s)	1.29 ± 0.13	$1.52 \pm 0.11^*$
SV 450 s^{-1} (mPa · s)	1.17 ± 0.11	$1.36 \pm 0.10^*$
Ht (%)	44.48 ± 3.20	44.59 ± 3.69
VBC (mL/min)	0.42 ± 0.07	$0.32 \pm 0.06^*$
EI 30 Pa	47.97 ± 3.67	$45.21 \pm 4.09^*$
EI 60 Pa	50.61 ± 3.23	$48.00 \pm 4.25^*$

* = $p < 0.001$ vs control subjects

AMI = acute myocardial infarction; BV = blood viscosity; PV = plasma viscosity; SV = serum viscosity; Ht = haematocrit; VBC = volume of blood cells (whole-blood filtration); EI = elongation index; Pa = Pascal.

Table 2 | Means ± SD of the haemorheological determinants in control subjects and AMI subjects subdivided according to the number of RF

	Control subjects	AMI subjects with 0-1 RF	AMI subjects with 2 RF	AMI subjects with >2 RF
BV 450 s ⁻¹ (mPa · s)	3.62 ± 0.44	4.34 ± 0.53 ^(c)	4.38 ± 0.42 ^(c)	4.31 ± 0.40 ^(c)
BV 225 s ⁻¹ (mPa · s)	3.90 ± 0.47	4.63 ± 0.56 ^(c)	4.76 ± 0.56 ^(c)	4.78 ± 0.65 ^(c)
BV 90 s ⁻¹ (mPa · s)	4.66 ± 0.63	5.38 ± 0.67 ^(c)	5.50 ± 0.70 ^(c)	5.57 ± 0.72 ^(c)
BV 2.37 s ⁻¹ (mPa · s)	10.36 ± 4.60	15.39 ± 4.01 ^(c)	15.06 ± 3.08 ^(c)	16.66 ± 5.26 ^(c)
BV 0.51 s ⁻¹ (mPa · s)	23.66 ± 10.50	30.37 ± 7.21 ^(b)	30.46 ± 6.97 ^(b)	33.73 ± 10.34 ^(c)
PV 450 s ⁻¹ (mPa · s)	1.29 ± 0.13	1.50 ± 0.12 ^(c)	1.51 ± 0.08 ^(c)	1.55 ± 0.13 ^(c)
SV 450 s ⁻¹ (mPa · s)	1.17 ± 0.11	1.34 ± 0.10 ^(c)	1.37 ± 0.09 ^(c)	1.38 ± 0.10 ^(c)
Ht (%)	44.48 ± 3.20	44.53 ± 3.84	44.88 ± 3.89	44.36 ± 3.30
VBC (mL/min)	0.42 ± 0.07	0.31 ± 0.08 ^(c)	0.31 ± 0.05 ^(c)	0.33 ± 0.06 ^(c)
EI 30 Pa	47.97 ± 3.67	44.97 ± 4.34 ^(b)	44.75 ± 4.03 ^(c)	45.96 ± 3.81 ^(a)
EI 60 Pa	50.61 ± 3.23	47.68 ± 4.48 ^(b)	47.54 ± 3.88 ^(c)	48.94 ± 4.37

^(a) *p* < 0.05 ^(b) *p* < 0.01 ^(c) *p* < 0.001 vs control subjects

AMI = acute myocardial infarction; RF = risk factors; BV = blood viscosity; PV = plasma viscosity; SV = serum viscosity; Ht = haematocrit; VBC = volume of blood cells (whole-blood filtration); EI = elongation index; Pa = Pascal.

of them, were evaluated using the Student’s t-test for unpaired data. The differences between AMI subjects at the different times of observation were evaluated using the Student’s t-test for paired data.

RESULTS

When we compared the whole group of young adults with AMI to control subjects, there was a significant increase in whole-blood viscosity at high and low shear rates, a significant increase in plasma and serum viscosity and a significant decrease in whole-

blood filtration and in erythrocyte deformability; no variation was evident in haematocrit (Table 1).

Subdividing the AMI subjects according to the number of principal cardiovascular risk factors (Table 2), it was apparent that in each AMI subgroup whole blood, plasma and serum viscosity, whole-blood filtration and erythrocyte deformability were significantly different in comparison with control subjects and there were no significant differences between AMI subgroups.

Subdividing the AMI group in accordance with the extent of CAD (Table 3) we observed a similar

Table 3 | Means ± SD of the haemorheological determinants in control subjects and AMI subjects subdivided according to the number of stenosed coronary vessels

	Control subjects	AMI without coronary stenosis	AMI with 1 vessel disease	AMI with 2-3 vessel disease
BV 450 s ⁻¹ (mPa · s)	3.62 ± 0.44	4.25 ± 0.58 ^(c)	4.31 ± 0.43 ^(c)	4.41 ± 0.41 ^(c)
BV 225 s ⁻¹ (mPa · s)	3.90 ± 0.47	4.53 ± 0.58 ^(c)	4.64 ± 0.47 ^(c)	4.96 ± 0.75 ^(c,d)
BV 90 s ⁻¹ (mPa · s)	4.66 ± 0.63	5.28 ± 0.67 ^(c)	5.39 ± 0.60 ^(c)	5.70 ± 0.87 ^(c)
BV 2.37 s ⁻¹ (mPa · s)	10.36 ± 4.60	15.52 ± 4.90 ^(c)	14.58 ± 2.71 ^(c)	16.68 ± 5.37 ^(c)
BV 0.51 s ⁻¹ (mPa · s)	23.66 ± 10.50	31.36 ± 8.67 ^(a)	28.99 ± 6.67 ^(a)	34.30 ± 10.34 ^(c,e)
PV 450 s ⁻¹ (mPa · s)	1.29 ± 0.13	1.51 ± 0.10 ^(c)	1.52 ± 0.11 ^(c)	1.54 ± 0.13 ^(c)
SV 450 s ⁻¹ (mPa · s)	1.17 ± 0.11	1.36 ± 0.10 ^(c)	1.35 ± 0.09 ^(c)	1.40 ± 0.11 ^(c)
Ht (%)	44.48 ± 3.20	44.11 ± 3.62	44.72 ± 3.30	45.60 ± 4.20
VBC (mL/min)	0.42 ± 0.07	0.32 ± 0.05 ^(c)	0.33 ± 0.06 ^(c)	0.32 ± 0.06 ^(c)
EI 30 Pa	47.97 ± 3.67	45.90 ± 4.23	44.83 ± 3.98 ^(c)	45.45 ± 3.85 ^(a)
EI 60 Pa	50.61 ± 3.23	48.53 ± 4.24	47.93 ± 4.42 ^(b)	47.95 ± 3.93 ^(b)

^(a) *p* < 0.05 ^(b) *p* < 0.01 ^(c) *p* < 0.001 vs control subjects

^(d) *p* < 0.05 vs AMI without coronary stenosis ^(e) *p* < 0.05 vs AMI with 1 vessel disease

AMI = acute myocardial infarction; BV = blood viscosity; PV = plasma viscosity; SV = serum viscosity; Ht = haematocrit; VBC = volume of blood cells (whole-blood filtration); EI = elongation index; Pa = Pascal.

Table 4 | Means \pm SD of the haemorheological determinants in 41 AMI subjects at baseline (T1), after 3 months (T2) and after 12 months (T3)

	AMI T1	AMI T2	AMI T3
BV 450 s ⁻¹ (mPa · s)	4.31 \pm 0.48	4.27 \pm 0.41	4.31 \pm 0.35
BV 225 s ⁻¹ (mPa · s)	4.69 \pm 0.59	4.66 \pm 0.54	4.80 \pm 0.75
BV 90 s ⁻¹ (mPa · s)	5.49 \pm 0.70	5.51 \pm 0.70	5.60 \pm 0.78
BV 2.37 s ⁻¹ (mPa · s)	15.85 \pm 4.95	14.88 \pm 2.70	15.50 \pm 3.64
BV 0.51 s ⁻¹ (mPa · s)	31.52 \pm 9.47	30.69 \pm 6.30	31.44 \pm 7.77
PV 450 s ⁻¹ (mPa · s)	15.85 \pm 4.95	14.88 \pm 2.70	15.50 \pm 3.64
SV 450 s ⁻¹ (mPa · s)	31.52 \pm 9.47	30.69 \pm 6.30	31.44 \pm 7.77
Ht (%)	44.85 \pm 3.50	44.79 \pm 3.43	45.98 \pm 3.53
VBC (mL/min)	0.31 \pm 0.06	0.29 \pm 0.10	0.33 \pm 0.10
EI 30 Pa	45.06 \pm 3.92	45.11 \pm 4.80	43.94 \pm 4.69
EI 60 Pa	48.07 \pm 4.38	47.90 \pm 4.53	47.25 \pm 4.69

AMI = acute myocardial infarction; BV = blood viscosity; PV = plasma viscosity; SV = serum viscosity; Ht = haematocrit; VBC = volume of blood cells (whole-blood filtration); EI = elongation index; Pa = Pascal.

behaviour pattern, with the exception of whole-blood viscosity at the shear rate of 225 s⁻¹, which was higher in AMI subjects with 2-3 vessel disease in comparison with those without coronary stenosis, and whole-blood viscosity at the shear rate of 0.51, which was higher in AMI subjects with 2-3 vessel disease in comparison with those with 1 vessel disease.

When we examined the AMI patients 3 and 12 months after AMI (Table 4), we found that at both times all the rheological parameters showed average values not statistically different from those observed during the first evaluation. Comparing AMI patients at T3 with control subjects (Table 5), the results were similar to those observed at T1.

Table 5 | Means \pm SD of the haemorheological determinants in control subjects and in 41 AMI subjects after 12 months (T3)

	Control subjects	AMI T3
BV 450 s ⁻¹ (mPa · s)	3.62 \pm 0.44	4.31 \pm 0.35 ^(a)
BV 225 s ⁻¹ (mPa · s)	3.90 \pm 0.47	4.80 \pm 0.75 ^(a)
BV 90 s ⁻¹ (mPa · s)	4.66 \pm 0.63	5.60 \pm 0.78 ^(a)
BV 2.37 s ⁻¹ (mPa · s)	10.36 \pm 4.60	15.50 \pm 3.64 ^(a)
BV 0.51 s ⁻¹ (mPa · s)	23.66 \pm 10.50	31.44 \pm 7.77 ^(a)
PV 450 s ⁻¹ (mPa · s)	1.29 \pm 0.13	1.48 \pm 0.10 ^(a)
SV 450 s ⁻¹ (mPa · s)	1.17 \pm 0.11	1.35 \pm 0.10 ^(a)
Ht (%)	44.48 \pm 3.20	45.98 \pm 3.53
VBC (mL/min)	0.42 \pm 0.07	0.33 \pm 0.10 ^(a)
EI 30 Pa	47.97 \pm 3.67	43.94 \pm 4.69 ^(a)
EI 60 Pa	50.61 \pm 3.23	47.25 \pm 4.69 ^(a)

(a) = $p < 0.001$ vs control subjects

AMI = acute myocardial infarction; BV = blood viscosity; PV = plasma viscosity; SV = serum viscosity; Ht = haematocrit; VBC = volume of blood cells (whole-blood filtration); EI = elongation index; Pa = Pascal.

DISCUSSION

Our data show that a hyperviscosity syndrome is present after AMI, as widely demonstrated in patients not selected for age. The rheological impairment was not related to the number of cardiovascular risk factors and only slightly influenced by the extent of coronary lesions. The persistence of the alteration was observed after three and twelve months.

We cannot exclude that the haemorheological abnormality found in our patients was related to the cardiovascular risk factors, whose effect on blood viscosity is well known, but the control group had a similar incidence of cardiovascular risk factors and there were no significant differences in haemorheological determinants between the two AMI subgroups with respectively 0-1 and > 2 risk factors. Moreover, although some risk factors were modified after AMI (many patients stopped smoking; dyslipidaemia, hyperglycaemia and arterial hypertension were more carefully controlled) the haemorheological pattern did not change significantly.

The hyperviscosity syndrome following AMI has been usually considered as part of an "acute phase reaction", and then its almost complete regression was expected within a few days or weeks. Such behaviour, in patients not selected for age, was in fact observed by some authors [15-17], but is different from that observed in other studies [18, 19].

The trend of haemorheological parameters 3 and 12 months after AMI seems to overlap the trend observed by us, in the same clinical condition, regarding the granulocyte count [20], their functional aspects [21] and the plasma elastase [20]. It is not possible to exclude that all these aspects may be related to the high prevalence of inflammatory gene polymorphism demonstrated in these young subjects with AMI [22-26].

Submitted on invitation.

Accepted on 3 April 2007.

References

- Fullhaas JU, Rickenbacher P, Pfisterer M, Ritz R. Long-term prognosis of young patients after myocardial infarction in the thrombolytic era. *Clin Cardiol* 1997;20:993-8.
- Imazio M, Bobbio M, Bergerone S, Barlera S, Maggioni AP. Clinical and epidemiological characteristics of juvenile myocardial infarction in Italy: the GISSI experience. *G Ital Cardiol* 1998;28:505-12.
- Doughty M, Mehta R, Bruckman D, Das S, Karavite D, Tsai T, Eagle K. Acute myocardial infarction in the young-The University of Michigan experience. *Am Heart J* 2002;143:56-62.
- Choudhury L, Marsh JD. Myocardial infarction in young patients. *Am J Med* 1999;107:254-61.
- Friedlander Y, Arbogast P, Schwartz SM, Marcovina SM, Austin MA, Rosendaal FR, Reiner AR, Psaty BM, Siscovick DS. Family history as a risk factor for early onset myocardial infarction in young women. *Atherosclerosis* 2001;156:201-7.
- Incalcaterra E, Hoffmann E, Averna MR, Caimi G. Genetic risk factors in myocardial infarction at young age. *Min Cardioangi* 2004;52:287-312.
- Dunn NR, Arscott A, Throgood M. The relationship between use of oral contraceptive and myocardial infarction in young women with fatal outcomes, compared to those who survive: results from the MICA case-control study. *Contraception* 2001;63:65-9.
- WHO Collaborative Study of Cardiovascular Disease and Steroid Hormone Contraception. Acute myocardial infarction and combined oral contraceptives: results of an international multicentre case-control study. *Lancet* 1997;349:1202-9.
- Kloner RA, Hale S, Alker K, Rezkalla S. The effects of acute and chronic cocaine use on the hearth. *Circulation* 1992;85:407-19.
- Corrado D, Thiene G, Cocco P, Frescura C. Non-atherosclerotic coronary artery disease and sudden death in the young. *Br Heart J* 1992;68:601-7.
- Warren SE, Thompson SI, Vieweg WV. Historic and angiographic features of young adults surviving myocardial infarction. *Chest* 1979;75:667-70.
- Reid HL, Barnes AJ, Lock PJ, Dormandy TL. A simple method for measuring erythrocyte deformability. *J Clin Pathol* 1976;29:855-60.
- Schmid-Schönbein H, Ruef P, Linderkamp O. The shear stress diffractometer Rheodyn SSD for determination of erythrocyte deformability. I. Principles of operation and reproducibility. *Clin Hemorheol* 1996;16:745-48.
- Ruef P, Pöschl JMB, Linderkamp O, Schmid-Schönbein H. The shear stress diffractometer Rheodyn SSD for determination of erythrocyte deformability. II. Sensitivity to detect abnormal erythrocyte deformability. *Clin Hemorheol* 1996;16:749-52.
- Jan KM, Chien S, Bigger JT. Observations on blood viscosity changes after acute myocardial infarction. *Circulation* 1975;51:1079-84.
- Caimi G, Raineri A, Sarno A. Blood rheology in acute myocardial infarction. *Acta Cardiologica* 1982;37:401-9.
- Turczynski B, Slowinska L, Szczesny S, Baschton M, Bartosik-Baschton A, Sezygula J, Wodniecki J, Spyra J. The whole blood and plasma viscosity changes in course of acute myocardial infarction. *Pol Arch Med Wewn* 2002;108:971-8.
- Ernst E, Krauth U, Resch KL, Paulsen HF. Does blood rheology revert to normal after myocardial infarction? *Br Heart J* 1990;64:248-50.
- Toth K, Mezey B, Juricskay I, Simor T, Javor T. Hemorheologic parameters during the 6 months following myocardial infarct. *Orvosi Hetilap* 1990;131:727-30.
- Lo Presti R, Montana M, Hoffmann E, D'Amico T, Amodeo G, Caimi G. Elastase in young subjects with acute myocardial infarction: evaluation at the initial stage and after 12 months. *Clin Hemorheol Microcirc* 2006;35:375-7.
- Lo Presti R, Tozzi Ciancarelli MG, Hoffmann E, Incalcaterra E, Canino B, Montana M, D'Amico T, Catania A, Caimi G. Persistence of the altered polymorphonuclear leukocyte rheological and metabolic variables after 12 months in juvenile myocardial infarction. *Clin Hemorheol Microcirc* 2006;35:227-30.
- Candore G, Balistreri CR, Lio D, Mantovani V, Colonna-Romano G, Chiappelli M, Tampieri C, Licastro F, Branzi A, Averna M, Caruso M, Hoffmann E, Caruso C. Association between HFE mutations and acute myocardial infarction: a study in patients from Northern and Southern Italy. *Blood Cells Mol Dis* 2003;31:57-62.
- Listi F, Candore G, Lio D, Cavallone L, Colonna Romano G, Caruso M, Hoffmann E, Caruso C. Association between platelet endothelial cellular adhesion molecule 1 (PECAM-1/CD31) polymorphisms and acute myocardial infarction: a study in patients from Sicily. *Eur J Immunogenet* 2004;31:175-8.
- Lio D, Candore G, Crivello A, scola L, Colonna-Romano G, Cavallone L, Hoffmann E, Caruso M, Licastro F, Caldarera CM, Branzi A, Franceschi C, Caruso C. Opposite effects of interleukin 10 common gene polymorphisms in cardiovascular diseases and in successful ageing: genetic background of male centenarians is protective against coronary heart disease. *J Med Genet* 2004;41:790-4.
- Listi F, Candore G, Lio D, Russo M, Colonna-Romano G, Caruso M, Hoffmann E, Caruso C. Association between C1019T polymorphism of connexin37 and acute myocardial infarction: a study in patients from Sicily. *Int J Cardiol* 2005;102:269-71.
- Grimaldi MP, Candore G, Vasto S, Caruso M, Caimi G, Hoffmann E, Colonna-Romano G, Lio D, Shinar Y, Franceschi C, Caruso C. Role of the pyrin M694V (A2080G) allele in acute myocardial infarction and longevity: a study in the Sicilian population. *J Leuk Biol* 2006;79:611-5.

Clinical haemorheology and microcirculation

Lucia Mannini, Emanuele Cecchi, Cinzia Fatini, Rossella Marcucci, Agatina Alessandriello Liotta, Marco Matucci-Cerinic, Rosanna Abbate and Gian Franco Gensini

Dipartimento di Area Critica Medico-Chirurgica, Centro Trombosi, Azienda Ospedaliero-Universitaria Careggi, Florence, Italy

Summary. Hyperviscosity, due to alterations of blood cells and plasma components, can induce microvascular damage. Nitric oxide (NO) is released by endothelium and plays a crucial role in flow-mediated vasodilation. An impaired availability of NO, due to polymorphisms of endothelial NO synthase (eNOS), may influence erythrocyte deformability thus increasing blood viscosity. We investigated haemorheological variables in patients with idiopathic sudden sensorineural hearing loss (ISSHL), retinal vein occlusion (RVO) and systemic sclerosis (SSc), as possible models of microvascular damage, and their relationship with eNOS gene T-786C, G894T and 4a/4b polymorphisms. Whole blood viscosity and plasma viscosity were assessed with a rotational viscosimeter and erythrocyte deformability index (DI) with Myrenne filtrometer. eNOS polymorphisms were analyzed in ISSHL and SSc patients. At multivariate analysis alterations of some haemorheological variables resulted significantly associated with ISSHL, RVO and SSc. A significantly higher prevalence of eNOS -786C and 894T was found in both ISSHL and SSc patients than in controls; at multivariate analysis these two polymorphisms significantly affected DI in both groups of patients. These results suggest that hyperviscosity, either determined by genetic susceptibility or not, can be involved in the pathophysiology of these clinical disorders and can be the target of new therapeutic strategies.

Key words: hyperviscosity, erythrocyte deformability, eNOS polymorphisms, idiopathic sudden sensorineural hearing loss, retinal vein occlusion, systemic sclerosis.

Riassunto (*Emoreologia clinica e microcircolo*). L'iperviscosità, dovuta ad alterazioni delle componenti cellulari e plasmatiche del sangue, può indurre un danno microvascolare. L'ossido nitrico (ON) è rilasciato dall'endotelio e svolge un ruolo cruciale nella vasodilatazione flusso-dipendente. Una ridotta disponibilità di ON, dovuta ai polimorfismi della nitrossido sintetasi endoteliale (NOSe), può alterare la deformabilità eritrocitaria incrementando la viscosità ematica. Abbiamo valutato le variabili emoreologiche in pazienti con sordità improvvisa (SI), occlusione venosa centrale della retina (OVCR) e sclerosi sistemica (ScS), come possibili modelli di patologia del microcircolo, e la loro relazione con i polimorfismi della NOSe T-786C, G894T e 4a/4b. Le viscosità del sangue totale e plasmatica sono state misurate con un viscosimetro rotazionale e l'indice di deformabilità eritrocitaria (ID) con il filtometro di Myrenne. I polimorfismi della NOSe sono stati analizzati nei pazienti con SI e ScS. All'analisi multivariata le alterazioni di alcune variabili emoreologiche sono risultate significativamente associate con la SI, l'OVCR e la ScS. Una prevalenza significativamente più alta degli alleli della NOSe -786C e 894T è stata osservata nei pazienti con SI e ScS rispetto al gruppo di controllo; all'analisi multivariata questi due polimorfismi sono risultati significativamente associati con un'alterazione dell'ID in entrambi i gruppi di pazienti. Questi risultati suggeriscono che l'iperviscosità, che sia o meno determinata da una suscettibilità genetica, può essere implicata nella fisiopatologia di queste malattie e può essere l'obiettivo di nuove strategie terapeutiche.

Parole chiave: iperviscosità, deformabilità eritrocitaria, polimorfismi dell'eNOS, sordità improvvisa, occlusione venosa retinica, sclerosi sistemica.

INTRODUCTION

Blood viscosity and erythrocyte deformability play a key role in maintaining and regulating microcirculation. Haemorheological variations due to alterations of blood cells and plasma components lead to hyperviscosity, which may slow

blood flow and facilitate occlusive events through erythrocyte rouleaux formation and platelet aggregation. Erythrocytes have unique flow-affecting properties namely aggregability, deformability and adherence to endothelial cells, which play a major role in blood flow. Low blood viscosity leads to an

improvement in microcirculatory flow, which enables the interactions between rheologic factors and the surrounding tissue [1]. Erythrocyte aggregation causes rheologic obstruction of the microcirculation, while damaged microcirculatory vessels in turn have a rheologic, functional and structural impact on erythrocytes. The alteration of erythrocyte membrane properties might be due to an oxidative injury, which occurs in microcirculatory disorders, mainly through lipid peroxidation.

Nitric oxide (NO) is released by the endothelium in response to shear stress and plays a crucial role in flow-mediated vasodilation [2, 3]; pharmacologic inhibition or a genetic deficiency of endothelial NO synthase (eNOS) impairs endothelium-dependent vasodilation and increases vascular resistance [4, 5]. NO, which is synthesized from L-arginine by at least 3 isoforms of NO synthase (NOS) (inducible, neuronal and endothelial) [6] contributes to vascular tone regulation [7] and maintains the functional and structural integrity of the vessel wall [8]. Finally *in vitro* and *in vivo* studies [9-12] suggested a role for NO in modulating erythrocyte deformability. An impaired availability of NO, due to nonsynonymous single-nucleotide polymorphisms (SNPs) in the coding region of *NOS3*, the gene for eNOS, may reduce shear stress, thus increasing blood viscosity and influencing erythrocyte deformability.

Since an impaired microvascular blood flow is at the basis of several clinical disorders, we sought to explore the role of hyperviscosity in patients with idiopathic sudden sensorineural hearing loss (ISSHL) [13], retinal vein occlusion (RVO) and systemic sclerosis (SSc) [14] as three possible models of microvascular damage. Moreover, to evaluate the role of eNOS polymorphisms in modulating haemorheological profile, the relationship between haemorheological variables and eNOS gene T-786C, G894T and 4a/4b polymorphisms was investigated in ISSHL [15] and SSc [14] patients.

STUDY POPULATIONS AND EXPERIMENTAL PROCEDURES

Idiopathic sudden sensorineural hearing loss, hyperviscosity and eNOS gene polymorphisms

Sixty-three consecutive ISSHL patients (30 males and 33 females), with a median age of 54 years (range 19-78 years), who referred to Florence Thrombosis Centre from January to July 2003 less than one week after the acute event, were enrolled. All patients underwent complete audiologic examination, complete history taking and general physical examination. The diagnosis of ISSHL was made by experienced audiologists of Audiological Clinic (University of Florence) by excluding other causes of sudden deafness such as viral, congenital, inflammatory, degenerative or traumatic. Sixty-seven healthy subjects matched for age and sex were also studied. Exclusion criteria for controls were a his-

tory of cardiovascular disease or other chronic diseases. Patients and controls were not on antithrombotic therapy at the time of the study.

A second study was performed in 80 ISSHL patients to evaluate the role of three eNOS gene polymorphisms (T-786C, G894T, 4a/4b) in affecting erythrocyte deformability.

Retinal vein occlusion and hyperviscosity

This study was performed to evaluate haemorheological variables in 180 consecutive patients affected by RVO, which was diagnosed by ophthalmoscopic fundus examination revealing disc swelling, venous dilation or tortuosity, retinal hemorrhages and cotton-wool spots and by fluorescein angiography demonstrating extensive areas of capillary closure, venous filling defects and increased venous transit time. The control population consisted in 180 healthy subjects matched for age and sex. Patients and healthy subjects with a personal history of glaucoma or cardiovascular disease were excluded from the study.

Systemic sclerosis, hyperviscosity and eNOS gene polymorphisms

Finally, we explored the role of haemorheological variables and eNOS gene polymorphisms also in 113 consecutive SSc patients who referred to the Division of Medicine I and Rheumatology of the University of Florence. Patients with symptoms overlapping with those of other connective tissue diseases were excluded from the study. Patients underwent complete clinical examinations and were also examined for nailfold capillaroscopy changes and tested for circulating autoantibodies characteristic of SSc (anti-topoisomerase I [anti-Scl-70], anticentromere and antinuclear with a nucleolar pattern); 108 of 113 patients presented with Raynaud's phenomenon. A detailed interview addressing personal and family history was performed in the context of a physical examination by expert physicians in order to identify symptom-free subjects and exclude those who were suspected of having any form of vascular disease (*i.e.* cardiovascular and cerebrovascular disease, venous thromboembolism or other chronic diseases). In order to evaluate the possible influence of calcium channel blockers (CCBs) on haemorheological parameters, we analyzed the rheologic profile in 20 SSc patients not receiving CCB therapy. One hundred-thirteen healthy subjects matched for age and sex were also studied as controls; exclusion criteria for controls were a positive history of cardiovascular disease, venous thromboembolism or other chronic diseases. All subjects in the patient and control groups were Caucasian, unrelated to each other and residing in the same area.

An extensive clinical profile was established for each SSc patient. Patients were classified as having limited cutaneous SSc (lcSSc) or diffuse cutaneous SSc (dcSSc) according to the criteria proposed by LeRoy *et al.* [16].

Skin involvement was evaluated with the modified Rodnan skin score, which was assessed by an experienced rheumatologist [17]. Nailfold videocapillaroscopy for analysis of microvascular abnormalities was performed as previously reported [14]. According to this analysis, patients were grouped as having capillaroscopy changes with an early, active or late pattern [18].

Two-dimensional echocardiogram and standard electrocardiogram were performed to assess cardiovascular involvement. Lung involvement was evaluated by forced vital capacity, diffusing capacity for carbon monoxide and high resolution computed tomography, and kidney involvement was evaluated by renal function tests (including 24-hour creatinine clearance) [19]. We determined the presence of antinuclear antibodies by indirect immunofluorescence on rat liver, anticentromere antibodies by indirect immunofluorescence on Hep-2 cells and by enzyme-linked immunosorbent assay (ELISA) for CENP antigen, anti-topoisomerase I antibodies by immunoblot analysis and rheumatoid factor by ELISA.

Exclusion criteria were as follows: age <18 years, pregnancy, stroke in the 4 months preceding the study, myocardial ischemia, heart failure, systemic arterial hypertension not pharmacologically controlled, thrombocytopenia (platelet count < 100×10^9 /liter), thrombocytosis (platelet count > 500×10^9 /liter), renal failure, chronic hepatitis, diabetes mellitus and malignancy. SSc patients treated with drugs potentially able to modify the evolution of the disease (corticosteroids, methotrexate, cyclophosphamide) were excluded, as were patients whose conditions did not allow a complete pharmacologic washout (patients with severe ulcers, severe pulmonary arterial hypertension, severe respiratory failure, congestive heart failure (NYHA class III-IV), creatinine values ≥ 1.5 mg/dL, megaeosophagus and/or malabsorption).

The presence of traditional cardiovascular risk factors was assessed on the basis of patient's interview and hospital records. Dyslipidemia was defined according to the Third Report of the National Cholesterol Education Program; hypertension in the presence of blood pressure above 130/80 mmHg and/or an antihypertensive treatment and diabetes according to American Diabetes Association criteria. Coronary artery disease was defined on the basis of a history of myocardial infarction or stable and unstable angina. Patients were considered overweight when their body mass index (BMI) was above 25 kg/m^2 . All subjects gave their informed consent for the experimental study which was approved by the Institutional Review Board.

Venous blood samples were obtained from overnight fasting subjects in a resting condition in the morning (from 8 to 10 am) by venepuncture of the antecubital vein with minimal stasis. To assess haemorheological profile 20 mL of blood were anticoagulated with EDTA. To determine PAI-1 plas-

ma levels an aliquot of 4.5 mL blood was collected into an ice-cold polypropylene tube containing 0.13 mol/L sodium citrate (0.5 mL; 1:10, V/V) and kept in melting ice. Finally, another aliquot of citrated blood was maintained at room temperature for Sonoclot analysis and measurement of fibrinogen plasma levels and factor VIII:C.

To determine homocysteine, whole venous blood was collected in tubes containing ethylenediaminetetraacetate (EDTA) 0.17 mol/L, immediately put in ice and centrifuged within 30 minutes at 4°C ($1500 \times g$ for 15 min).

Haemorheological studies were performed by assessing whole blood viscosity (WBV), plasma viscosity (PLV) and erythrocyte deformability index (DI) as already reported [13]. WBV and PLV were measured at 37°C using the Rotational Viscosimeter Low Shear 30 (Contraves, Zürich, Switzerland). WBV was analyzed at shear rates of 0.512 s^{-1} and 94.5 s^{-1} and was determined at native hematocrit. PLV test was only performed at 94.5 s^{-1} shear rate. Erythrocyte filtration was measured by a microcomputer-assisted filtrometer, model MF4 (Myrenne GmbH, Roetgen, Germany). Erythrocyte deformability was estimated by a curve indicating erythrocyte filtration through a 10 min recording in order to determine rheologic properties of erythrocytes, passing them through polycarbonate filters with $5 \mu\text{m}$ micropores (Nucleopore®, Pleasanton, CA). The initial flow rate from the microcomputer generated curves was taken for assessing DI. Blood count was performed by a Coulter counter (Coulter Corporation, Miami, Florida).

Sonoclot analysis, a global test to assess whole blood coagulation, was performed by a special device (Sonoclot Analyzer, Sienco Inc, Morrison, CO, USA) [20]. The Sonoclot device consists of an open-ended disposable plastic probe, mounted on an ultrasonic transducer, which is immersed in a cuvette containing 1.5 mg of celite, which is used as clotting activator, and $360 \mu\text{L}$ of whole blood. The viscous force of the forming clot creates impedance to the vibrating probe, which is converted to an output signal [20]. The changes in the viscoelastic properties of blood clot are recorded in the form of a graph ("Sonoclot Signature"). Sonoclot variables taken into consideration were: 1) the SonACT (the time until onset of initial fibrin formation) expressed in seconds (s); 2) the clot rate value (used to evaluate the acceleration of clotting formation) expressed as % slope/min; 3) the time to peak (the time till fibrin formation is completed) expressed in min.

Fibrinogen was assayed according to the Clauss method. Factor VIII was measured by a clotting method using factor VIII:C-deficient plasma (DADE Behring, Marburg, Germany) and an ELISA was used to determine PAI-1 antigen (ag) plasma levels (Asserachrom® PAI-1, Stago, Asnieres-sur-Seine, France) in ISSHL patients. Plasma levels of total homocysteine (free and pro-

tein bound) were determined by fluorescence polarization immunoassay (IMX Abbott Laboratories, Oslo, Norway) in RVO patients.

Polymorphisms of *NOS3* were analyzed in ISSHL and SSc patients after genomic DNA extraction from peripheral blood leukocytes using a QIAmp Blood kit (Quiagen, Hilden, Germany), as previously described [15].

Statistical analysis was performed using the STATA 7.0 program (Stata Corporation, College Station, Texas, USA) for the first study and Statistical Package for the Social Sciences software for Windows, version 11.5 (SPSS, Chicago, IL) for the others. All odds ratios (OR) are given with their 95% confidence intervals. A value of $p < 0.05$ was chosen as the cut-off level for statistical significance.

RESULTS

Idiopathic sudden sensorineural hearing loss, reduced erythrocyte deformability, hypercoagulability and eNOS gene polymorphisms

Among the variables studied, hematocrit, WBV at both 0.512 s^{-1} and 94.5 s^{-1} , PLV, DI, SonACT, clot rate, time to peak, factor VIII:C and PAI-1ag resulted significantly altered in ISSHL patients than in controls. In *Table 1* data obtained from both univariate and multivariate analysis are reported. At multivariate analysis WBV at 94.5 s^{-1} , DI, SonACT, clot rate, factor VIII:C and PAI-1ag plasma levels remained significantly and independently associated with ISSHL after adjustment for sex, age, dyslipidemia, smoking habitus, hypertension, hematocrit, fibrinogen, haemorheological and haemostatic variables. Significant correlations (Spearman's rank correlation coefficient) were found between haemostatic (clot rate, factor VIII:C and PAI-1ag) and haemorheological variables (WBV at both 0.512 s^{-1} and 94.5 s^{-1} , DI). Significant correlations were also found between clot rate values and both factor VIII:C ($r = 0.32$, $p < 0.001$) and PAI-1ag ($r = 0.23$, $p < 0.01$) plasma levels.

eNOS gene genotype distribution and allele frequency were in agreement with those predicted by Hardy-Weinberg equilibrium in patients and controls. A significant higher prevalence of eNOS -786C and 894T, but not of 4a allele was observed in patients in comparison to controls.

When we assumed a dominant model of inheritance (*i.e.* eNOS -786CC+TC *vs* -786TT) a significant association between the eNOS gene -786C and 894T rare variants and the disease was found. The multivariate analysis, adjusted for gender, age and traditional cardiovascular risk factors (hypertension, dyslipidemia and smoking habit) revealed that eNOS 894T rare variant was an independent predisposing factor to ISSHL. When the eNOS -786C and 894T rare variants were present (-786CC+TC and 894TT+GT combined genotype),

the OR for the predisposition to the disease was 2.99 (95%CI 1.43-6.20; $p = 0.003$) and in subjects carrying all three eNOS rare alleles (-786CC+TC and 894TT+GT and 4a4a+4a4b combined genotype), the OR was 3.6 (95%CI 1.83-7.18; $p = 0.0002$).

We observed a higher percentage of altered erythrocyte deformability in subjects carrying the eNOS rare variants in comparison to those carrying the wild-type allele: DI was altered in 73.2%, 70% and 74% of patients carrying the eNOS -786C, 894T and 4a rare variants, respectively, and in 41.7%, 53.3% and 56.6% of patients carrying the -786T, 894G and 4b wild-type alleles. The same pattern was observed in control subjects: erythrocyte deformability was altered in 9.3%, 8.6% and 8.3% of controls carrying the eNOS -786C, 894T and 4a rare variants, respectively, and in 2.7%, 4.4% and 5.4% of controls carrying the -786T, 894G and 4b wild-type alleles. To evaluate the influence of eNOS polymorphisms on erythrocyte deformability apart from the disease we used a logistic model in which erythrocyte deformability was considered the dependent variable; from the univariate analysis, eNOS -786C and 894T rare alleles significantly affected the altered erythrocyte deformability, and the influence on this parameter was higher in subjects carrying these two variants. After adjustment for traditional cardiovascular risk factors, the eNOS rare variants remained associated with altered erythrocyte deformability, and the presence of -786C and 894T alleles significantly modified the influence on erythrocyte deformability.

Table 1 | Univariate and multivariate analysis of clinical and laboratory characteristics in ISSHL patients and controls

	Univariate analysis OR (95% CI)	Multivariate analysis ^o OR (95%CI)
Hematocrit (%)	1.18 (1.05-1.32)**	1.06 (0.86-1.32)
WBV 0.512 s^{-1} (mPa·s)	6.97 (3.12-15.55)**	1.43 (0.34-5.95)
WBV 94.5 s^{-1} (mPa·s)	17.08 (6.85-42.59)**	5.62 (1.28-24.77)*
PLV (mPa·s)	4.73 (1.75-12.76)**	3.92 (0.90-17.06)
DI	12.20 (5.32-27.97)**	5.96 (1.61-22.03)**
SonACT (s)	4.93 (1.93-12.57)**	4.79 (1.02-22.48)*
Clot rate (%/min)	7.63 (2.87-20.23)**	5.41 (1.30-22.59)*
Time to peak (min)	1.07 (0.33-3.51)	1.31 (0.18-9.70)
Fibrinogen (mg/dL)	1.66 (0.45-6.17)	0.76 (0.08-7.32)
Factor VIII:C (%)	2.95 (1.18-7.39)*	5.02 (1.02-24.69)*
PAI-1ag (ng/mL)	2.60 (1.21-5.56)*	3.74 (1.01-13.87)*

* $p < 0.05$; ** $p < 0.01$

^o Adjusting for sex, age, hypertension, dyslipidemia, smoking habitus, haemorheological and Sonocot variables, factor VIII:C, PAI-1ag, hematocrit, fibrinogen.

WBV = whole blood viscosity; PLV = plasma viscosity; DI = deformability index; SonACT = activated clotting time; PAI-1ag = plasminogen activator inhibitor 1 antigen.

Table 2 | Multivariate logistic regression analysis of clinical and laboratory characteristics in RVO patients and controls

	Model 1*		Model 2**		Model 3***	
	OR (95%CI)	p	OR (95%CI)	p	OR (95%CI)	p
Age	0.99 (0.98-1.02)	0.9	0.99 (0.97-1.02)	0.8	0.99 (0.96-1.02)	0.7
Gender (males vs females)	1.08 (0.68-1.69)	0.7	1.27 (0.78-2.07)	0.3	1.23 (0.68-2.23)	0.5
Hypertension	3.15 (1.94-5.12)	< 0.0001	3.19 (1.91-5.23)	< 0.0001	3.20 (1.74-5.88)	< 0.0001
Diabetes	2.09 (0.93-4.73)	0.07	2.29 (0.97-5.4)	0.06	2.91 (1.11-7.68)	0.03
Smoking habit	2.34 (1.35-4.07)	0.002	2.24 (1.24-4.03)	0.007	2.05 (1.02-4.12)	0.04
WBV at 94.5 s ⁻¹ shear rate, mPa·s						
1 st tertile	Reference		Reference		Reference	
2 nd tertile	1.6 (0.82-3.16)	0.2	1.68 (0.82-3.45)	0.2	1.90 (0.72-5.06)	0.2
3 rd tertile	4.29 (2.52-7.31)	< 0.0001	4.08 (2.30-7.21)	0.006	8.97 (3.72-21.63)	< 0.0001
WBV at 0.512 s ⁻¹ shear rate, mPa·s						
1 st tertile	Reference		Reference		Reference	
2 nd tertile	0.55 (0.29-1.04)	0.06	0.57 (0.29-1.09)	0.9	1.17 (0.48-2.84)	0.7
3 rd tertile	2.78 (1.15-6.72)	0.005	1.73 (1.00-3.00)	0.05	2.78 (1.15-6.72)	0.02
Deformability Index						
1 st tertile	4.99 (2.76-9.05)	< 0.0001	4.75 (2.53-8.94)	< 0.0001	4.84 (2.05-11.44)	< 0.0001
2 nd tertile	1.20 (0.61-2.36)	0.6	1.13 (0.54-2.34)	0.7	1.02 (0.37-2.79)	0.9
3 rd tertile	Reference		Reference		Reference	

* Adjusted for age, gender, hypertension, diabetes, smoking habit.
** Adjusted for age, gender, hypertension, diabetes, smoking habit and white blood cells.
*** Adjusted for age, gender, hypertension, diabetes, smoking habit, white blood cells, hematocrit, fibrinogen and homocysteine.

Retinal vein occlusion and hyperviscosity

Among the traditional cardiovascular risk factors, hypertension, smoking habit and diabetes, but not dyslipidemia, were significantly more frequent in patients than in healthy subjects. With regard to laboratory parameters, a significant difference in WBV at both 0.512 s⁻¹ and 94.5 s⁻¹, white blood cells, DI and homocysteine, but not PLV, hematocrit and fibrinogen, was observed between patients and controls. In order to investigate the possible association between RVO and haemorheological parameters the study population was divided into tertiles of WBV at 0.512 s⁻¹ and 94.5 s⁻¹ and DI and a logistic regression analysis was performed which has shown, at univariate analysis, a significant association of the highest tertiles of WBV at 0.512 s⁻¹ (OR: 2.31, 95%CI 1.42-3.77; $p < 0.0001$), WBV at 94.5 s⁻¹ (OR: 4.91, 95%CI 2.95-8.17; $p < 0.0001$), and the lowest tertile of DI (OR: 5.53, 95%CI 3.13-9.75; $p < 0.0001$) with the disease.

After adjustment for age, sex, hypertension, smoking habit and diabetes (model 1 analysis), white blood cells (model 2) as well as for hematocrit, fibrinogen and homocysteine (model 3) the highest tertiles of WBV at both shear rates and the lowest tertile of DI were found to be significantly associated with the disease (Table 2).

Systemic sclerosis, haemorheologic profile and eNOS polymorphisms

A marked alteration of all haemorheological parameters in SSc was found. Levels of fibrino-

gen and C-reactive protein (CRP), but not hematocrit, were significantly higher in SSc patients than in controls. Patients with either lcSSc (n = 75) or dcSSc (n = 38) showed altered haemorheological variables compared with controls ($p < 0.0001$). A significant difference in CRP levels was observed between the lcSSc and dcSSc groups. No relationship was found between high CRP levels and rheologic parameters ($p > 0.05$ for all variables); no correlation was detected between the haemorheologic profile and ulcers (n = 54 patients) ($p > 0.05$ for all rheologic parameters).

On videocapillaroscopy, 57 patients had an early pattern, 41 had an active pattern and 15 had a late pattern of changes. The haemorheologic profile was not different among the three groups (data not shown). In Table 3, data obtained from univariate and multivariate analyses are reported. In multivariate analysis, WBV at 94.5 s⁻¹, DI and PLV remained significant and independent risk factors for SSc after adjustment for age, sex, hypertension, hematocrit, fibrinogen, NOS3 polymorphisms and haemorheological parameters. In 20 SSc patients not receiving CCB therapy, we analyzed the rheologic profile. No difference was observed between SSc patients receiving CCB therapy and those not receiving CCB therapy ($p = 0.3$ for WBV at 0.512 s⁻¹, $p = 0.5$ for WBV at 94.5 s⁻¹, $p = 0.8$ for PLV and $p = 0.4$ for DI, by Mann-Whitney test for unpaired data).

No deviation from the expected population genotype proportions predicted by Hardy-Weinberg equilibrium was detected at *NOS3* polymorphisms site. A significant difference in genotype distribution for the *NOS3* 894G > T polymorphism, but not for the -786T > C and 4a/4b polymorphisms, was observed between SSc patients and controls; with regard to the *NOS3* allele frequency, we found a significantly higher prevalence of the *NOS3* -786C ($p = 0.04$) and 894T ($p = 0.007$) rare alleles, but not of the 4a rare allele, in patients than in controls. Fifty-nine of 113 patients (52.2%) carried the -786C/894T haplotype. At univariate analysis, by using a dominant model of inheritance, *NOS3* -786C and 894T alleles influenced the predisposition to SSc ($p = 0.02$ and $p = 0.003$, respectively). After adjustment for age, sex and hypertension, only the simultaneous presence of the -786C and 894T alleles represented a susceptibility factor for SSc ($p = 0.004$). Nevertheless, after adjustment for haemorheological parameters as well, the simultaneous presence of these 2 alleles did not remain a factor predisposing to the disease.

In order to evaluate the influence of *NOS3* polymorphisms on haemorheological parameters, we used a logistic model in which the single haemorheological parameter was considered the dependent variable apart from the disease; in the univariate analysis, the *NOS3* -786C and 894T alleles, but not the 4a allele, significantly influenced all rheologic parameters; nevertheless, after adjustment for age, sex, hypertension, hematocrit and fibrinogen, these *NOS3* rare variants significantly influenced the DI (Table 4). In subjects carrying the *NOS3* -786C and 894T alleles we observed that *NOS3* -786C/894T haplotype significantly influenced the DI, but not the other rheologic parameters, at both univariate and multivariate analyses (OR 4.26, 95%CI 2.37-7.65, $p < 0.0001$ and OR 2.65, 95%CI 1.24-5.67, $p = 0.01$, respectively).

The role of *NOS3* polymorphisms in influencing the haemorheologic profile was also tested in the control population. We observed that in subjects carrying the *NOS3* 894T allele, the percentages of altered WBV and DI were higher than those in subjects carrying the 894G wild-type allele (WBV

at 0.512 s^{-1} , 17.6 % vs 11.3 %; WBV at 94.5 s^{-1} , 17.6 % vs 6.5 %; DI, 17.6 % vs 4.8 %). Interestingly, the *NOS3* 894T allele influenced the DI, but not the other rheologic parameters, at both univariate and multivariate analyses (OR 4.21, 95%CI 1.08-16.50, $p = 0.04$ and OR 3.97, 95%CI 1.00-17.58, $p = 0.05$, respectively).

DISCUSSION

The results of these studies suggest that hyperviscosity is associated with some clinical disorders in whom a microvascular damage is invoked as possible pathophysiological mechanism. Impairment of blood fluidity may significantly affect tissue perfusion and result in functional deterioration, especially if disease processes also disturb vascular properties. In particular, in the first study, we focused our attention on both haemorheological factors and parameters of haemostatic system. The findings obtained document, in fact, a high prevalence of alterations of blood rheology associated with haemostatic changes which suggest blood clotting activation in ISSHL patients. Interestingly, at multivariate analysis WBV at high shear rates and erythrocyte filtration represent risk factor for ISSHL with OR > 5. These data suggest a role for an altered erythrocyte deformability, hypercoagulability and hypofibrinolysis in the pathophysiology of blood flow reduction in cochlear microvascular district eventually leading to sudden hearing loss. Actually, at low shear rates, erythrocytes form rouleaux and WBV is predominantly a function of erythrocyte concentration and aggregation properties, whereas at high shear rates erythrocyte act as free particles, and WBV is primarily determined not only by erythrocyte concentration but also by PLV and erythrocyte deformability [21]. In the first study DI and WBV at high shear rate but not PLV and hematocrit, resulted independently associated with ISSHL, so suggesting that reduced erythrocyte deformability may be a relevant mechanism in determining ISSHL. Among the possible causes of decreased erythrocyte deformability, which is mainly determined by the physical properties of the membrane skeleton, we have analyzed the role

Table 3 | Haemorheological profile and systemic sclerosis: univariate and multivariate analysis

Variable	Univariate analysis			Multivariate analysis*			Multivariate analysis**		
	OR	95% CI	p	OR	95% CI	p	OR	95% CI	p
WBV 0.512 s^{-1} (mPa.s)	12.4	6.4-24.1	< 0.0001	1.4	0.4-5.02	0.6	1.5	0.4-5.5	0.5
WBV 94.5 s^{-1} (mPa.s)	15.8	7.9-31.8	< 0.0001	5.4	1.4-20.5	0.01	5.4	1.4-19.9	0.01
PLV (mPa.s)	8.0	4.4-14.5	< 0.0001	2.8	1.2-6.5	0.01	2.8	1.2-6.5	0.01
Deformability index	10.6	5.2-21.4	< 0.0001	3.7	1.4-9.9	0.01	3.9	1.4-10.8	0.007
Fibrinogen	4.8	2.5-9.2	< 0.0001	2.6	1.1-6.3	0.04	2.6	1.1-6.5	0.04

*Adjusted for age, gender, hypertension, hematocrit, and fibrinogen.

**Adjusted for age, gender, hypertension, hematocrit, fibrinogen, *eNOS* -786T > C and 894G > T polymorphisms, and for haemorheological variables.

Table 4 | Haemorheological profile and eNOS polymorphisms in SSc patients: univariate and multivariate analysis

Dependent variable	Variable	Univariate analysis			Multivariate analysis*		
		OR	95% CI	p	OR	95% CI	p
Deformability index	eNOS-786CC+TC	3.9	2.1-7.4	< 0.0001	2.3	1.01-5.4	0.04
	eNOS 894TT+GT	3.1	1.6-5.9	0.001	2.2	1.01-4.8	0.04
	eNOS aa+ab	1.3	0.7-2.4	0.3	-		
WBV 0.512 s ⁻¹	eNOS-786CC+TC	2.2	1.2-3.8	0.008	1.2	0.4-3.3	0.8
	eNOS 894TT+GT	3.6	2.04-6.4	< 0.0001	2.6	0.9-7.4	0.07
	eNOS aa+ab	1.1	0.6-2.03	0.6	-		
WBV 94.5 s ⁻¹	eNOS-786CC+TC	2.2	1.2-3.9	0.008	0.9	0.3-2.6	0.9
	eNOS 894TT+GT	3.3	1.8-5.8	< 0.0001	1.0	0.4-2.8	0.9
	eNOS aa+ab	1.5	0.8-2.6	0.2	-		
PLV	eNOS-786CC+TC	1.9	1.1-3.3	0.02	1.2	0.6-2.4	0.6
	eNOS 894TT+GT	1.7	1.02-2.9	0.04	0.8	0.4-1.7	0.6
	eNOS aa+ab	1.7	0.9-3.1	0.06	-		

*Adjusted for age, gender, fibrinogen, hematocrit, hypertension, and haemorheological parameters.

of eNOS polymorphisms causing a reduced nitric oxide availability. In fact, experimental studies [9, 11, 12, 22] suggested that NO may modulate erythrocyte deformability and aggregation with a concentration-dependent effect and demonstrated that NOS inhibition resulted in an impairment of erythrocyte deformability, which could be restored by NO donors. Though, the mechanism responsible for the effect of NO on erythrocyte deformability has yet to be fully defined. A NO regulatory effect on red cell deformability by soluble guanylate cyclase, involved in the production of cGMP, has been hypothesized [23] and experimental studies showed a role of NO in modulating ion transport across the red cell membrane [24, 25]. To date, L-arginine, a precursor of NO, exhibits activity as a vasodilator, platelet aggregation inhibitor and modulator of immunologic processes and epithelial permeability [26]; so arginine supplementation might represent a therapeutic benefit in the presence of eNOS polymorphism related to reduced NO availability. The presence of eNOS gene rare variants, which are related to impaired NO availability, affect red blood cell deformability and blood viscosity, so possibly contributing to microcirculatory alterations, such as those found in ISSHL, which represent a suitable model. However, further studies are needed to address the molecular mechanism by which the eNOS gene is involved in the modulation of haemorheologic profile in patients suffering from other microvascular disorders.

Interestingly, we found a significant association between haemorheological alterations and changes in haemostatic system in ISSHL patients, suggesting that the occurrence of rheological modifications may be relevant in determining microvascular occlusion by triggering blood clotting activation and impaired fibrinolysis in these pa-

tients. Nevertheless in these patients factor VIII:C, coagulation parameters measured in whole blood test and PAI-1ag remained important risk factors for ISSHL after adjustment for haemorheological parameters. These results are in agreement with previous studies reporting both increased plasma levels of PAI-1ag and factor VIII:C as risk factors for arterial and venous thrombosis [27, 28]. A stimulated endothelium may account for the elevated levels of PAI-1 found in ISSHL patients which, in turn, contribute to the thrombophilic state. High wall shear stress, such as that occurring in stenosed vessels or due to blood hyperviscosity, may perturb vascular endothelium [29] and, thus, stimulate platelet adhesion and aggregation and the expression of procoagulant activities. At the same time high factor VIII levels may enhance thrombin generation and, thus, result in increased platelet activation and fibrin formation processes. In keeping with this finding are the results of the global evaluation of haemostasis by Sonoclot analysis that has shown significant alterations in SonACT and clot rate values in ISSHL patients with respect to controls. Clot rate is influenced by the rapid increase in blood viscosity, due to the conversion of fibrinogen to fibrin and reflects the speed at which the clot is being formed. In ISSHL patients hypercoagulability is suggested by shorter SonACT values and by higher clot rate values, indicating an enhanced rate of thrombin generation and fibrin formation, and by higher factor VIII:C plasma levels than in controls.

We hypothesized that the altered erythrocyte deformability and the consequently increased blood viscosity may account for these haemostatic changes. Actually, the luminal surface of the blood vessel is constantly exposed to haemodynamic shear stress, that, according to Poiseuille's law, is proportional to blood flow viscosity and inversely

proportional to the third power of internal radius. This condition may create a vicious circle between endothelial damage and erythrocyte deformability, which can influence each other, thus leading to microvascular occlusion.

As ISSHL patients were investigated during the first week after the acute event we cannot rule out that elevated PAI-1ag and factor VIII:C plasma levels might be, at least in part, related to the acute phase reaction. However this seems unlikely because levels of fibrinogen were not different between patients and controls. A limitation of this study is that these parameters were measured after the event and there is no evidence here that those in the population who have such blood alterations will be at higher risk of ISSHL. However, this happens for all retrospective studies.

The observed changes in viscosity, blood clotting and fibrinolysis may contribute, at least in part, to the pathophysiological mechanism of ISSHL. Since the more recent studies performed in patients affected by ISSHL have shown inconsistent effects of haemodilution alone as a possible therapeutic option [30, 31], the clinical implications of these results are that not only hyperviscosity but overall hypercoagulability should be the target for therapeutic approaches in these patients.

Interestingly, hyperviscosity has been also found to be associated with the occurrence of retinal vein occlusive disease, in particular as regard the highest tertile of WBV at both shear rates as well as the lowest tertile of erythrocyte deformability index. Contrasting data has been previously reported by some studies concerning a possible association between alterations of haemorheological variables and the occurrence of RVO but no conclusive results have been obtained [32-37]. Such conflicting results can be explained by either the scanty number of patients studied in most of these studies or by the fact that only some of these studies analyzed the whole pattern of haemorheology in association with the disease. Our study, evaluating the entire haemorheological profile together with inflammatory parameters and hematocrit, in a relevant number of RVO patients and healthy subjects, confirms the significant role of haemorheological variables in the occurrence of this disease.

Our findings are in keeping with some previous studies evaluating haemorheological variables in RVO patients [33, 36]. In our study, WBV has been found to be associated with an increased risk of RVO at both shear rates investigated, after multiple statistical adjustment. This allows us to state that blood viscosity plays a relevant role in the pathogenesis of RVO. Indeed, haemorheology in RVO seems important particularly because altered blood fluidity could lead to further decreased flow, initiating and/or causing progression of vessel wall alterations.

Another relevant finding of our study is the observation that an increased erythrocyte deformability

is significantly protective against RVO. Erythrocyte deformability plays an important role in determining blood viscosity in the presence of slow venous flow and high vascular resistance, conditions that are normally present in the central retinal vein at the level of lamina cribrosa. Hence, an altered pattern of deformability for red cells can lead to a venous stasis and then to a reduced blood flow, by determining occlusion of retinal vessels. In our study, abnormalities of DI have been found to be present in a high percentage of RVO patients as compared to age and gender-comparable healthy subjects and have been observed to be significantly associated with an increased risk of the disease. Previous studies investigated red cell deformability in RVO patients but inconclusive data were obtained [32-34]. This can be ascribed to the different methods used for the measurement of such parameter.

At variance with previous studies, conversely, we did not find a significant association between plasma viscosity and RVO [34, 35, 37]. This conflicting result can be explained by the differences among these studies in terms of study populations, methods of measurements as well as control populations and main cardiovascular risk factors.

Notably, however, the results obtained in our study can be helpful for the clinical management of RVO patients. Up to now, no established treatment for RVO is available. The increasing role of hypercoagulability in these patients supports the role of antithrombotic drugs, but medical management of patients with RVO consists primarily on the treatment of the underlying systemic diseases. The presence of an altered haemorheological profile, on the other hand, can give to physicians a further therapeutic option for the treatment of RVO patients. Currently, some reports indicating a possible beneficial role of haemodilution therapy in the management of RVO have been reported, but data are limited [32, 38]. Moreover, a beneficial effect of treatment with pentoxifylline, a therapeutic agent able to determine a significant improvement of perfusion to occluded vessels, as well as of haemorheology, has been proposed in RVO patients by hypothesizing a relevant role for prohaemorheological agents in the clinical management of this occlusive disease, but data supporting this approach are lacking [39].

To date, statins and antiplatelet drugs have been reported to significantly influence haemorheological profile [40, 41] and, interestingly, a recent report showed a role for platelet activation in the pathogenesis of RVO [42]. Thus, the results of our study likely suggest a possible usefulness of the approach with these drugs to RVO patients. This is also in line with a recent meta-analysis of studies evaluating thrombophilia in RVO, which suggests that these patients have a risk profile of "arterial" more than of "venous" type [43].

In conclusion, recent literature and our findings point to a possible approach to RVO with haemodi-

lution, statins and antiplatelet drugs. Randomized controlled trials are needed to confirm usefulness of such treatment in these patients.

Finally, we documented a marked alteration of haemorheological variables and the role of *NOS3* gene -786T > C and 894G > T polymorphisms in influencing the haemorheologic profile in SSc patients. We found haemorheological alterations not only in dcSSc and in the presence of cutaneous ulcers, but also in lcSSc in the absence of cutaneous ulcers. This result may indicate that the haemorheologic status is involved in SSc "per se", independently of clinical manifestations. Our results confirm the effect of two *NOS3* polymorphisms in modulating the rheologic phenotype and, in particular, the erythrocyte deformability also in SSc patients. Indeed, these results highlight a possible mechanism by which a potential reduced availability of NO, related to *NOS3* -786T > C and 894G > T polymorphisms, might influence the predisposition to SSc. Actually, we demonstrated that an altered haemorheologic profile represents an independent risk factor for SSc, as described in ISSHL and RVO, two other clinical conditions in which a microcirculatory alteration is involved. Thus, it could be hypothesized that these polymorphisms might modulate susceptibility to the disease by influencing the haemorheologic profile in addition to their influence on vascular biology. The effect of the *NOS3* polymorphisms on the haemorheologic environment, related to potentially reduced NO levels, might be supported by our observation of a higher percentage of altered haemorheologic parameters in healthy subjects carrying the *NOS3* 894T rare allele.

Previous studies involving a limited number of patients indicated rheologic disorders related to erythrocyte aggregation and PLV in SSc [44, 45]. This is the first study to evaluate all rheologic parameters, such as PLV, WBV and DI; their alteration may be involved in the modification of the microvascular district found in SSc.

The pathogenetic mechanism of SSc are not yet completely defined. However, we know that impaired endothelial production of NO is involved in the breakdown of vascular tone control and vessel patency.

To date, there is evidence for impaired NO production as a potential result of the 894G > T polymorphism in exon 7 and of the -786T > C polymorphism, which reduces the promoter activity by ~ 50%, thereby lending experimental support for the notion of a physiologic role of this SNP. Data from experimental studies demonstrated that homozygosity for the rare variant of the -786T > C polymorphism in the promoter region of the *NOS3* gene is associated with a deficit of eNOS expression in human endothelial cells exposed to laminar shear stress, as well as with a reduced NO-mediated vasomotor function [46]. Interestingly, a re-

cent report by Sandrim *et al.* [47] suggested that there is a genetic contribution of *NOS3* haplotype to the development of endothelial dysfunction in hypertensive patients, and thus this contribution is obscured when specific *NOS3* genotypes alone are considered. Similarly, we demonstrated that the *NOS3* -786C/894T haplotype significantly affected the rheologic parameters in SSc, thus supporting the hypothesis that studies based on haplotypes may provide more reliable information than SNP-based studies.

Our results, which confirm that *NOS3* polymorphisms represent a susceptibility factor for SSc [48], are concordant with those of Metzger *et al.* [49], who reported an association between *NOS3* gene haplotype and lower circulating nitrate and nitrite concentrations. In contrast, the results of our study are not concordant with those of other studies that did not demonstrate the association between *NOS3* polymorphisms and SSc [50, 51]. These conflicting findings might be a result of the interethnic differences in the distribution of genetic polymorphisms [52], thus explaining the different clinical significance in each ethnic group from a different genetic background. At present, the number of candidate genes analyzed is really limited for revealing the complex nature of this disease and its heterogeneous phenotype.

Nonetheless, the results of this study confirm that also in SSc patients a potential reduction in NO availability related to *NOS3* polymorphisms may modulate erythrocyte deformability, thus contributing to endothelial injury with the same pathophysiological mechanism above discussed for ISSHL patients.

In the present study, in addition to erythrocyte involvement, we observed an increased PLV in SSc patients. This datum is attributable not only to increased fibrinogen levels, but also to the increase of other plasma components, such as albumin and immunoglobulins [53]. Since CCB therapy has been reported to modulate rheologic parameters in hypertension, we investigated the rheologic profile in 20 additional SSc patients not receiving CCB therapy. Actually, an altered rheologic profile has been observed in SSc patients independently of CCB therapy, possibly suggesting that the microcirculatory alteration is more relevant to rheologic parameters than the benefit derived from CCB therapy.

This study has two main limitations. First, apart from the -786T > C polymorphism, which is known to suppress *NOS3* gene transcription, thus lending experimental support to its physiologic role, the effects of the 894G > T and 4a/4b polymorphisms remain at present a matter of debate. Actually, the 894G > T polymorphism in exon 7 results in a conservative amino acid substitution and could affect eNOS activity, but the initial suggestion that the 894T variant is more susceptible to proteolytic cleavage [54] might be

attributed to experimental conditions. Finally, a functional role for the 4a/4b polymorphism in intron 4 has not been demonstrated, even though it has been reported to be associated with altered plasma NO levels [55] and responsible for variations in the genetic control of plasma nitrite and nitrate levels [56].

The second limitation lies in the lack of studies about the possible benefit of therapy with NO donors in SSc patients. These experimental data might shed light on the potential link between the *NOS3* genotypes and the rheologic parameters, thus substantiating the relevance of our results.

Our findings document an altered rheologic profile in SSc patients and demonstrate that this alteration is modulated by *NOS3* polymorphisms. This seems to shed light on a novel mechanism that might influence the microcirculation in SSc and allows us to comprehend how disease genotypes associated with the basic biology become clinical phenotypes. These findings suggest further inves-

tigation of the molecular mechanism by which the *NOS3* gene is involved in the modulation of the rheologic profile. Elucidation of additional interactions mediated by *NOS3* polymorphisms might offer exciting opportunities for future investigations and new therapeutic possibilities.

In conclusion, the results of our investigations suggest that alterations in haemorheological variables, either determined by genetic susceptibility or not, can be involved in the pathophysiological mechanism of some clinical disorders in which a disturb of the microvascular district is invoked and can be the target of new possible therapeutic strategies. However, prospective studies are needed to strengthen our findings in patients with microvascular disorders.

Submitted on invitation.

Accepted on 3 April 2007.

References

- Klingel R, Fassbender C, Fassbender T, Erdtracht B, Berrouschot J. Rheopheresis: rheologic, functional, and structural aspects. *Ther Apher* 2000;4:348-57.
- Pohl U, Holtz J, Busse R, Bassenge E. Crucial role of endothelium in the vasodilator response to increased flow in vivo. *Hypertension* 1986;8:37-44.
- Cooke JP, Rossitch E Jr, Andon NA, Loscalzo J, Dzau VJ. Flow activates an endothelial potassium channel to release an endogenous nitrovasodilator. *J Clin Invest* 1991;88:1663-71.
- Rees DD, Palmer RM, Moncada S. Role of endothelium-derived nitric oxide in the regulation of blood pressure. *Proc Natl Acad Sci U S A* 1989;86:3375-8.
- Huang PL, Huang Z, Mashimo H, Bloch KD, Moskowitz MA, Bevan JA, Fishman MC. Hypertension in mice lacking the gene for endothelial nitric oxide synthase. *Nature* 1995;377:239-42.
- Moncada S, Higgs A. The L-arginine-nitric oxide pathway. *N Engl J Med* 1993;329:2002-12.
- Ignarro LJ. Endothelium-derived nitric oxide: actions and properties. *FASEB J* 1989;3:31-6.
- Loscalzo J. Nitric oxide insufficiency, platelet activation, and arterial thrombosis. *Circ Res* 2001;88:756-62.
- Korbut R, Gryglewski RJ. Nitric oxide from polymorphonuclear leukocytes modulates red blood cell deformability in vitro. *Eur J Pharmacol* 1993;234:17-22.
- Starzyk D, Korbut R, Gryglewski RJ. The role of nitric oxide in regulation of deformability of red blood cells in acute phase of endotoxaemia in rats. *J Physiol Pharmacol* 1997;48:731-5.
- Bor-Kucukatay M, Wenby RB, Meiselman HJ, Baskurt OK. Effects of nitric oxide on red blood cell deformability. *Am J Physiol Heart Circ Physiol* 2003;284:H1577-84.
- Bateman RM, Jagger JE, Sharpe MD, Ellsworth ML, Mehta S, Ellis CG. Erythrocyte deformability is a nitric oxide-mediated factor in decreased capillary density during sepsis. *Am J Physiol Heart Circ Physiol* 2001;280:H2848-56.
- Mannini L, Paniccia R, Cecchi E, Alessandrello Liotta A, Leprini E, Berloco P, Pagnini P, Abbate R, Gensini GF, Prisco D. Reduced erythrocyte deformability and hypercoagulability in idiopathic sudden sensorineural hearing loss. *Clin Hemorheol Microcirc* 2005;33:47-55.
- Fatini C, Mannini L, Sticchi E, Rogai V, Guiducci S, Conforti ML, Cinelli M, Pignone AM, Bolli P, Abbate R, Matucci-Cerinic M. Hemorheologic profile in systemic sclerosis: role of *NOS3* -786T > C and 894G > T polymorphisms in modulating both the hemorheologic parameters and the susceptibility to the disease. *Arthritis Rheum* 2006;54:2263-70.
- Fatini C, Mannini L, Sticchi E, Cecchi E, Bruschetti A, Leprini E, Pagnini P, Gensini GF, Prisco D, Abbate R. eNOS gene affects red cell deformability: role of T-786C, G894T, and 4a/4b polymorphisms. *Clin Appl Thromb Hemost* 2005;11:481-8.
- LeRoy EC, Black C, Fleischmajer R, Jablonska S, Krieg T, Medsger TA Jr, Rowell N, Wollheim F. Scleroderma (systemic sclerosis): classification, subsets and pathogenesis. *J Rheumatol* 1988;15:202-5.
- Clements P, Lachenbruch P, Seibold J, White B, Weiner S, Martin R, Weinstein A, Weisman M, Mayes M, Collier D. Inter and intraobserver variability of total skin thickness score (modified Rodnan TSS) in systemic sclerosis. *J Rheumatol* 1995;22:1281-5.
- Cutolo M, Sulli A, Pizzorni C, Accardo S. Nailfold videocapillaroscopy assessment of microvascular damage in systemic sclerosis. *J Rheumatol* 2000;27:155-60.
- Kahaleh B, Meyer O, Scorza R. Assessment of vascular involvement. *Clin Exp Rheumatol* 2003;21(3 Suppl 29):S9-14.
- Hett DA, Walker D, Pilkington SN, Smith DC. Sonoclot analysis. *Br J Anaesth* 1995;75:771-6.
- Gatehouse S, Gallacher JE, Lowe GD, Yarnell JW, Hutton RD, Ising I. Blood viscosity and hearing levels in the Caerphilly Collaborative Heart Disease Study. *Arch Otolaryngol Head Neck Surg* 1989;115:1227-30.
- Korbut R, Gryglewski RJ. The effect of prostacyclin and nitric oxide on deformability of red blood cells in septic shock in rats. *J Physiol Pharmacol* 1996;47:591-9.

23. Petrov V, Lijnen P. Regulation of human erythrocyte Na⁺/H⁺ exchange by soluble and particulate guanylate cyclase. *Am J Physiol* 1996;271:C1556-64.
24. de Oliveira EM, Tavares de Lima W, Vannuchi YB, Marcourakis T, da Silva ZL, Trezena AG, Scavone C. Nitric oxide modulates Na⁺, K⁺-ATPase activity through cyclic GMP pathway in proximal rat trachea. *Eur J Pharmacol* 1999;367:307-14.
25. Pernollet MG, Lantoine F, Devynck MA. Nitric oxide inhibits ATP-dependent Ca²⁺ uptake into platelet membrane vesicles. *Biochem Biophys Res Commun* 1996;222:780-5.
26. Smulders RA, Aarsen M, Teerlink T, De Vries PM, Van Kamp GJ, Donker AJ, Stehouwer CD. Haemodynamic and biochemical responses to L-arginine and L-lysine infusions in normal subjects: L-arginine-induced vasodilatation cannot be explained by non-specific effects of cationic amino acids. *Clin Sci (Lond)* 1997;92:367-74.
27. Prisco D, Chiarantini E, Boddi M, Rostagno C, Colella A, Gensini GF. Predictive value for thrombotic disease of plasminogen activator inhibitor-1 plasma levels. *Int J Clin Lab Res* 1993;23:78-82.
28. Kamphuisen PW, Eikenboom JC, Bertina RM. Elevated factor VIII levels and the risk of thrombosis. *Arterioscler Thromb Vasc Biol* 2001;21:731-8.
29. Galbusera M, Zoja C, Donadelli R, Paris S, Morigi M, Benigni A, Figliuzzi M, Remuzzi G, Remuzzi A. Fluid shear stress modulates von Willebrand factor release from human vascular endothelium. *Blood* 1997;90:1558-64.
30. Mosnier I, Bouccara D, Atassi-Dumont M, Sterkers O. [Treatments of idiopathic sudden sensorineural hearing loss: retrospective study of 144 cases]. *Rev Laryngol Otol Rhinol (Bord)* 1998;119:119-28.
31. Ziegler EA, Hohlweg-Majert B, Maurer J, Mann WJ. Epidemiological data of patients with sudden hearing loss - a retrospective study over a period of three years. *Laryngorhinootologie* 2003;82:4-8.
32. Wiek J, Schade M, Wiederholt M, Arntz HR, Hansen LL. Haemorheological changes in patients with retinal vein occlusion after isovolaemic haemodilution. *Br J Ophthalmol* 1990;74:665-9.
33. Piermarocchi S, Segato T, Bertoja H, Midena E, Zucchetto M, Girolami A, Procidano M, Mares M. Branch retinal vein occlusion: the pathogenetic role of blood viscosity. *Ann Ophthalmol* 1990;22:303-11.
34. Arend O, Remky A, Jung F, Kiesewetter H, Reim M, Wolf S. Role of rheologic factors in patients with acute central retinal vein occlusion. *Ophthalmology* 1996;103:80-6.
35. Remky A, Arend O, Jung F, Kiesewetter H, Reim M, Wolf S. Haemorheology in patients with branch retinal vein occlusion with and without risk factors. *Graefes Arch Clin Exp Ophthalmol* 1996;234 (Suppl 1):S8-12.
36. Williamson TH, Rumley A, Lowe GD. Blood viscosity, coagulation, and activated protein C resistance in central vein occlusion: a population controlled study. *Br J Ophthalmol* 1996;80:203-8.
37. Lip PL, Blann AD, Jones AF, Lip GY. Abnormalities in haemorheological factors and lipoprotein (a) in retinal vascular occlusion: implications for increased vascular risk. *Eye* 1998;12:245-51.
38. Hansen LL, Wiek J, Wiederholt M. A randomised prospective study of treatment of non-ischaemic central retinal vein occlusion by isovolaemic haemodilution. *Br J Ophthalmol* 1989;73:895-9.
39. De Sanctis MT, Cesarone MR, Belcaro G, Incandela L, Steigerwalt R, Nicolaidis AN, Griffin M, Geroulakos G. Treatment of retinal vein thrombosis with pentoxifylline: a controlled, randomized trial. *Angiology* 2002;53:S35-8.
40. Muravyov AV, Yakusevich VV, Surovaya L, Petrochenko A. The effect of simvastatin therapy on hemorheological profile in coronary heart disease (CHD) patients. *Clin Hemorheol Microcirc* 2004;31:251-6.
41. Houtsmuller AJ, Vermeulen JA, Klompe M, Zahn KJ, Henkes HE, Baarsma GS, Tijssen J. The influence of ticlopidine on the natural course of retinal vein occlusion. *Agents Actions Suppl* 1984;15:219-29.
42. Leoncini G, Bruzzese D, Signorello MG, Armani U, Piana A, Ghiglione D, Camicione P. Platelet activation by collagen is increased in retinal vein occlusion. *Thromb Haemost* 2007;97:218-27.
43. Janssen MC, den Heijer M, Cruysberg JR, Wollersheim H, Bredie SJ. Retinal vein occlusion: a form of venous thrombosis or a complication of atherosclerosis? A meta-analysis of thrombophilic factors. *Thromb Haemost* 2005;93:1021-6.
44. Picart C, Carpentier PH, Galliard H, Piau JM. Blood yield stress in systemic sclerosis. *Am J Physiol* 1999;276:H771-7.
45. Picart C, Carpentier PH, Brasseur S, Galliard H, Piau JM. Systemic sclerosis: blood rheometry and laser Doppler imaging of digital cutaneous microcirculation during local cold exposure. *Clin Hemorheol Microcirc* 1998;18:47-58.
46. Cattaruzza M, Guzik TJ, Slodowski W, Pelvan A, Becker J, Halle M, Buchwald AB, Channon KM, Hecker M. Shear stress insensitivity of endothelial nitric oxide synthase expression as a genetic risk factor for coronary heart disease. *Circ Res* 2004;95:841-7.
47. Sandrim VC, Coelho EB, Nobre F, Arado GM, Lanchote VL, Tanus-Santos JE. Susceptible and protective eNOS haplotypes in hypertensive black and white subjects. *Atherosclerosis* 2006;186:428-32.
48. Fatini C, Gensini F, Sticchi E, Battagliani B, Angotti C, Conforti ML, Generini S, Pignone A, Abbate R, Matucci-Cerinic M. High prevalence of polymorphisms of angiotensin-converting enzyme (I/D) and endothelial nitric oxide synthase (Glu298Asp) in patients with systemic sclerosis. *Am J Med* 2002;112:540-4.
49. Metzger IF, Souza-Costa DC, Marroni AS, Nagassaki S, Desta Z, Flockhart DA, Tanus-Santos JE. Endothelial nitric oxide synthase gene haplotypes associated with circulating concentrations of nitric oxide products in healthy men. *Pharmacogenet Genomics* 2005;15:565-70.
50. Allanore Y, Borderie D, Lemarechal H, Ekindjian OG, Kahan A. Lack of association of eNOS (G894T) and p22phox NADPH oxidase subunit (C242T) polymorphisms with systemic sclerosis in a cohort of French Caucasian patients. *Clin Chim Acta* 2004;350:51-5.
51. Assassi S, Mayes MD, McNearney T, Fischbach M, Reveille JD, Arnett FC, Tan FK. Polymorphisms of endothelial nitric oxide synthase and angiotensin-converting enzyme in systemic sclerosis. *Am J Med* 2005;118:907-11.
52. Marroni AS, Metzger IF, Souza-Costa DC, Nagassaki S, Sandrim VC, Correa RX, Rios-Santos F, Tanus-Santos JE. Consistent interethnic differences in the distribution of clinically relevant endothelial nitric oxide synthase genetic polymorphisms. *Nitric Oxide* 2005;12:177-82.
53. Tietjen GW, Chien S, Leroy EC, Gavras I, Gavras H, Gump FE. Blood viscosity, plasma proteins, and Raynaud syndrome. *Arch Surg* 1975;110:1343-6.
54. Tesaro M, Thompson WC, Rogliani P, Qi L, Chaudhary PP, Moss J. Intracellular processing of endothelial nitric oxide synthase isoforms associated with differences in se-

- verity of cardiopulmonary diseases: cleavage of proteins with aspartate vs glutamate at position 298. *Proc Natl Acad Sci U S A* 2000;97:2832-5.
55. Wang XL, Mahaney MC, Sim AS, Wang J, Wang J, Blangero J, Almasy L, Badenhop RB, Wilcken DE. Genetic contribution of the endothelial constitutive nitric oxide synthase gene to plasma nitric oxide levels. *Arterioscler Thromb Vasc Biol* 1997;17:3147-53.
56. Tsukada T, Yokoyama K, Arai T, Takemoto F, Hara S, Yamada A, Kawaguchi Y, Hosoya T, Igari J. Evidence of association of the eNOS gene polymorphism with plasma NO metabolite levels in humans. *Biochem Biophys Res Commun* 1998;245:190-3.

The blood rheology in renal pathology

Bruno de Cindio^(a), Domenico Gabriele^(a), Gerardo Catapano^(a), Paola Fata^(a), Rene Hackel^(a), and Renzo Bonofiglio^(b)

^(a)*Dipartimento di Ingegneria Chimica e dei Materiali, Università della Calabria, Arcavacata di Rende (CS), Italy*

^(b)*Unità Operativa di Nefrologia, Dialisi e Trapianti, Azienda Ospedaliera dell'Annunziata, Cosenza, Italy*

Summary. The blood is a viscoelastic material often studied as a Newtonian or non-linear liquid. Some pathologies and extracorporeal blood treatment processes may affect both the liquid and solid blood component. An adequate rheological technique, able to detect these alterations, may provide clinicians with an important diagnostic aid. Creep tests consisting in the application of a constant stress are very promising because they may roughly separate the liquid-like (*i.e.*, at long response times) from the solid-like (*i.e.*, at short response times) component of the blood rheological behaviour. In this paper, some preliminary results obtained in creep tests on healthy and uremic individuals are reported showing the potentiality of this technique.

Key words: blood, creep, elasticity, renal pathology.

Riassunto (*L'influenza di alcune patologie renali sul comportamento reologico del sangue*). Il sangue è un materiale viscoelastico spesso studiato come un liquido Newtoniano o al massimo non lineare. Alcune patologie e trattamenti farmacologici o extracorporei del sangue possono alterarne sia la componente solida che quella liquida. Tecniche reologiche adeguate in grado di individuare queste alterazioni potrebbero costituire un importante strumento diagnostico a disposizione del clinico. Tra le varie possibili tecniche il *creep*, che consiste nell'applicazione al campione di uno sforzo costante, sembra estremamente promettente grazie alla sua capacità di separare, seppur in modo approssimativo, la componente solida del comportamento reologico del sangue, valutata a tempi brevi di risposta, da quella liquida, valutata a tempi lunghi. In questo lavoro sono riportati i risultati preliminari ottenuti nello studio di campioni di sangue da individui sani e con patologie renali, con l'obiettivo di dimostrare le potenzialità di questa tecnica.

Parole chiave: sangue, *creep*, elasticità, patologie renali.

INTRODUCTION

The blood can be considered a tissue consisting of liquid plasma and cells (*i.e.*, red blood cells, white blood cells and platelets). From a rheological point of view, it can be considered a suspension of interacting deformable particles of different shapes and dimensions in a suspending liquid (generally assumed Newtonian). The blood is characterised by a viscoelastic behaviour, mainly due to the properties of the suspended particles. Traditionally, also for some experimental difficulties, only its liquid-like component is characterised yielding the viscosity as the only measured rheological parameter.

Differences between healthy and uremic individuals are generally overlooked also in the design and testing of medical. However, some pathologies and drug or extracorporeal treatments may affect the blood rheology by changing either its liquid (*e.g.*, protein, fat or salt concentrations) or solid (*e.g.*, cell deformability, shape, dimension, etc.) component, or both. In some cases, the cell properties have been characterised with

empirical instruments or complex techniques [1] often requiring sample dilution that might strongly affect the final measurement.

Fundamental rheological tests, already used in other fields for the characterisation of suspensions, might be effectively used for the blood to characterise properties related to its microstructure.

Fundamental tests are performed under well known kinematic conditions: either a deformation field is applied and the corresponding stress field is measured, or a stress field is applied and the induced deformation is measured [2]. However, the fundamental tests commonly used for the characterisation of viscoelastic materials (and consisting in small amplitude oscillations) were not proven sensitive enough for blood characterisation, possibly as an effect of the simultaneous evaluation of the liquid-like and the solid-like components, the former being greater than the latter.

These considerations suggest that transient tests might be a feasible alternative capable to roughly separate the blood liquid-like from its solid-like rheologi-

cal behaviour. It is known that if the observation or process characteristic time is lower than the material relaxation time (*i.e.*, the Deborah number is $De > 1$), a solid-like response is observed, whilst if it is greater (*i.e.*, $De < 1$), a liquid-like behaviour is observed [2, 3]. Among other transient tests, creep tests in which a step stress of known amplitude is applied for a definite time, is very promising because weakly structured systems seem more sensitive to stress than to strain challenges. It is also worth to remind that low stress creep tests should cause a minimal damage to the material structure, and the measured parameters could be directly related to the material properties and should not depend on the deformation history.

In this paper, some preliminary results obtained in the course of creep tests performed at low stress on blood from healthy and diseased individuals are reported to validate creep for blood rheological characterization.

RHEOLOGICAL ANALYSIS

Creep tests are based on the application of a sudden constant stress (τ_0) to the sample and on the measurement of the induced deformation (γ). Experimental results are usually expressed in terms of the material compliance $J(t)$, *i.e.*, the strain-to-stress ratio, as follows [2, 3]:

$$J(t) = \frac{\gamma(t)}{\tau_0} \quad (1)$$

A typical plot of the time varying compliance of a viscoelastic material is shown in *Figures 1a, 1b*. It is possible to identify the following three regions [4]:

- the instantaneous elastic compliance at time zero, related to the pure elastic behaviour (often negligible or difficult to measure experimentally);
- the delayed elastic compliance, caused by the viscoelastic effects;
- the long-term viscous compliance, mainly related to the pure liquid behaviour.

Creep data have been analysed according to different techniques. The most common approach uses a mechanical model consisting of a Maxwell element in series with one or more Kelvin-Voigt elements [4]. This model features many fitting parameters poorly related to the material structure.

In this paper, starting from a pioneering work [5], a rather novel approach to creep analysis was used that is based on the identification of two different regions:

- a region at long response times, where the blood exhibits a liquid-like behavior. In this region, the reciprocal slope of the compliance *vs* time curve can be interpreted as its viscosity at the applied stress;
- a region at short response times, where the viscoelastic behaviour is dominant. The hysteresis area between the extrapolated behaviour at long response times and the actual blood behaviour provides a measure of the total blood elasticity (*Figure 2*). A cell specific elasticity can be estimated as the ratio between the hysteresis area in a differential time interval, $A(t, t+dt)$, and the total hysteresis area.

This approach yields two parameters strictly related to the specific material properties (*i.e.*, viscosity and cell specific elasticity), and can be very useful for a true material characterization. Experimental viscosities estimated at the applied stress were related to the haematocrit according to the model proposed by Dintenfass, as follows [6]:

$$\eta_r = (1 - kTC)^{-2.5} \quad (2)$$

where: C is the red blood cell (RBC) concentration, k is the RBC packing density, kC represents the effective RBC volume, T is the Taylor factor (related to the apparent RBC internal viscosity to the plasma viscosity ratio), and η_r is the dimensionless viscosity of the blood relative to plasma:

$$\eta_r = \frac{\eta_{\text{blood}}}{\eta_{\text{plasma}}} \quad (3)$$

In the course of pure viscosity measurements, all these parameters depend on the actual shear rate (or stress) that is applied. In this work, the viscosity was always evaluated at the same 0.09 Pa stress. Plasma

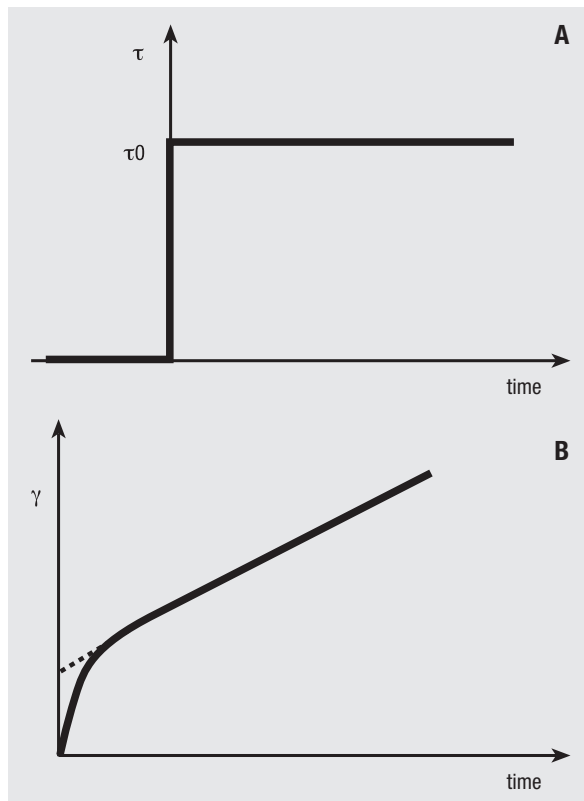


Fig. 1 | Scheme of creep test operation: a) the applied stress; b) a typical deformation induced in a viscoelastic material.

viscosity, assumed constant with the shear rate, was evaluated according to a literature correlation as a function of the actual blood cholesterol (*Chol*), fibrinogen (*Fib*), trygliceride (*Tg*), and high density cholesterol (*HDL*) concentration by means of the fitting coefficients *a*, *b*, *c*, *d*, and *e*, as follows [7]:

$$\eta_{plasma} = a + b \cdot Chol + c \cdot Fib + d \cdot Tg + e \cdot HDL \quad (4)$$

The plasma viscosity estimated according to equation 4 ranged between 1.47 mPa·s and 1.51 mPa·s, in good agreement with literature values [6, 8]. Cell concentration, *C*, is usually replaced with the haematocrit, *Hct*. *kT* is a sort of cell rigidity that, in this work, was used as a fitting parameter. Its value was reported to be about 0.9 for healthy individuals [6].

MATERIALS AND METHODS

Blood samples were collected with EDTA (0.5 µl/ml blood) from healthy individuals and from patients with renal insufficiency (RI), nephrotic syndrome (NS) or subjected to kidney transplantation (Tx). Tests were performed on blood donated by three individuals of each sex in each group. Haematocrit and some information on the pathology and drug treatment of the donors is reported in *Table 1*. The investigated transplant patients were immune suppressed with different doses of either tacrolimus or cyclosporine. The extent of renal damage of the investigated RI patients was characterised in terms of the patients' plasma creatinine concentration, *CL*, where $1 < CL < 3$ suggests minimal damage and $CL > 3$ an extensive damage. Creep tests were performed on a Rheometrics DSR200 controlled stress rheometer equipped with parallel plates ($\phi = 40$ mm) and a Peltier temperature control system. Tests were performed at 37 °C, a 1.5 ± 0.1 mm

Table 1 | Information on patients' identity, haematocrit (normal values reported under the column title) and sex of healthy individuals

Donor ID	Haematocrit (%) (Female 36-46; Male 41-53)	Sex
GF	45.3	M
FR	46.3	M
PG	46.9	M
AF	33.4	F
EF	37.4	F
PF	42.0	F

constant gap for up to 1000 s at 0.09 Pa, the lowest stress permitted by the instrument to minimize the damages to the blood. A few tests were performed at a 9 Pa stress to evaluate the damage to the blood structure caused by higher stresses. Water loss from the sample was minimized by using a cell cover supplied by Rheometrics. Direct inspection of the blood sample at the end of each test confirmed that no significant alteration had occurred during the test. Experiments were performed in triplicates on each sample. The blood samples were also analysed by optical microscopy at 1000x magnification (OPTECH Biostar B4, Germany) after coloration with the May-Grunwald Giemsa reactant, to study the cell morphology immediately before and after each the rheological test. The biochemistry of all samples was characterised as routinely done in the clinics.

RESULTS AND DISCUSSION

The typical compliance vs time curve that was obtained for blood at low stress is shown in *Figure 3*.

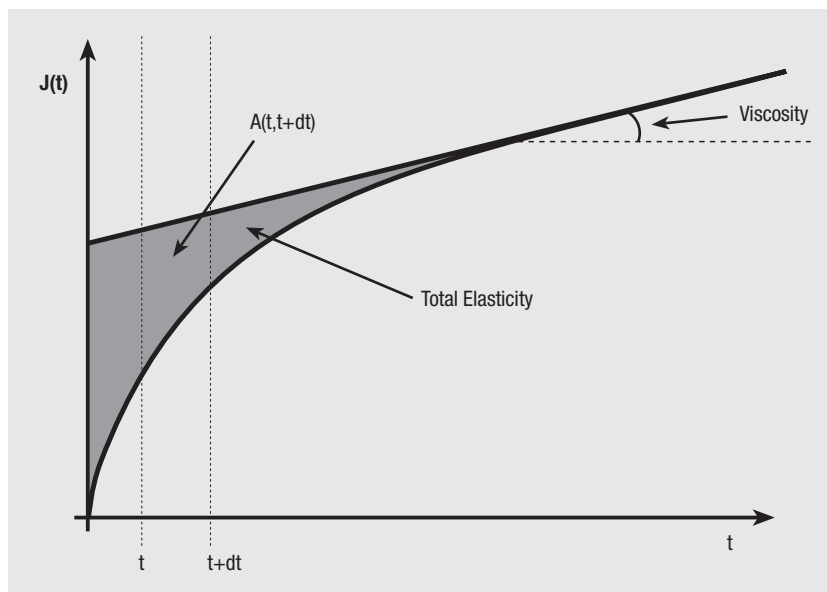


Fig. 2 | Typical compliance vs time curve obtained in the course of a creep test: the analysis proposed in this paper characterizes the blood behaviour in terms of viscosity (at long response times) and total elasticity (at short response times).

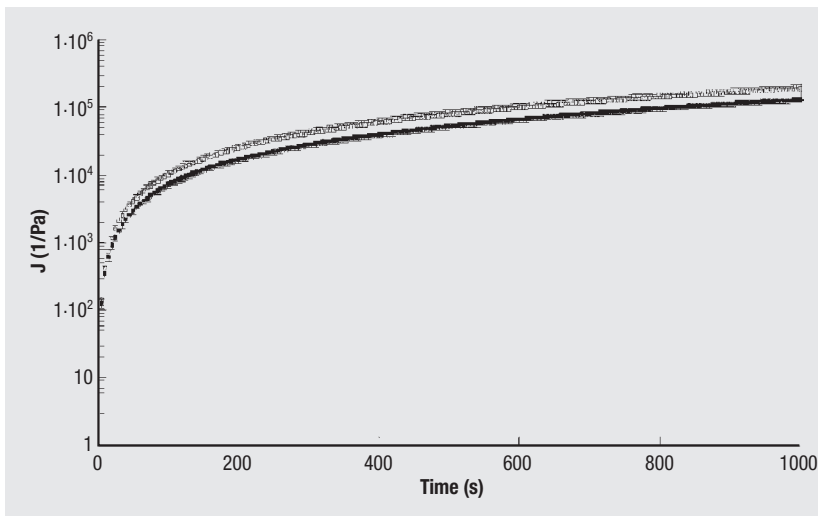


Fig. 3 | Compliance vs time curves obtained for healthy individuals: female, open symbols; male, closed symbols.

Figure 3 shows also that these curves were highly reproducible for healthy individuals of either sex. The difference observed for individuals of different sex is likely caused by the different haematocrit, as shown in Table 1. In fact, compliance is a bulk property that is affected by both the single particle property (*e.g.*, its morphology, rigidity, etc.) and the particle concentration. Similar curves were obtained with the blood of the other investigated individuals. The standard deviation of each experimental compliance point typically averaged 10%, and never exceeded 15%.

Figures 4a, 4b show that creep tests performed at low stress did not cause observable damages to the tested blood. Hence, the measured properties may be expected to provide information on the actual blood structure. Figures 4a, 4c show that creep tests at a 9 Pa stress damaged and fragmented many cells in the blood sample, opposite to that observed at a stress two orders of magnitude lower.

The measured relative viscosity of the blood of healthy individuals was in good agreement with those reported in literature and with the predictions of Equation 2. Consistently, the kT parameter was estimated to be 0.904 ± 0.018 in good agreement with the

0.9 value reported for healthy individuals [6]. The agreement of the relative viscosity of the blood of diseased individuals with those predicted by Equation 2 was not as good as for healthy individuals. In fact, Equation 2 consistently overpredicted the relative viscosity. This is particularly true for Tx and NS patients, as shown in Figures 5 and 6, where relative viscosity is reported as haematocrit function in a linear scale. Possibly, this is to be blamed on effect of the pathology on both the humoral and the cellular blood component, viscosity depending on the blood composition rather than on the cell properties only. However, no clear trend was observed.

The total blood elasticity of healthy individuals, estimated as the total hysteresis area, decreased with the haematocrit, although the paucity of available data did not permit to establish a clear statistical trend. This suggests that the blood deformability decreases as the haematocrit increases, as was expected higher particle concentrations causing an enhancement of the solid-like behaviour of the blood.

Specific information on the cell properties, rather than on the blood as a whole, were obtained by normalizing the hysteresis area in a differential time interval, $A(t, t+Dt)$, over the total hysteresis area to

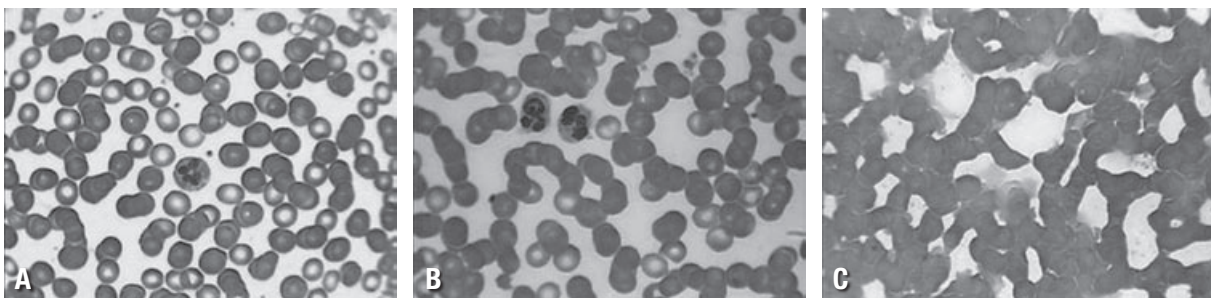


Fig. 4 | Microscopic take of blood from a healthy female individual, 1000x magnification: a) before the creep test, b) after a creep test stress at 0.09 Pa; c) after a creep test at 9 Pa.

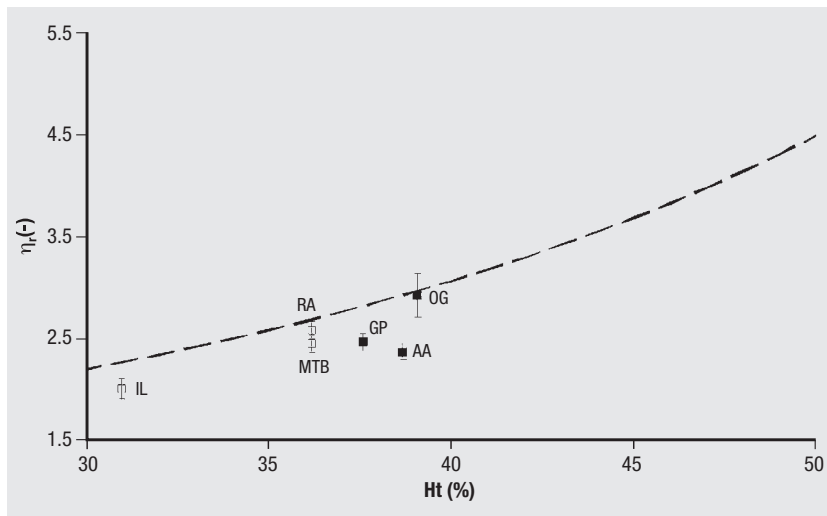


Fig. 5 | Relative viscosity of the blood of kidney transplantation (TX) patients as a function of the haematocrit: experimental values for female (open symbols) and male (full symbols) patients; best-fit predictions from equation 2 (line).

give a specific elasticity. Practically identical curves were obtained for all healthy individuals independent of their sex. This result suggests that the specific elasticity does not depend on the haematocrit and provides intensive information on the cell properties that do not change with sex, as was expected.

Figures 7a, 7b show that the specific elasticity of

the blood of transplant patients is not significantly different from that of the controls. Table 2 shows that these patients were given either one of two different immunosuppressive drugs (*i.e.*, tacrolimus or cyclosporine), which have been reported to have different effects on the blood cells. In fact, tacrolimus was reported to deteriorate the rheological prop-

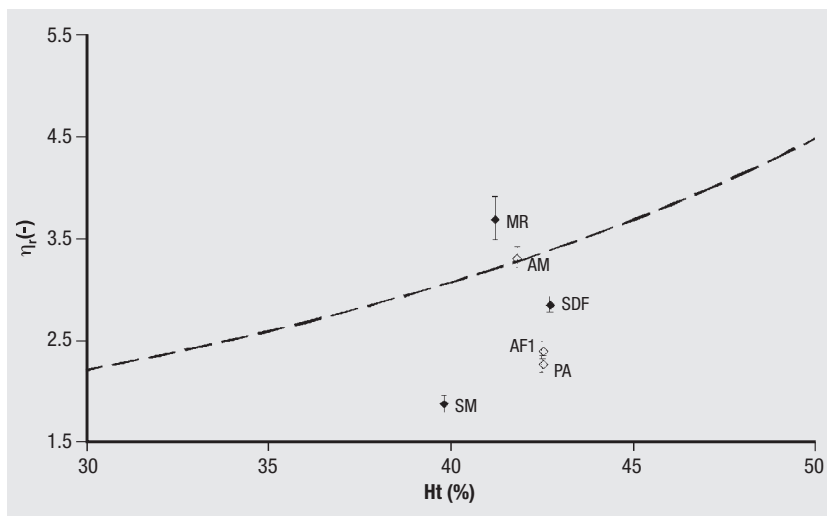


Fig. 6 | Relative viscosity of the blood of nephrotic syndrome (NS) patients as a function of the haematocrit: experimental values for female (open symbols) and male (full symbols) patients; best-fit predictions from equation 2 (line).

Table 2 | Information on patients' identity, haematocrit (normal values reported under the column title) drug treatment, and sex of patients with kidney transplantation

Donor ID	Haematocrit (%) (Female 36-46; Male 41-53)	Drug treatment	Drug daily amount per bodyweight (mg/d/kgBW)	Sex
GP	37.6	Tacrolimus	High	M
OG	39.1	Tacrolimus	Low	M
AA	38.7	Cyclosporine	High	M
IL	31.0	Cyclosporine	Low	F
RA	38.6	Tacrolimus	Low	F
MTB	36.2	Cyclosporine	High	F

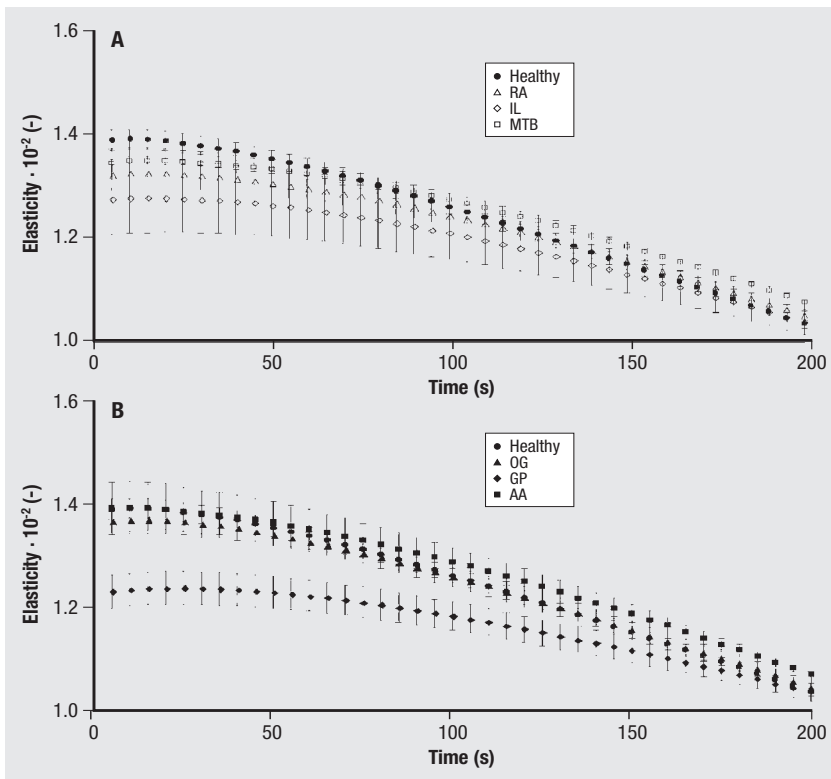


Fig. 7 | Experimental specific elasticity vs time curves for kidney transplantation (Tx) patients: a) female; b) male.

erties of RBCs by negatively affecting both their aggregability and deformability [1]. Cyclosporine was reported to reduce RBC deformability but to

increase their aggregability causing an enhanced solid-like behaviour [1]. Figure 7b shows that only in the case of the male patient taking the highest

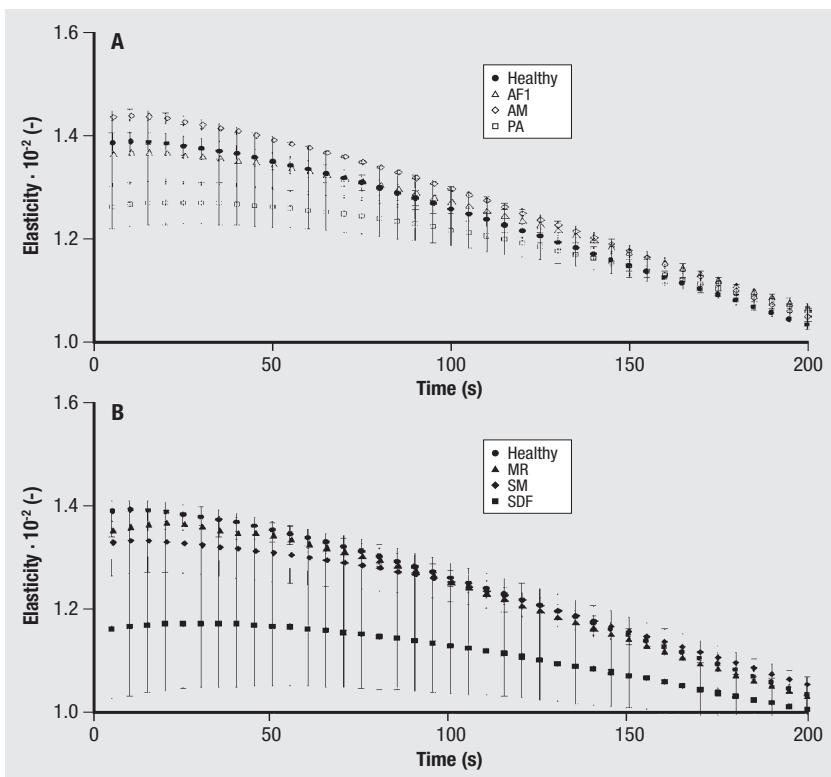


Fig. 8 | Experimental specific elasticity vs time curves for nephrotic syndrome (NS) patients: a) female; b) male.

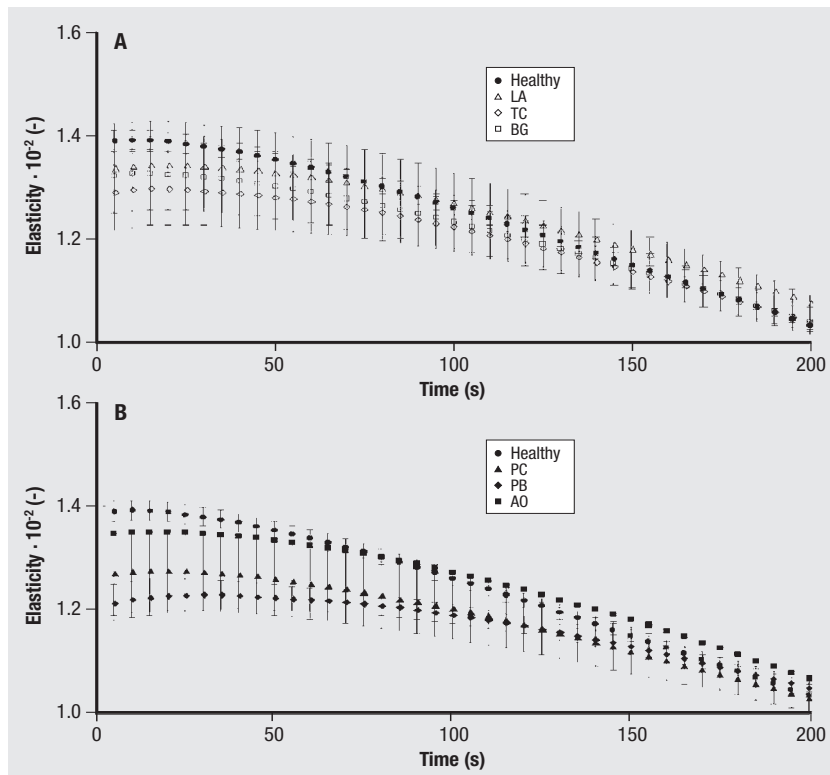


Fig. 9 | Experimental specific elasticity vs time curves for renal insufficiency (RI) patients: a) female; b) male.

dose of tacrolimus (*i.e.*, GP) the specific elasticity was consistently lower than the controls over the first 200 s of testing. Sub-toxic drug doses and the opposed effect of cyclosporine on cell aggregability and deformability might have caused minimal differences from the controls in the other investigated patients.

Haematocrit values and sample ID for NS patient were reported in Table 3; Figures 8a, 8b show that the specific elasticity of the blood of the NS patients was also generally very close to that of the controls. Only in the case of the two patients (*i.e.*, SDF and PA) with *Lupus erythematosus* the specific elasticity was significantly and consistently lower than the controls.

Figures 9a, 9b show that the specific elasticity of the blood of RI patients with slightly elevated

creatinine clearance (reported in Table 4) was only slightly lower than that of the controls. In the case of RI patients with an elevated creatinine clearance (Table 4) the specific elasticity was consistently lower than that of the controls over the first 200 s of testing. These results suggest that the observed reduction might be correlated to the extent of the renal damage.

In all the cases in which a reduced specific elasticity was observed, the difference with respect to the controls was consistently more evident within the first 50 s from the stress application. It is also worth noticing that the estimated blood viscosity of these patients was not far from that of the controls suggesting that, at least in these cases, the measurement of the specific elasticity was a more sensitive marker of the blood alterations caused by the pathology.

Table 3 | Information on patients' identity, haematocrit (normal values reported under the column title) and sex of patients with nephrotic syndrome

Donor ID	Haematocrit (%)		Sex
	(Female 36-46; Male 41-53)		
SM	39.8		M
MR	41.2		M
SDF	42.7		M
AM	41.8		F
AF1	37.7		F
PA	42.5		F

CONCLUSIONS

The results reported in this paper suggest that creep tests might be useful for the diagnostic monitoring of renal pathologies and provides support for further research. In fact, creep tests may be quickly performed and yield in one shot reliable measurements of both the liquid-like (*i.e.*, the viscosity) and the solid-like (*i.e.*, the elasticity) component of the blood rheological behaviour.

Viscosity measurements provide information only on massive alterations to both the humoral and the cellular blood components but are not sensitive to pathological alterations to the blood cell properties only.

Table 4 | Information on patients' identity, haematocrit (normal values reported under the column title), plasma creatinine concentration, and sex of patients with renal insufficiency

Donor ID	Haematocrit (%) (Female 36-46; Male 41-53)	Creatinine conc (mg/dL)	Sex
AO	34.8	1<CL<3	M
PC	37.6	CL>3	M
PB	33.8	CL>3	M
BG	40.8	1<CL<3	F
LA	40.8	1<CL<3	F

The specific elasticity obtained from low stress creep tests as the ratio between the hysteresis area in a differential time interval and the total hysteresis area

may provide information on the blood cell properties (e.g., their deformability and aggregability) independent of the actual cell volume fraction (i.e., the haematocrit), as was shown for healthy individuals. The tests on blood from RI patients suggest that the specific elasticity might even be related to the progression of the renal damage caused by the pathology.

Work is under way to seek for possible correlations between the specific elasticity and markers of the extent of the renal damage for different renal pathologies in the attempt to validating the use of creep tests as a diagnostic tool.

Submitted on invitation.

Accepted on 3 April 2007.

References

1. Chmiel B, Harkoszka H, Cierpka L, Wiecek A. Rheological properties of red blood cells in kidney transplant recipients: the role of lipid profile and type of immunosuppression. *Transplantation Proceedings* 2005;37:1885-8.
2. Tanner R. *Engineering rheology*. Oxford: Oxford University Press; 2000.
3. Ferry JD. *Viscoelastic properties of polymers*. New York: John Wiley and sons; 1980.
4. Whorlow RW. *Rheological techniques*. London: Ellis Horwood Limited; 1980.
5. de Cindio B. *Bioreologia: modelli di comportamento e metodi sperimentali*. Roma: Istituto Superiore di Sanità; 2003. (Rapporti ISTISAN 03/13).
6. Dintenfass D. *Rheology of blood in diagnostic and preventive medicine: An introduction to clinical haemorheology*. London: Butterworths; 1976.
7. Eterovic D, Pintaric I, Tocilj J, Reiner Z. Determinants of plasma viscosity in primary hyperlipoproteinemias. *Clin Hemorheol* 1995;15:841-50.
8. Rosenson RS, McCormick A, Uretz EF. Distribution of blood viscosity values and biochemical correlates in healthy adults. *Clin Chem* 1996;42:1189-95.

Sickle cell anemia: haemorheological aspects

Maria Cristina Martorana^(a), Giorgio Mojoli^(b), Paolo Cianciulli^(c), Anna Tarzia^(d), Emilio Mannella^(a) and Patrizia Caprari^(d)

^(a)Centro Aziendale Produzione Emocomponenti (CAPE), Azienda Ospedaliera San Camillo-Forlanini, Rome, Italy

^(b)Rheology Application Specialist, Miane, Treviso, Italy

^(c)Day Hospital Talassemici, S. Eugenio Hospital, Rome, Italy

^(d)Dipartimento di Ematologia, Oncologia e Medicina Molecolare, Istituto Superiore di Sanità, Rome, Italy

Summary. The maintenance of erythrocyte shape and membrane integrity is bound to the modification of deformability and/or permeability. Usually, these features are not investigated with normal laboratory tests. The membrane stiffness, the cell geometry, and the viscoelasticity components are influencing factors on survival and functionality of the erythrocytes. Only few studies have analyzed the viscoelastic characteristics of red blood cells, even less are the studies on patients affected by sickle cell disease (SCD), a pathology characterized by acute and chronic impairment of cell flexibility due to the formation of intracellular sickle haemoglobin (Hb S) polymers. A critical point of SCD is represented by the rheologic alterations of sickle cells determined by the transition from sol to gel of haemoglobin producing a dramatic change in cell viscosity and viscoelastic properties. We have investigated the behaviour of the blood in SCD, from an original rheological point of view, by evaluating the viscoelastic properties of sickle cells in oscillating harmonic sinusoidal mode. A comparison between patients with different severity of the disease, with transfusion dependence (TD) or without transfusion dependence (NTD), has been carried out. This study has confirmed the rheologic impairment of SC blood. The TD patients showed a minor heterogeneity of rheologic behaviour in comparison with NTD patients, because of the normalizing effect of transfusion. The analysis of viscoelastic properties might be an additional useful tool for monitoring transfusional and pharmacological treatments.

Key words: sickle cell disease, blood viscosity, erythrocyte deformability, blood visco-elastic properties.

Riassunto (*Anemia falciforme: aspetti emoreologici*). Le alterazioni morfologiche, la modificazione in deformabilità e/o permeabilità dell'eritrocita a cui seguono danni di tipo emoreologico, normalmente non sono evidenziabili con i normali test di laboratorio, e innescano una serie di reazioni a catena che possono determinare un danno irreversibile con conseguente sequestro da parte degli organi emocateretici. Non molti sono gli studi sulle caratteristiche viscoelastiche degli eritrociti, ancora meno sono quelli su pazienti portatori di anemia falciforme (AF), una patologia caratterizzata da un danno acuto e cronico della flessibilità cellulare dovuta alla formazione di polimeri intracellulari di emoglobina S. Un aspetto critico della AF è rappresentato dalle alterazioni reologiche delle cellule falcemiche determinate dalla transizione da sol a gel dell'emoglobina accompagnata da un drammatico cambiamento della viscosità e delle proprietà viscoelastiche del globulo rosso. In questo lavoro sono stati studiati pazienti sia omozigoti per AF che portatori di doppia eterozigosi S/α o β - talassemia, trasfusione dipendenti (TD) e non trasfusione dipendenti (NTD), valutando le proprietà viscoelastiche tramite regime oscillatorio. Questo studio ha confermato la presenza di alterazioni reologiche nella AF. I pazienti TD, essendo normalizzati dall'effetto della trasfusione, hanno mostrato una minore eterogeneità rispetto ai pazienti NTD. La valutazione in regime oscillatorio delle proprietà viscoelastiche potrebbe essere un ulteriore utile strumento che permette di monitorare trattamenti trasfusionali e farmacologici.

Parole chiave: anemia falciforme, emoreologia, deformabilità dei globuli rossi, proprietà viscoelastiche del sangue.

INTRODUCTION

"The history of our understanding of sickle cell disease can be likened to the opening of the proverbial Russian egg: at once another egg appears with-

in, and inside that another and yet another and so on. Thus, in the study of sickle cell disease, first we see the ailing and anemic patient, then his deoxygenated, sickling red cell, then its abnormal haemoglob-

in, and finally, hidden away inside the beta chain of the molecule, a single displaced amino acid" [1].

Oral history passed down through African generations told of an inherited illness with episodes of sudden onset bone pains and of many infantile deaths. The earliest known medical paper with the original name of "sickle cell disease" was published in 1874 by Africanus Horton [2].

The scientific pathway from man to molecule begins with the recognition of the clinical aspects of sickle cell disease (SCD) at the beginning of the past century. Herrick's initial description in 1910 of elongated crescent-shaped cells led to a variety of *in vitro* experiments which attempted to explain this phenomenon.

Many later studies showed that the formation of sickle polymer is complex and involves multiple types of chemical interactions. A large body of precise and coherent informations has been gathered on the mechanisms underlying the polymerization of S hemoglobin (Hb S). They form the cornerstone of our understanding of the pathogenesis of SCD [3-6].

SICKLE CELL DISEASE: A FOUNDER MUTATION

SCD, marked by misshapen red blood cells, is usually caused by a founder mutation. It fits in the germ-line mutations category and it is passed down intact over generations [7].

The SC mutation today can be found in five different haplotypes (Senegal, Benin, Bantu, Arab-India, Cameroon) leading to the conclusion that the mutation appeared independently five times in five different founders in human history. Their highest frequency occurs in tropical areas but the population migrations have ensured that they are encountered in most different countries [8].

The frequency of a founder mutation in the population is governed by two competing forces in which the beneficial effects drive the frequency of the mutant gene up, while the harmful effects damp down the frequency. The SCD is a well-known example of the so called balancing selection: it apparently arose repeatedly in regions ridden by malaria, in Africa and the Middle East. A single copy of SC gene helps the carrier to survive malarial infection (protective effect) while two copies produce a homozygous sick state with lower survival rates [7].

As a result of heterozygote advantage against malaria, the inherited haemoglobin disorders are the commonest monogenic disease [8]. The inherited disorders are classified into two groups: the structural variants and the thalassaemias (thal). The first group results from single-amino-acid substitutions in α or β chains; the second group is characterized by abnormal globin gene function resulting in total absence or in quantitative reduction of α or β globin chain synthesis. The α - and β -thalassaemias are a heterogeneous group of haematological disorders with a high incidence in a wide areas extending from

Mediterranean and African regions, the Middle East, the Indian sub-continent, South-East Asia, Melanesia and Pacific Islands [8].

The distribution of the β^s gene in the Old World corresponds to that of falciparum malaria [9-11]. In the various populations of equatorial Africa, the gene frequency ranges from 5% to more than 14%; it is about 4% among Caribbeans, Europeans, and North and South Americans of African descent. The sickle gene is also indigenous to Sicily, Greece, India, Saudi Arabia, Israel, Turkey and Iran [9-14].

SICKLING DISORDERS

The sickle cell picture shows the propensity of the red blood cells to assume a sickled configuration when blood is deoxygenated, accompanied by the loss of potassium and water which it provides an inhospitable environment for the parasite of *Plasmodium Falciparum*.

SCD pathophysiology is mediated by acute and chronic impairment of cell flexibility due to the formation of intracellular Hb S polymers as cells are partially deoxygenated in the microcirculation.

The vicious circle of the erythrocyte membrane damage of SCD is well-known. The sickling phenomenon depends on the formation of deoxyhaemoglobin S and the transition from a sol to a gel is accompanied by a dramatic increase in viscosity. The consequent increase in intracellular haemoglobin concentration accelerates and potentiates the rate of deoxygenation of the erythrocytes at which further polymerization can occur. This is the beginning of the numerous structural and functional abnormalities of sickle red blood cell [3-6, 13-16].

The clinical manifestations of SCD vary enormously between and among the major genotypes ranging from asymptomatic subjects to patients disabled by recurrent pain and chronic complications. Typically, patients are anaemic but lead a relatively normal life with painful episodes. Virtually every organ system in the body is subject to vaso-occlusion, which accounts for the characteristic acute and chronic multisystem failure of this disease.

In the homozygous state (Hb SS) and in double heterozygous conditions (Hb S/ β thalassaemia), the presence of Hb S induces heterogeneous morbidity, that can be grouped in four major categories: chronic haemolytic anaemia, systemic manifestations with increased susceptibility to infections, vaso-occlusive episodes or painful "crises" of varying severity and frequency, organ damage as consequence of multiple vaso-occlusive events [15].

SICKLE BLOOD CELL RHEOLOGY

The whole blood viscosity is a function of both the number of erythrocytes and their deformability and of the plasma proteins. It is known that the blood is a non-Newtonian fluid and its viscosity is markedly dependent on shear rate. The plasma has a high

protein-mediated effects and exhibits RBC-RBC adhesive interactions at lower shear rates that are mediated by large plasma proteins (*i.e.* fibrinogen) [4-8, 17-19].

In SCD the viscosity is dominated by HbS gelation and by the presence of dense sickle cells. As reported by Ballas and Mohandas [18], a wide number of interrelated factors influence the micro – and macro – rheology of the sickle blood: plasma components, haematocrit (Hct), the unsickling-sickling red cells cycles, the cellular dehydration, the erythrocyte deformability and mechanical fragility, vascular factors, α -globin genotypes and β globin apotypes, the white cell populations, the haemostatic factors, the epistatic genes, and the environment. All the above-mentioned determinants together with the alterations of the Virchow triad on the haemostatic system and genetic factors [19-21] are responsible for aberrant interaction of sickle RBC with vascular endothelium and can modulate the SCD severity.

Upon deoxygenation the viscosity of sickle blood rises sharply, because the polymerization of deoxy-HbS, therefore in SCD the presence of anaemia with a decrease in Hct can be considered protective of microcirculatory flow. The increase in Hct by transfusion therapy, used in severe cases of SCD, can rise the viscosity and upset this balance resulting in hyperviscosity and clinical deterioration. The transfusion guidelines for SCD have defined the post-transfusional Hct value is less than 0.35 (or Hb concentration of <11-12 g/dL) and sickle red blood cells (SS-RBCs) between 30 and 50 % [22, 23]. Until today the management of SCD is of supportive care and the red cell membrane deformability and the hypoxia are the cardinal points of the pharmacodynamic research. The use of hydroxyurea (HU), a rheological drug, has been proposed for its ability to rise the level of fetal haemoglobin (Hb F), increase mean cell volume and reduce neutrophil count. Therefore, HU increases the whole cell deformability with a consequent better oxygen supply to the tissues [2, 22].

The viscoelastic properties of the sickle gel depend on both the density and rigidity of the component fibers. Thus, rheological measurements on sickle gels have not only provided new insights into the structure of the gel but also have clear-cut implications regarding the deformability of sickle cells *in vivo* [15].

The effects of the rheological properties of the gel and the intrinsic behaviour of haemoglobin S, with or without other genetically determined abnormalities of the α or β chain, can be regarded as the proximate and most immediate cause of the vaso-occlusive manifestations in these patients. In fact, a hallmark of these patients is the vaso-occlusion of small and sometimes large vessels that allow a higher morbidity and mortality, because of the involvements of the vaso-occlusive formations.

Decreased deformability of sickle cells has been documented using a variety of techniques, includ-

ing viscosimetry, filtration, ektacytometry, and micropipette aspiration of individual cells [18-21] that have pointed out, respectively, an increased viscosity of blood, decreased filtration rate of diluted cell suspension through narrow pores, decreased ability of cells to undergo deformation in shear fields, and increased aspiration pressures needed to induce entry of cells into micropipets. These studies have demonstrated a marked heterogeneity in the extent of erythrocytes rheologic abnormalities in different SCD subjects and often in the same individual blood sample [18-21].

In order to study the rheological behaviour of sickle blood cells in SCD, a comparison between transfusion dependent (TD) or no-transfusion dependent (NTD) patients with different severity of the disease was carried out by evaluating the viscoelastic properties of sickle cells in oscillating harmonic sinusoidal mode.

MATERIALS AND METHODS

Blood samples

The blood samples were collected by venepuncture using plastic tubes containing 4.7 mM K_3 ethylenediaminetetra-acetic acid (EDTA K_3) and processed within 2 hours. The samples from SCD patients (Day Hospital Talassemici, S. Eugenio Hospital, Rome, Italy) were analyzed in triplicates and in comparison with samples from healthy blood donors as controls (periodic healthy blood donors of Donors Group – Italian Red Cross, Centro Aziendale Produzione Emocomponenti – Azienda Ospedaliera San Camillo – Forlanini).

Patients

Ten SCD patients (mean age 33 years) were analyzed: n. 5 subjects TD and n. 5 subjects NTD. Both groups included two HbSS and three HbS/ β thalassaemia patients. Moreover, two TD patients and one NTD patient carried a combined 3.7 alfa globin gene mutation. All TD patients showed a rate of HbS less than 35% whereas the rate of NTD ranged from 66 to 68%.

The regular transfusional therapy of TD patients was justified by clinical severity of the disease: bone infarction, hepatobiliary injury, priapism, skin ulcers and cardiac complications. The NTD group showed a milder clinical picture with the exception of the patient n.8 that had manifested the avascular necrosis of the femoral head.

Haemorheological assays

For the haemorheological assays a rotational viscosimeter RV20 was used with the couette measuring system CV100. The coaxial cylinder sensor systems are known as ME 31. Shear rate and test temperature were controlled through the rheocontroller RC-20 (HAAKE - Karlsruhe, Germany). Blood samples were analyzed according to the Recommendation of the International Committee for Standardization in

Haematology (ICSH) [24]. Each blood sample was measured at 37 °C in oscillation harmonic sinusoidal mode to determine its viscoelastic properties. The oscillating movement allows us to investigate the structure of the fluid and to study its dynamic and mechanical behaviour.

Viscoelastic properties were analyzed by elastic modulus G' and viscous modulus G'' . G' represents the elastically stored energy in a sample subjected to oscillating deformation, while G'' marks the amount of energy which is dissipated into heat as the result of viscous flow.

We used two analytical procedures to evaluate the rheological behaviour: strain and frequency tests. Strain test was used to determine the deformability pattern of the sample in order to analyze the linear viscoelastic region. The test was conducted at constant ω (deformation velocity), varying the strain (amplitude of deformation). Frequency test was used to measure the dynamic and mechanical properties of the fluid which enables us to investigate its viscoelastic behavior under several stress conditions.

We studied the tangent of phase shift angle ($\tan \delta = G''/G'$) as a function of strain rate at a constant value of deformation amplitude, selected on the previously determined linear viscoelastic range by strain test. The frequency test was evaluated in the range from 0.1 to 10 Hz. ($f = \omega/2\pi$).

For the evaluation of G' and G'' values we used the mathematical model known as "Power law":

$$X = K * Y^n$$

where X is the independent variable and Y is the dependent variable.

It is possible to associate different variables to the X and Y value and to calculate the related constants. In this way we can evaluate all the behaviours of interest using only two constants instead of a large number of experimental data.

The meaning of each constant depends on the considered variable.

The function is represented by a curve, the constant "K" is associated with the position of the curve inside the graph plane, and the constant "n", with the slope of the curve. The calculated constants were compared with those obtained from healthy controls.

RESULTS

The distribution of the viscoelastic behaviours expressed as $\tan \delta$, G' , and G'' , are shown in Figures 1-4.

The $\tan \delta$ curves obtained by TD patients (1-5), NTD patients (6-10) and normal control (C) have been evaluated in the linear viscoelastic range from 0.1 to 10 Hz. The $\tan \delta$ curve of the normal control was independent from the applied strain rate, while the $\tan \delta$ curves of both TD and NTD groups showed different trends. In the TD-patients 1 and 5 (Figure 1) $\tan \delta$ values were higher than control ones at 0.1 Hz, while were comparable to control values at 10 Hz. In the TD-patients 2, 3, 4 the slope of the $\tan \delta$ was comparable with that of control in the explored frequency region (0.1-10 Hz). As concerns TD-patient 2, a particular behaviour was observed being $\tan \delta$ value comparable to control value at 0.1 Hz but increased at 10 Hz.

Similarly, the $\tan \delta$ curves of the NTD patients (Figure 2) presented two different trends. In NTD-patients n. 6, 8 and 10, the $\tan \delta$ values were higher than the control ones at 0.1 Hz, while the curves of the NTD-patients n. 7 and 9 ran together with the control one. It is noteworthy that the $\tan \delta$ values of patients n. 6 and 8 were very low at 10 Hz as compared with the control ones.

Since $\tan \delta$ curves represents the G''/G' ratio, we have also analysed G' and G'' separately in order to evaluate the relationship between elastic G' and viscous G'' modulus in TD and NTD patients.

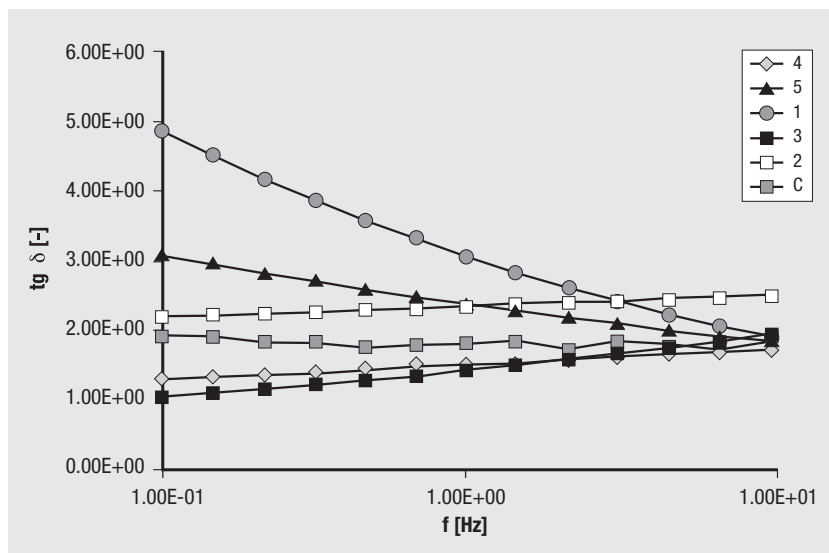


Fig. 1 | Analysis of tangent δ ($\tan \delta$) in transfusion dependent SCD patients (1-5). C = control.

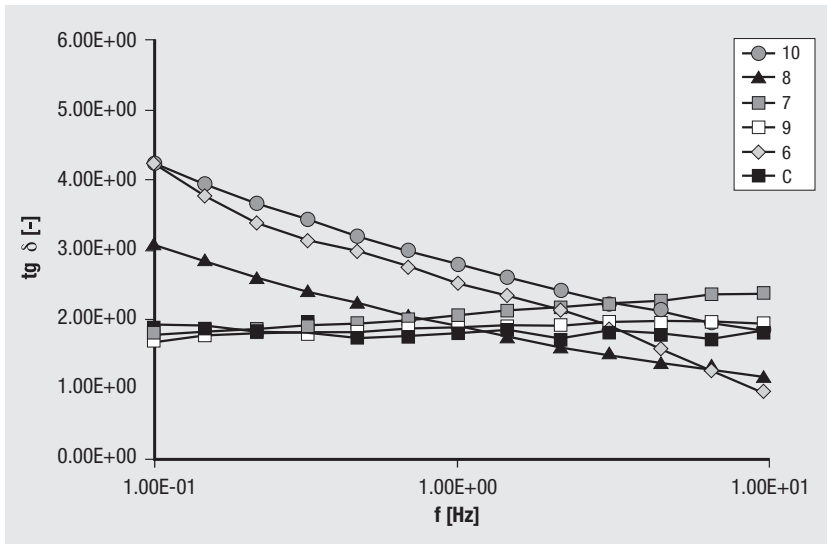


Fig. 2 | Analysis of tangent δ ($tg \delta$) in no-transfusion dependent SCD patients (6-10). C = control.

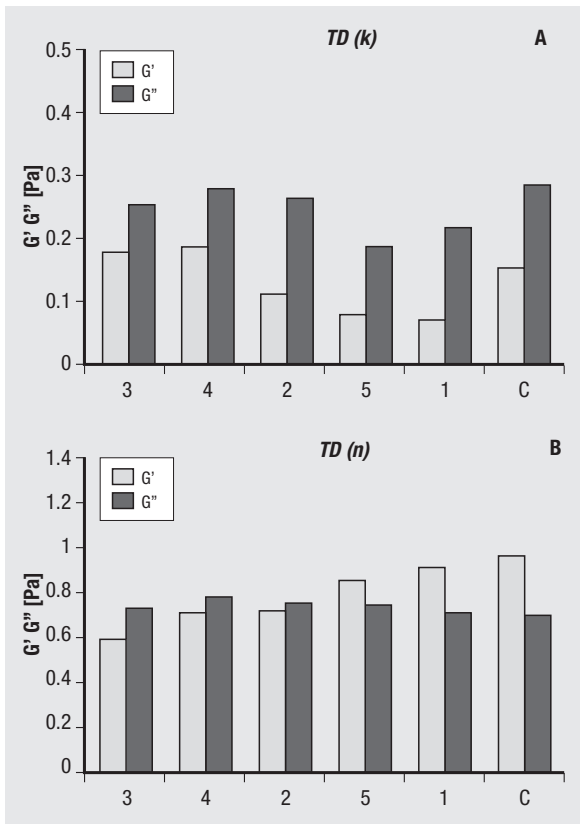


Fig. 3 A-B | Analysis of G' elastic modulus and G'' viscous modulus in transfusion dependent SCD patients (1-5). C = control; K = width constant; n = behaviour coefficient; TD = transfusion dependent.

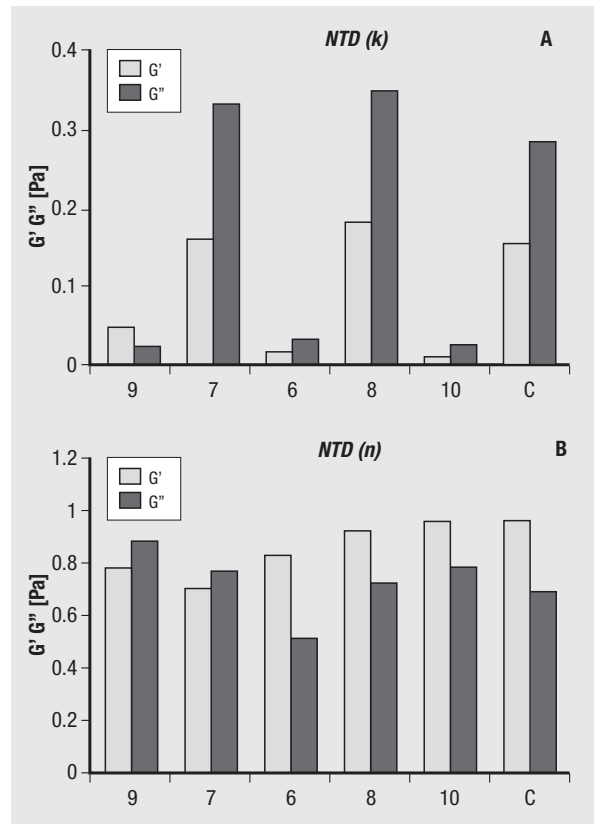


Fig. 4 A-B | Analysis of G' elastic modulus and G'' viscous modulus in no-transfusion dependent SCD patients (1-5). C = control; K = width constant; n = behaviour coefficient; NTD = no-transfusion dependent.

As regards the TD patients (Figures 3A-B), the most relevant observations were a decrease in the constant K values in TD-patients 1, 2, and 5, while the TD-patients 3 and 4 reported K values similar to control ones.

The constant n values, that are associated with the slope of the G' and G'' curves, presented viscous modulus greater than elastic one ($G'' > G'$) in the TD-patients 2, 3 and 4, while the trend of G' and G'' was comparable to control in the TD-patients 1 and 5.

As regards the NTD patients (*Figures 4A-B*), the analysis of G' and G'' moduli demonstrated a wide heterogeneity of K values, and in particular a marked decrease in G' and G'' was observed in NTD-patients 6, 9 and 10. About the constant n the viscous modulus was greater than the elastic one ($G'' > G'$) in NTD-patients 7 and 9 by showing a reversal of control trend.

DISCUSSION

Today, people affected by SCD have a “quality-adjusted life-years” and it is important to study this complicated disease with a multidisciplinary approach. It is not yet well understood the relationship between the physiological and rheological aspects and between the drug treatments and/or transfusional therapy and the rheological informations.

The red cell membrane viscosity and deformability in SCD has been showed to be different from those of normal erythrocytes, being sickled cells poorly deformable and this decrease in deformability leads to an increase in whole blood viscosity. Consequently, an increased impediment to flow induces an irregular erythrocyte aggregation, producing a reduction in oxygen saturation and resulting finally in further sickling of cells and vaso-occlusion in the microcirculation.

The measurement of viscoelasticity of the blood is a direct indicator of both the elastic and the viscous responses of the whole blood structure. The elastic (storage) modulus G' represents the assessment of the elastic storage of energy primarily due to kinetic deformability of the erythrocytes while the viscous (loss) modulus G'' is the assessment of the rate of energy dissipation due to cell deformation.

We have investigated the behaviour of the blood in SCD, from an original rheological point of view, by evaluating the viscoelastic properties of sickle cells in oscillating harmonic sinusoidal mode. A comparison between patients with different severity of the

disease, with TD or without NTD, has been carried out.

This study has confirmed the rheologic impairment of SC blood and has allowed to evidence an improvement of blood rheologic properties due to transfusion therapy. The TD patients showed a minor heterogeneity of rheologic behaviour in comparison with NTD patients, because of the normalizing effect of the transfusion. Furthermore, two different trends of $\tan \delta$ were observed independently by the treatment: a control-like behaviour and a marked slope. The evaluation of G' and G'' moduli has allowed to identify the different rheologic abnormalities of the patients, in particular the more solid-like behaviour of NTD patients with a decreased deformability. In spite of the undeniable damages of the transfusional therapy [23-25], up to today it seems to be a treatment strategy to prevent further complications of vasoocclusive events. Nevertheless, some silent subclinical processes can be masked for the existence of the chronic hypercoagulable state and in the presence of diminished flow and stasis.

The analysis of viscoelastic properties might be an additional useful tool in monitoring transfusional and pharmacological treatments and their effectiveness by providing particular insights into the deformability characteristics of sickle blood. Furthermore, the viscoelastic behaviour might give qualitative informations about the flow behaviour of the sickle blood and how the erythrocyte deformability affects the blood flow under different conditions.

Acknowledgments

The authors have greatly appreciated the superb technical assistance in data collection and management and in the preparation of the manuscript provided by Maria Gabriella Paolizzi. We are indebted to Mauro Pelella for his kindness.

Submitted on invitation.

Accepted on 3 April 2007.

References

1. Castle WB. From man to molecule and back to mankind. *Semin Hematol* 1976;13:59-69.
2. Opkala IE. New therapies for sickle cell disease. *Hematol Oncol Clin North Am* 2005;19:974-87.
3. Emmel WE. A study of the erythrocytes in a case of severe anemia with elongated and sickle-shaped red blood corpuscles. *Arch Intern Med* 1917;20:586-8
4. Pauling L, Itano H, Singer SJ, Wells IC. Sickle cell anemia: a molecular disease. *Science* 1949;110:543-65.
5. Weatherall DJ, Clegg JB. *The thalassaemia syndromes*. 3.ed. St.Louis (MI), USA: Blackwell Science Publishing; 1981.
6. Huisman THJ, Jonxis JHP. The hemoglobinopathies. *Clinical and Biochemical analysis* 1982;6:20-33.
7. Drayna D. Founder mutations. *Scientific American* 2005; 953: 60-7.
8. Weatherall DJ, Clegg JB. Inherited disorders: an increasing global health problem. *Bulletin WHO* 2001;79:704-12.
9. Platt OS. The sickle syndromes. In: Handin RI, Lux SE and Stossel TP (Ed.). *Blood: principles and practise of haematology*. Philadelphia: J.B. Lippincott Company; 1995. pp. 1645-700.
10. Silvestroni E, Bianco I. New data on microdrepanocytic disease. *Blood* 1955;10:623-32.
11. Lehmann H, Huntsman RG. *Man's s*. Amsterdam: North-Holland Publishing Company; 1966.
12. Mears JG, Beldjord C, Benabadi M, Belghiti YA, Baddou MA, Labie D, Nagel RL. The sickle gene polymorphism in North Africa. *Blood* 1981;58:599-601.
13. Nagel RL. Malaria and hemoglobinopathies. In: Steinberg MH. *Disorders of hemoglobin*. New York: Cambridge University Press; 2001. 832-60.
14. Bianco Silvestroni I. *Le talassemie: un problema medico-sociale ieri e oggi*. Roma: Istituto Italiano di Medicina Sociale; 1998. p. 329-39.
15. Ingram V. Sickle cell disease – molecular and cellular pathogenesis. In: Bunn HF, Forget BG (Ed.). *Hemoglobin: mo-*

- lecular, genetic and clinical aspects*. Philadelphia (PA): WB Saunders Company; 1986. p 452-501.
16. Hebbel RP & Vercellotti GM. The endothelial biology of sickle cell disease. *J Lab Clin Med* 1997;129:288-93.
 17. Briehl, R.W & Nikolopoulou P. (1993) Kinetics of hemoglobin S polymerization and gelation under shear: I. Shape of the viscosity progress curve and dependence of delay time and reaction rate on shear rate and temperature. *Blood* 1993;81:2420-8.
 18. Ballas SK, Mohandas N. Sickle red cell microrheology and sickle blood rheology. *Microcirculation* 2004;11:209-25.
 19. Dobbe JGG, Hardeman MR, Streckstra GJ, Strackee J, Ince C, Grimbergen CA. Analyzing red blood cell-deformability distributions. *Blood Cells, Molec and Dis* 2002;28:373-84.
 20. Stuart J, Nash GB. Red cell deformability and haematological disorders. *Blood Review* 1990;4:141-7.
 21. Handerman MR, Ince C. Clinical potential of *in vitro* measured red cell deformability, a myth? *Clin Hemorheol Microcirc* 1999;21:277-84.
 22. Gee B. Transfusion therapy. In: Eckman J, Platt A. (Ed.). Sickle cell information center-problem-oriented clinical guidelines (monograph on the internet 2004) Atlanta: Sickle Cell Information; 1997. Available from:<http://www.scinfo.org>
 23. Alexy T, Pais E, Armstrong JK, Meiselman HJ, Johnson CS, Fisher TC. Rheological behavior of sickle and normal red blood cell mixtures in sickle plasma: implication for transfusion therapy. *Transfusion* 2006;46:912-8.
 24. International Committee for Standardization in Haematology (ICSH). Expert panel on blood rheology. guidelines for measurement of blood viscosity and erythrocyte deformability. *Clinical Hemorheology* 1986;6:439-53.
 25. Serjeant G. Blood transfusion in sickle cell disease: a cautionary tale. *Lancet* 2003;361:1659-60.

Plasma exchange in acute and chronic hyperviscosity syndrome: a rheological approach and guidelines study

Marco Ballestri^(a), Federica Ferrari^(a), Riccardo Magistri^(a), Maria Mariano^(b), Giovanni Battista Ceccherelli^(b), Giorgio Milanti^(b), Marisa De Palma^(b) and Alberto Albertazzi^(a)

^(a) *Divisione e Cattedra di Nefrologia Dialisi e Trapianto renale;* ^(b) *Medicina Trasfusionale, Azienda Ospedaliero-Universitaria di Modena, Modena, Italy*

Summary. Therapeutic plasma exchange is an extra-corporeal technique able to remove from blood macromolecules and/or replace deficient plasma factors. It is the treatment of choice in hyperviscosity syndrome, due to the presence of quantitatively or qualitatively abnormal plasma proteins such as paraproteins. In spite of a general consensus on the indications to therapeutic plasma exchange in hyperviscosity syndrome, data or guide lines about the criteria to plan the treatment are still lacking. We studied the rheological effect of plasma exchange in 20 patients with plasma hyperviscosity aiming to give data useful for a rational planning of the treatment. Moreover, we verified the clinical applicability of the estimation of plasma viscosity by means of Kawai's equation. Plasma exchange decreases plasma viscosity about 20-30% for session. Only one session is required to normalize plasma viscosity when it is < 2.2 mPas, whereas a maximum of 3 sessions are required when it is > 2.2 till to 6 mPas. A fourth session is useless, especially if the inter-session interval is < 15 days. By means of a polynomial equation, knowing basal-plasma viscosity and the disease of a patient, we can calculate the decrease of viscosity obtainable by each session of plasma exchange then the number of session required to normalize the viscosity. Kawai's equation is able to evaluate plasma viscosity in healthy volunteers, but it is not clinically reliable in paraproteinemias.

Key words: therapeutic apheresis, plasma viscosity, hyperviscosity syndrome, plasma exchange.

Riassunto (Plasma exchange nella sindrome da iperviscosità acuta e cronica: approccio reologico e studio di linee guida). Il plasma exchange è una tecnica terapeutica extracorporea che consente di rimuovere dal sangue macromolecole lesive e/o supplementare fattori plasmatici carenti. Costituisce il trattamento di elezione della sindrome da iperviscosità, dovuta alla presenza nel plasma di proteine quantitativamente o qualitativamente anomale. Nonostante l'ampio consenso all'impiego del plasma exchange nella sindrome da iperviscosità, non vi sono al momento istruzioni operative o linee guida per la pianificazione del trattamento. Abbiamo studiato gli effetti emoreologici del plasma exchange in 20 pazienti con iperviscosità plasmatica al fine di ricavare dati utili per una pianificazione razionale della terapia aferetica. Abbiamo inoltre verificato l'applicabilità clinica della formula di Kawai per il calcolo teorico della viscosità plasmatica. Una singola seduta di plasma exchange riduce la viscosità plasmatica del 20-30%. Una sola seduta normalizza la viscosità plasmatica quando questa è < 2.2 mPas, mentre sono necessarie 3 sedute quando la viscosità è > 2.2, fino a 6 mPas. Una quarta seduta non risulta utile, specie se eseguita ad un intervallo < 15 giorni. Conoscendo la viscosità plasmatica iniziale e la patologia del paziente, utilizzando un'equazione polinomiale, è possibile calcolare il decremento di viscosità per ogni seduta ed il numero di sedute necessarie per normalizzarla. L'equazione di Kawai non consente un calcolo attendibile della viscosità plasmatica nei pazienti con paraproteinemia.

Parole chiave: aferesi terapeutica, viscosità plasmatica, sindrome da iperviscosità, plasma exchange.

INTRODUCTION

Therapeutic plasma exchange (TPE) is an extra-corporeal blood purification technique able to remove from plasma macromolecules not removable by means of haemodialysis and/or to replace deficient plasma factors [1]. About twenty years after

the birth and the empirical application of TPE [2], authoritative studies typed the diseases in which TPE may be useful and looked for guidelines in indications for TPE. Four categories of diseases had been identified [1, 3, 4]: the first category includes the diseases in which controlled trials suggested TPE as the

standard therapy *i.e.* thrombotic thrombocytopenic purpura or hyperviscosity; second category includes the diseases for which there is available evidence suggesting efficacy of TPE, *i.e.* systemic vasculitis, or myeloma-paraproteinemias; third category includes the disorders which have not adequately tests of efficacy of TPE at this time, *i.e.* progressive systemic sclerosis or multiple sclerosis; fourth category includes the disease for which it's not demonstrated efficacy of TPE in controlled trials, *i.e.* psoriasis or amyotrophic lateral sclerosis. Despite of a large consensus on guidelines concerning the indications to TPE, data or guidelines about the criteria to plan the treatment are still lacking [4].

We studied the use of TPE in dysproteinemias which can cause different kidney lesions (*i.e.* cast nephropathy, light chain deposition disease) and/or plasma hyperviscosity. Acute hyperviscosity syndrome (HS) can occur when the normal plasma viscosity (PV) of 1.4 mPas increase up to 4-5 mPas and it is more common in Waldenström's macroglobulinemia, than multiple myeloma or cryoglobulins [5]. In particular, acute HS can appear when plasmatic IgM is > 5 gr/dL or IgG3 and monomeric IgA > 4-5 gr/dL or polimeric IgA > 10-11 gr/dL. Clinical manifestations of acute HS are due to both vascular occlusion and impaired haemostasis; it includes ocular, neurological and cardiovascular dysfunctions and bleeding [6]. Really, acute HS is a very rare event whereas we often observe patients with asymptomatic light or mild plasma hyperviscosity, 2-3 mPas, due to paraproteins, high levels of immunoglobulins, alfa globulin or lipids. TPE is the treatment of choice of acute HS and it is however able to effectively and rapidly correct plasma viscosity during the period that other therapeutic interventions such as chemotherapy take effect. It's well known that the efficiency of TPE is different for different molecules and ranges from 15 to 75%; it is highest for IgM because of their prevalent intravascular distribution and is 4-5 fold lower for IgG because of their wide extravascular distribution [1, 7]. In spite of this, quantitative data about the rheological effect of TPE are lacking and parameters regarding the start, the frequency and the end point of TPE are usually empirically settled.

Aims of the study were: a) to get a status-report of our clinical behaviour; b) to quantify the rheological efficacy of TPE; c) to give data useful in planning TPE; d) to create a model for computation the number of TPE-sessions required to normalizing PV in each patient on the basis of his basal PV and his disease; e) to verify the clinical applicability of the estimation of PV by means of Kawai's equation (KE). In fact, KE could be very helpful in hospital units where viscometers or rheometers are unavailable.

METHODS

We studied 20 patients undergone to TPE for a total of 51 treatments. The mean age of the pa-

tients was 65±14 years. They were undergoing to TPE because of multiple myeloma (MM) 30%, Waldenström's macroglobulinemia (WM) 25%, monoclonal gammopathy of undetermined significance (MGUS) 5%, cryoglobulinemia (CG) 25%, other inflammatory disease (ID) 15% with increased alfa-globulins and/or polyclonal immunoglobulins, such as collagenopathies.

The technique of plasma exchange was: continuous flow system; mean volume of exchange 40 ml/kg/session; acid-citrate-dextrose as anticoagulant. Replacement solution composition: albumin 3.3%, Na 154 mEq/L, K 3 mEq/L, Ca 2.5 mEq/L.

We measured PV with the rheometer Hakke-CV100 (Hakke GmbH, Karlsruhe, Germany) at even temperature of 37 °C and shear rate 300 s⁻¹, accordingly with the indications of the International Committee for Standardization in Haematology standards [8]. The measures had been done pre and post TPE. In CG, the PV had been measured at temperature of 30 °C too.

Moreover, we estimated the rough PV pre and post TPE and in 30 healthy volunteers by means of the equation of Kawai [9, 10]:

$$PV = 0.204 + (0.177 \times PT)$$

where PV is plasma viscosity expressed as mPas and PT are plasma proteins expressed as g/dL.

All the data concerning PV were analyzed after the end point of TPE program, therefore results and values of PV did not influence planning and frequency of the treatments.

RESULTS AND DISCUSSION

First of all, we could obtain a status-report of our clinical behaviour at this time. Empirically, we prescribed 3 TPE for patients with MGUS, 4 for MM and 5 for WM. In CG and ID we tend to prescribe a major number of treatments, till to 7. The interval between the treatments was less than a week (from 1 to 5 days) for the first 4 sessions, and usually above 15 days for following sessions. The end point of TPE was empirically decided for patients with paraproteinemias, whereas for the other diseases, included CG, it was determined especially on the basis of laboratory and clinical signs of remission.

Figure 1 shows the rheological effects of each TPE-session. The rheological efficiency (RE) of TPE in decreasing PV was major when major was basal-PV. By the analysis of the figure we can roughly foresee that the normalization of a basal-PV < 2.2 mPas requires only one TPE-session; whereas, the required sessions are almost 2 when basal-PV is > 2.2 till up to 6 mPas. Nevertheless, it must be considered that the RE of each session is varying during a TPE program. In fact, the RE tended to progressively decrease in relation to the progressive decrease of PV. Really, as shown in Figure 2a, a significant fall of RE appeared only during the fourth consecutive

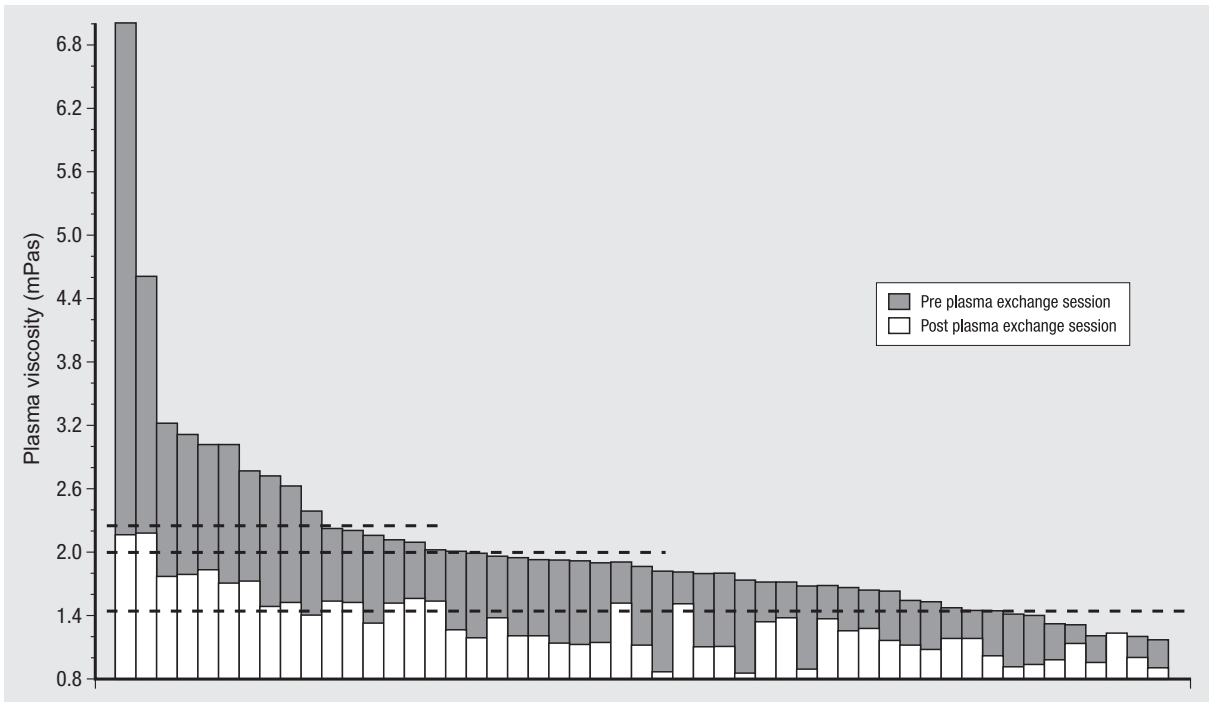


Fig. 1 | Rheological effects of each therapeutic plasma exchange session. Higher is basal plasma viscosity therefore greater is the decrease of viscosity post apheresis. A single one session of plasma exchange normalizes plasma viscosity when it is < 2.2 mPas. Whereas 2 sessions are required when plasma viscosity is > 2.2 till to 6 mPas.

session of TPE. Moreover, TPE is very able to remove molecules, but it don't stop their production and PV could tend to rise during the break between the sessions. *Figure 2b* shows the mean increasing

of PV between consecutive sessions of TPE, due to redistribution and/or neo-production of plasma proteins and/or paraproteins. Really, PV reached again to the starting levels only in occasion of the

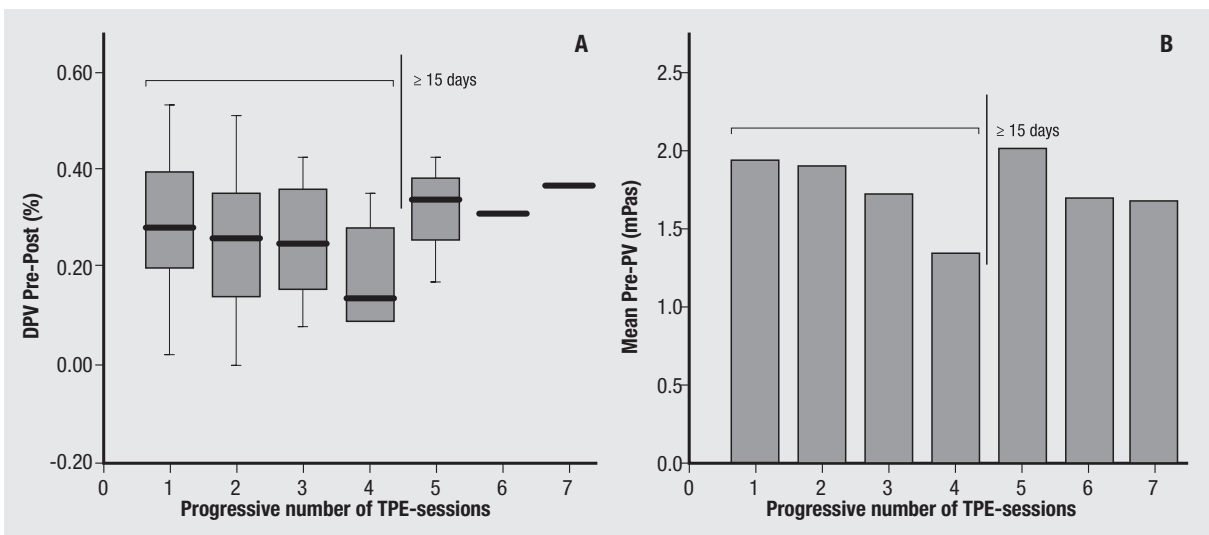


Fig. 2 | a) the fall in rheological efficiency of plasma exchange (DPV pre-post) was significant only during the fourth consecutive session. It increased again after an interval ≥ 15 days, when plasma viscosity (PV) was increased too. Whereas, the break between the first four sessions was ≤ 5 days. b) mean plasma viscosity pre-plasma exchange (PrePV) during consecutive session. PrePV progressively decreased till to a nadir after the third session and increase again after the break ≥ 15 days.

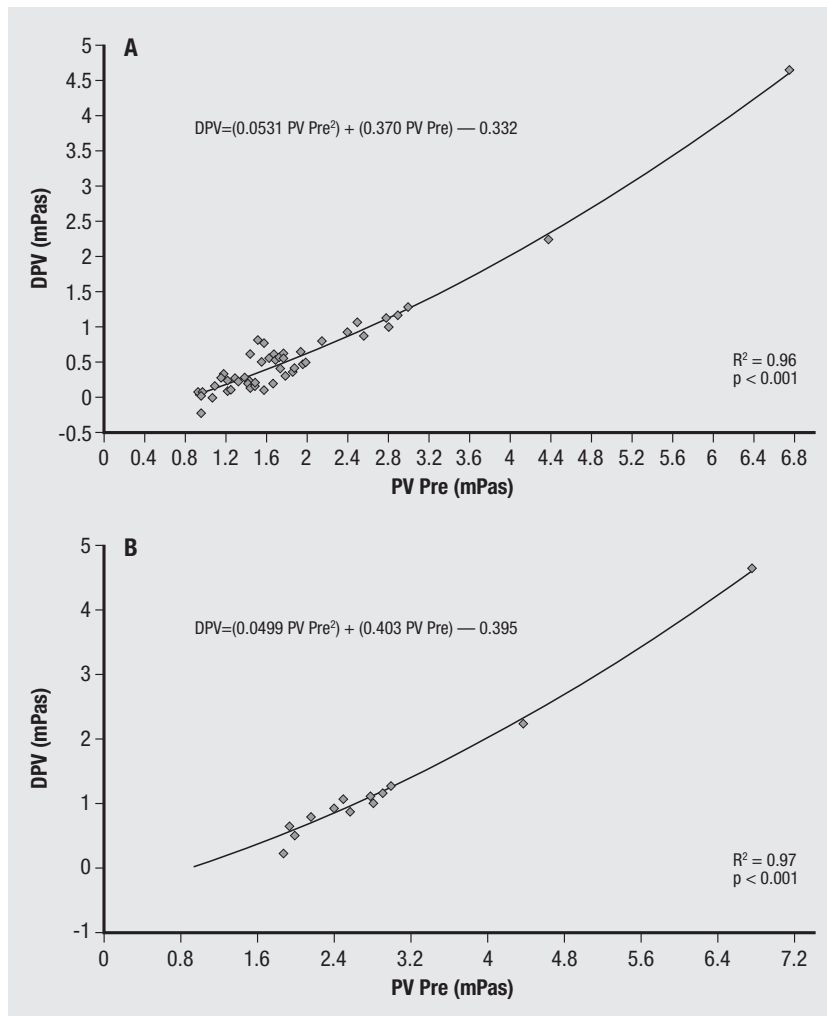


Fig. 3 | Correlation between gradient of plasma viscosity pre and post apheresis (DPV) in function of basal plasma viscosity (PV). It's possible to roughly calculate a polynomial relation by mean of which the DPV of each plasma exchange can be predicted. Then, the number of sessions required to normalize PV can be estimated. a) Curve calculated on the basis of the overall cases. b) Curve calculated on the basis of GM and MM patients.

fifth session, usually performed ≥ 15 days after the fourth. Nevertheless, we take into account that rate of productions can be very variable and depending to type and severity of the disease and to medical treatments such as chemotherapy.

The study of rheological effect of the TPE-sessions in the different diseases confirmed the greatest efficacy in decreasing PV in WM (about $33 \pm 0.12\%$), because of the prevalent intravascular distribution of IgM [1]. The decrease was $20 \pm 0.21\%$ in MM, $17 \pm 0.04\%$ in MGUS, $19 \pm 0.12\%$ in CG and $33 \pm 0.09\%$ in ID. The high rheological efficiency of TPE obtained in ID could be explained by the complex genesis of hyper-PV, probably due to synergic effect of alfa- and gamma-globulins. On the contrary, in CG, the influence of immunoglobulins became evident only when we measured PV at temperature 30°C , whereas at 37°C , the hyper-PV seemed mainly due to alfa-globulins. Nevertheless, because of the little number of cryoglobulinemic patients, we did not obtain the statistical significance.

The analysis of PV-decreasing in function of basal-PV showed a polynomial relation expressed by the following equation (Figure 3):

$DPV = (0.0531 PV Pre^2) + (0.370 PV Pre) - 0.332$ where DVP is the gradient of PV pre-post a single session of TPE and PV Pre is PV at the start of the session.

The standard error of this equation is 0,1 ($R^2 = 0.96$; $p = 0.000$). The error lightly increases when PV Pre is < 2 mPas, but in this case only one session of TPE is sufficient to normalize PV and no long planning is request. Testing the correlation in the different diseases, we could confirmed a more closely correlation only in the lympho-immunoproliferative disorders and we could be define more specific numeric coefficients to reduce the standard error. In particular, $DPV = (0.045 PV Pre^2) + (0.4485 PV Pre) - 0.4533$ for MM ($R^2 = 0.99$; $p = 0.000$); $DPV = (0.0347 PV Pre^2) + (0.4584 PV Pre) - 0.4307$ for WM ($R^2 = 0.95$; $p = 0.000$) and $DPV = (0.0499 PV Pre^2) + (0.403 PV Pre) - 0.3949$ ($R^2 = 0.97$; $p = 0.000$) for MM + WM.

KE was perfectly reliable when applied to estimate PV in healthy volunteers and in patients affected by ID (Table 1). On the contrary, it was not reliable in calculating PV pre-TPE in patients with paraproteinemias because of an evident undervaluation. KE was again reliable post TPE-session, that is after

Table 1 | Difference between plasma viscosity (PV) measured (M) and roughly calculate with Kawai's equation (KE)

		HV	AI	MM	WM	MGUS	CG	ID
PV Pre	M (mPas)	1.47 ± 0.10	1.96 ± 0.99	2.94 ± 1.93	2.02 ± 0.43	1.42 ± 0.20	1.47 ± 0.27	1.70 ± 0.19
	KE	1.47 ± 0.06	1.58 ± 0.30	1.93 ± 0.26	1.66 ± 0.18	1.35 ± 0.01	1.25 ± 0.15	1.74 ± 0.12
	p	n.s.	0:03	n.s.	0.008	n.s.	0:02	n.s.
PV Post	M (mPas)		1.21 ± 0.23	1.20 ± 0.03	1.33 ± 0.27	1.18 ± 0.24	1.09 ± 0.21	1.22 ± 0.22
	KE		1.14 ± 0.18	1.64 ± 0.28	1.15 ± 0.03	1.07 ± 0.03	1.01 ± 0.08	1.19 ± 0.08
	p		n.s.	n.s.	n.s.	n.s.	n.s.	n.s.

PV Pre: PV pre plasma exchange; PV Post: PV post plasma exchange; HV: healthy volunteers; MM: multiple myeloma; WG: Waldenström's macroglobulinemia, MGUS; monoclonal gammopathy of undetermined significance; CG: cryoglobulinemia; ID: other inflammatory diseases. Kawai's equation (KE).

removal of paraproteins from plasma. The absence of statistic significance in MM and MGUS group was due respectively to the high variance and to the small dimension of the sample. These observations confirm that hyperviscosity in paraproteinemias is due not only to the concentrations of paraproteins [5], but also to their abnormal shape, abnormal polymerisation, and/or interaction with other plasma-proteins. On the contrary, the increase of PV in ID is due to an excess of normal plasma proteins (mainly alfa-globulins and/or polyclonal immunoglobulins) and only their concentration influences PV.

CONCLUSIONS

TPE is a useful technique able to rapidly correct HS and mainly decrease PV about 20-30% each session. Probably, the existing empirical approach to planning TPE-treatment in hyper-PV causes a little overdose of this therapy. Only one TPE-session is required to normalize PV when it is < 2.2 mPas, whereas a maximum of 2-3 session are required when it is > 2.2 till up to 6 mPas. In general, a fourth session is useless especially if the inter-session period is < 10-15 days.

We can roughly calculate the decrease of PV obtainable by each TPE-session and the number of session required to normalize PV, knowing basal-PV and the dis-

ease of a patient. The polynomial equation suggested is: $= (0.0499 PV Pre^2) + (0.403 PV Pre) - 0.395$. However it is possible to use more disease's specific coefficients.

KE is not clinically reliable to evaluate PV in paraproteinemias because paraproteins can influence PV by means of interaction mechanisms and independently by their concentrations.

Actually we are performing studies on larger populations, this effort will permit to develop a simply software for automatic planning of TPE-treatment in HS.

Moreover, we need studies able to clarify when the correction of hyper-PV is indicated. Acute HS is of very rare occurrence, therefore light or mild chronic asymptomatic hyper-PV is of very frequent observation in patients with paraproteins, inflammation disorders, hyper-fibrinogenemia, hyper-lipoproteinemia, metabolic syndrome and so on. The rule of chronic hyperviscosity in stimulating endothelial responses is probably underestimated and we cannot exclude the existence of a chronic HS (CHS) able to impair microcirculation and promote progression of target organ-damage. Probably, TPE will not be the treatment of choice for CHS: it will be a new venture.

Submitted on invitation.

Accepted on 3 April 2007.

References

- McCulloch J. Therapeutic apheresis In: McCulloch J. (Ed.) *Transfusion Medicine*. Philadelphia: Elsevier Churchill Livingstone, 2005; p. 517-47.
- McCarthy L. Therapeutic apheresis: current prospectives. *Ther Apher* 2002;6:1.
- Smith JV. Therapeutic apheresis in the United States: current indications and directions. *Ther Apher* 1999;3:1-3.
- Teruya J. Practical issues in therapeutic apheresis. *Ther Apher* 2002;6(4):288-9.
- Metha J, Singhal S. Hyperviscosity syndrome in plasma cell dyscrasias. *Semin Thromb Hemost* 2003;29:467-71.
- Rampling MW. Hyperviscosity as a complication in a variety of disorders. *Semin Thromb Hemost* 2003;29:459-65.
- Zarkovic M, Kwaan HC. Correction of hyperviscosity by apheresis. *Sem Thromb Hemost* 2003;29:535-42.
- International Committee for Standardization in Hematology. Guidelines for measurement of blood viscosity and erythrocyte deformability. *Clin Hemorheol* 1996;8:83-8.
- H Kawai. Proceedings, 4th Congress on rheology, New York, 1965.
- Remuzzi A, Brenner BM, Pata V, Tebaldi G, Mariano R, Belloro A, Remuzzi G. Three-dimensional reconstructed glomerular capillary network: blood flow distribution and local filtration. *Am J Physiol* 1992;263(3 Pt 2):562-72.
- Baskurt OK, Meiselman HJ. Blood rheology and hemodynamics. *Sem Thromb Hemost* 2003;29:435-50.
- Lehoux S, Castier Y, Tedgui A. Molecular mechanisms of the vascular responses to haemodynamics forces. *J Int Med* 2006;259:381-92.

Deformability and viability of irradiated red cells

Roberto Reverberi^(a), Maurizio Govoni^(b) and Marina Verenini^(b)

^(a)*Servizio di Immunoematologia e TrASFusionale, Arcispedale S. Anna, Ferrara, Italy*

^(b)*Servizio di Immunoematologia e Medicina TrASFusionale, Ospedale Maggiore, Bologna, Italy*

Summary. The irradiation of blood components with X or gamma rays is necessary to prevent the graft-versus-host disease, but it also provokes untoward effects. In particular, red cells are damaged and have a decreased *in vivo* recovery, an increased *in vitro* haemolysis, and a leakage of potassium in the supernatant. The results of the clinical studies show that the loss of viability progressively increases with the storage after irradiation. On the other hand, the storage before irradiation is inconsequential. The mechanism through which irradiation causes the loss of viability is unknown, but a critical examination of the literature and our results indicate that the erythrocyte deformability is the only parameter related to viability to show sufficiently precocious and important changes. We also tried to identify the mechanism by which irradiation influences deformability and examined, in particular, the changes in the mean cell volume (MCV) and vesiculation. However, the temporal behaviour of both suggests no causal relationship.

Key words: irradiation, erythrocyte viability, erythrocyte deformability, erythrocyte filterability.

Riassunto (*Deformabilità e vitalità di globuli rossi irradiati*). L'irradiazione degli emocomponenti con raggi gamma o X è indispensabile per prevenire la graft-versus-host disease, ma provoca anche effetti collaterali. In particolare, i globuli rossi subiscono un danno che si evidenzia come diminuita vitalità *in vivo*, aumento di emolisi *in vitro* e rilascio di potassio nel soprannatante. I risultati degli studi clinici dimostrano che la perdita di vitalità aumenta progressivamente con la conservazione dopo irradiazione. Al contrario, la conservazione prima dell'irradiazione è ininfluenza. Il meccanismo con il quale l'irradiazione provoca la perdita di vitalità è ignoto ma un esame critico della letteratura e dei nostri risultati mostra che la deformabilità eritrocitaria è l'unico parametro correlato con la vitalità che subisce variazioni abbastanza precoci ed importanti dopo irradiazione. Noi abbiamo cercato di identificare anche il meccanismo che lega l'irradiazione e la perdita di deformabilità ed, in particolare, abbiamo rivolto la nostra attenzione ai cambiamenti di volume corpuscolare medio dei globuli rossi (MCV) ed alla vescicolazione. Tuttavia, il comportamento nel tempo di ambedue non suggerisce una relazione causale.

Parole chiave: irradiazione, vitalità eritrocitaria, deformabilità eritrocitaria, filtrabilità eritrocitaria.

INTRODUCTION

In 1989, 10.1% of all blood components transfused in the USA were irradiated to prevent the graft-versus-host disease and the percentage has certainly increased in more recent years [1]. Some experts even advocate universal irradiation of cellular blood components [2].

The recommended dose of radiation (25 to 30 Gy of gamma or X rays) [3] is remarkably effective in abrogating the T-lymphocyte proliferation, but also entails untoward effects. In particular, erythrocytes suffer a damage, which manifests itself as a decreased post-transfusion viability, an increased haemolysis and a leakage of potassium in the extracellular space [1]. Surprisingly little data are available about the mechanism(s) that impair viability. One of the factors involved could be the erythrocyte deformability. We studied the deformability changes

after irradiation, together with other cell properties and characteristics, and tried to correlate them to the loss of viability. In the first part of the present review, we will examine the data on viability and the possibly related parameters. In the second part, we will discuss the mechanism(s) underlying the loss of deformability after irradiation.

IRRADIATION AND RED BLOOD CELL VIABILITY

The kinetics of *in vivo* survival of red cells, transfused after a long storage *in vitro*, is usually composed of a steep initial decrease, followed by a slower linear decline. It is a classic two-component curve, with the first component due to the rapid removal of non-vital red cells from circulation, whilst the second is caused by progressive aging. The two

components are influenced by different factors [4] and therefore they are (partially) independent. The initial component is estimated 24 h after transfusion (24-h recovery). The second requires measurements more prolonged in time (long-term survival).

The first studies on the effects of irradiation on red cell viability were performed during experimental research on extracorporeal irradiation of blood as a therapy for leukaemia [5]. The dose levels varied from 350 to 2000 Gy, one or two orders of magnitude greater than those used today. Autologous blood was irradiated in the extracorporeal circulation, labelled with ^{51}Cr and immediately reinfused. Schiffer *et al.* [5] noticed the two-component curve. The 24-h recovery correlated linearly with the dose. On the contrary, the relationship with long-term survival was exponential, with a modest variation up to 500 Gy and marked effects at higher doses.

The first study on stored blood was conducted by Button *et al.* [6] (Table 1). The viability of packed red cells or whole blood, stored 21 days in citrate-phosphate-dextrose (CPD) and irradiated before transfusion, was measured in 17 and 16 pa-

tients, respectively, and compared with non-irradiated controls. The dose ranged from 50 to 200 Gy. The authors observed no significant difference in the 24-h recovery, but long-term survival was impaired at all dose levels, although the difference was statistically significant with 200 Gy only (T_{50} : 23.2 days, vs 28.7 in the controls).

Considering the first results, it is surprising that long-term survival was reported in two further studies only [7, 8]. In both cases, the dose was 25 Gy and survival was slightly reduced [7] or not varied [8].

Studies reporting the 24-h recovery were more numerous (Table 1). In most cases, authors utilized volunteers who were transfused, at an appropriate interval of time, with autologous irradiated or non-irradiated red cells. This kind of experimental design permits to lessen the influence of the variability between subjects and to obtain significant results studying just a few cases. Friedman *et al.* [9] used red cells stored in Nutricel (AS3), irradiated (20 Gy) on day 1 and transfused after 21 or 28 days of storage (6 volunteers). They observed that the 24-h recovery was significantly decreased by irradiation,

Table 1 | Summary of available data on 24-h recovery of irradiated red blood cells

Author	Storage solution	Dose (Gy)	Day of		24-h Recovery (%)		P	Note
			Irradiation	Transfusion	Irradiated	Control		
Button [6]	CPD	50	21	21	78.0		NS	Whole blood
		100	21	21	84.3	81.2	NS	
		200	21	21	77.5		NS	
		50	21	21	82.6		NS	
		100	21	21	83.8	81.7	NS	
		200	21	21	78.4		NS	
Friedman [9]	AS3	20	1	21	82.7	90.4	≤0.03	
			1	28	80.7	85	≤0.03	
Davey [10]	AS1	30	0	42	68.5	78.4	<0.02	
Moroff [7]	AS1	25	1	28	78.5	83.7	NR	
			14	42	69.5	76.4	NR	
Suda [12]	AS1	15	0	6	90.9	91.1	NS	Frozen
Mintz [13]	AS1	30	0-1	35	78.0	81.8	NS	
Miraglia [13]	CPDA-1	35	0	5	89.7	90.6	NS	Frozen
			7	14	85.3	83.7	NS	Frozen-rejuvenated
			14	18	79.5	82.6	NS	
Davey [15]	AS3	25	0	42	78.9	/	0.012	Leucoreduced
					72.3			Non leucoreduced
Moroff [8]	AS1	25	1	28	78.1	84.8	<0.01	
			14	42	68.8	76.3	<0.01	
			14	28	81.3	84.3	NS	
			26	28	80.7	82.0	NS	
Valeri [14]	CPDA-1	25	3-6	6-9	86.0	83.2	NS	Frozen

NS = Not significant.

NR = Not reported.

tion (21 day storage: 82.7 vs 90.4%; 28 day storage: 80.7 vs 85.0%), although it remained higher than 75%. A similar study, with red cells stored in Adsol (AS1), irradiated on day 0 (30 Gy) and transfused on day 42, confirmed the decreased recovery (68.5 vs 78.4%) [10]. In 6 out of 8 irradiated blood units, recovery was lower than 75%, whilst that only happened in 1 case out of 8, with control red cells. These results were substantially confirmed by Moroff *et al.* [7], again with red cells in AS1 and a dose of 25 Gy (Table 1). On the contrary, Mintz and Anderson [11], in similar conditions (red cells in AS1, 30 Gy) found no significant difference after 35 days of storage from irradiation.

A more complex experimental design was used by Moroff *et al.* [8], in order to verify the influence of storage before and after irradiation. Results showed convincingly that storage before irradiation entailed no difference in viability with the controls. On the contrary, the more the storage after irradiation was prolonged, the more viability was decreased (Table 1).

In three studies, red cells were irradiated before [12, 13] or during [14] the frozen storage. In those experiments, the dose levels ranged from 15 to 35 Gy and the storage after irradiation was at most 6 days. No difference in recovery was observed. Finally, only one study evaluated the effect of leucoreduction [15]. Red cells from 7 volunteers were collected in AS3, irradiated on day 0 with 25 Gy and transfused on day 42. Half of the blood units had been leucoreduced by filtration before irradiation. They showed a slightly but significantly better recovery (78.0 vs 72.3%).

Altogether, it may be concluded that 24-h recovery is impaired by irradiation and the difference between irradiated and control red cells increases as storage after irradiation is prolonged (about 2% per week [16]). On the other hand, storage before irradiation seems to be inconsequential. In the light of these facts, the recommendation by Food and Drug Administration (FDA) that red cells should not be stored more than 28 days after irradiation seems appropriate [17]. On the contrary, the European guidelines [18] (and the Italian law [19]) appear unjustified in forbidding irradiation after the 14th day of storage: data clearly show that it is better to irradiate the blood units after 28 days of storage, rather than storing up to day 28 red cells irradiated on day 14.

The few data on survival suggest that at the current dose levels the effect of irradiation is minimal or absent. Finally, it may be noticed that all studies cited in Table 1 come from North America: this explains why red cells stored in SAGM, the solution used in Europe, were not studied.

FACTOR(S) RESPONSIBLE FOR THE DECREASED VIABILITY

From the above-mentioned considerations, some characteristics emerge, which must be possessed by

the factor(s) responsible for the decreased viability. In principle, the following characteristics could be used to identify the factor(s): it must differ between irradiated and control red cells; the difference must increase with the dose and the length of storage after irradiation; however, it must not vary immediately after irradiation; moreover, it should presumably be a factor also influencing viability prescinding from irradiation.

Role of adenosine-triphosphate (ATP)

Bearing in mind the data accumulated on the relationship between ATP and erythrocyte viability [20], ATP concentration or total adenine nucleotide concentration are the most plausible candidates. However, many studies found no significant difference between irradiated and control red cells [9, 15, 21-23]. Moroff *et al.* [8] reported that ATP was decreased, in comparison to the controls, in red cells irradiated on day 14 and measured on day 42. However, in the same study, the difference was not significant in blood units irradiated on day 1 and measured on day 28. In both cases, *in vivo* recovery was significantly different. *Vice versa*, ATP was significantly decreased in blood units irradiated on day 14 and measured on day 28, but *in vivo* recovery was not. A discrepancy between *in vivo* recovery and ATP concentration, with the first one significantly decreased and the second not, was also found by Friedman *et al.* [9] and Davey *et al.* [15]. A decreased ATP concentration, in comparison to controls, was described by Moore and Ledford [24] (40 Gy) and Leitner *et al.* [25] (30 Gy), after 21 days of storage post-irradiation; by Hillyer *et al.* [26] (35 Gy) and Davey *et al.* [10] (30 Gy), after 42 days. Notwithstanding the statistical significance, Moore and Ledford [24] commented that the difference was small, similar to that encountered between different data sets collected in the same conditions. They supposed, therefore, that it would not have been biologically significant. Finally, in the three studies in which ATP concentration was measured systematically every 7-14 days [24-26], the difference between irradiated and control red cells did not increase progressively in time. This last fact, and the modest variation in comparison to the controls, indicates that ATP is not the factor responsible for the impaired viability.

In vitro haemolysis

Irradiation causes immediate haemolysis of red cells, but only at much higher doses than currently used [27]. In those circumstances, the cell membrane is damaged, ions can freely diffuse across and this causes an osmotic lysis. At usual doses, haemolysis does not appear immediately after irradiation [24, 25, 28]. During the storage post-irradiation, haemolysis increases more markedly in the irradiated red cells than in the controls, but the difference is only significant after 4 [8], 5 [24, 25] or 6 weeks [10, 26]. In fact, we found that the irradiated samples showed

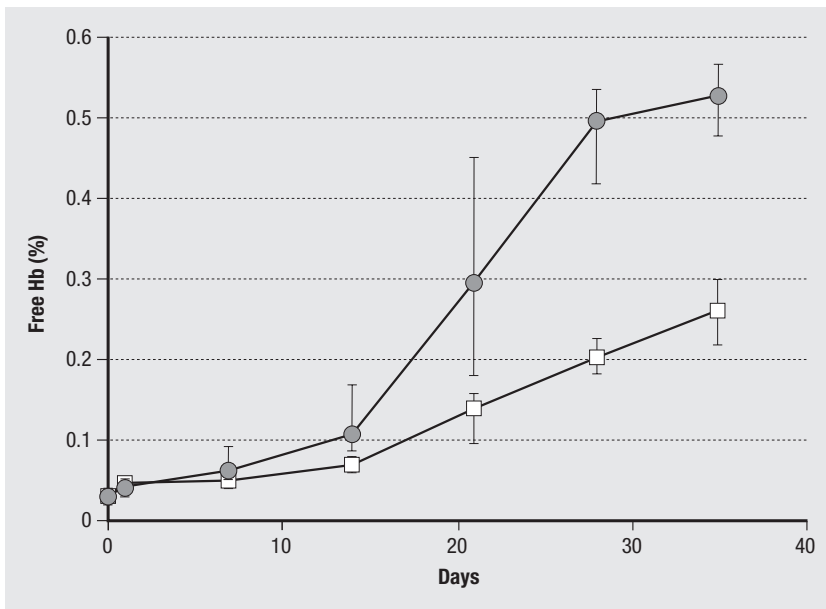


Fig. 1 | Free haemoglobin (haemolysis), expressed as a percentage of the total haemoglobin content, after irradiation with 25 Gy of gamma rays. Irradiation was performed on day 1. Data are medians of 6-12 samples. Error bars connect the first and the third quartile. (Closed circles: irradiated; open squares: non irradiated)

a greater haemolysis since the first week of storage, in comparison to the controls (*Figure 1*). However, haemolysis was very low in the first weeks of storage and, in any case, values remained lower than 1% even after 5 weeks. Therefore, haemolysis represents no more than a small percentage of the red cells that do not survive after 24 hours.

Osmotic resistance

In a classic study on red cell storage, osmotic resistance (more exactly, haemolysis in 0.6% NaCl) was the parameter best correlated with the *in vivo* recovery, excepting ATP concentration [29]. Osmotic resistance actually measures the surface/volume ratio, which decreases during storage because of the loss of part of the cell membrane [30]. One of the first studies on irradiation of red cells reported surprising results about the osmotic resistance: immediately after irradiation there was no difference with the controls, but after an incubation at 37 °C for 24 hours, osmotic resistance increased with doses of 500-1000 Gy and markedly decreased with 2000 Gy [5]. The authors offered no explanation for this phenomenon but, 40 years later, we are able to formulate a plausible conjecture: the decreased resistance at the higher dose probably reflects the severe membrane damage also responsible for immediate haemolysis (see above). The increased resistance at lower doses is probably provoked by a less severe damage but sufficient to activate, during the 37 °C incubation, the K-Cl cotransport [31]. This, on its part, causes dehydration and an increase in the surface/volume ratio. The only other study [32] that reported data on osmotic resistance, utilized a dose of radiation much nearer (50 Gy) to the recommended one. Before measurement, red cells were incubated at 37 °C for an hour. Contrarily to the study cited above [5], irradiation caused a modest but signifi-

cant increase of haemolysis in 0.65% NaCl. The difference with the controls was already evident after a week of storage but did not increase afterwards. In the presence of a powerful antioxidant (tirilazad mesylate), haemolysis in 0.65% NaCl halved in both the irradiated sample and the control. Autologous plasma (final haematocrit 42-47%) was even more effective (six fold reduction). Authors attributed the erythrocyte damage by irradiation and storage to oxidative processes, and the protective effects of plasma to antioxidant properties. In conclusion, osmotic resistance is influenced by factors not related to erythrocyte viability [4] and, therefore, it cannot be directly responsible for the loss of viability after irradiation.

Deformability and other rheologic parameters

A close relationship between erythrocyte deformability and viability was described four decades ago by Haradin *et al.* [33]. They used a rudimentary filterability technique and the measurement of viscosity. However, examining their published graphs, the inferred relationship could be explained by the fact that both viability and the rheologic modifications are time-dependent. A more convincing demonstration was offered by Card *et al.* [34], who studied a subject whose red cells lose viability at an accelerated pace during storage. All haematological and biochemical parameters (including ATP) were normal, except deformability (measured with the ektacytometer), which worsened much faster than in the controls. There are just a few studies on the rheology of irradiated red cells. A Japanese group evaluated the elongation of erythrocytes under various shear stresses (deformation index) [21, 35, 36]. Red cells in mannitol, adenine, phosphate (MAP), irradiated with 15 or 35 Gy of X rays, showed a lower deformation index, in comparison to controls, starting from

2-3 weeks of storage [35]. The difference in terms of percentage of erythrocytes not deformable at low shear stress (33 dyn/cm^2) was even more evident. Similar results were obtained with gamma rays (35 Gy) [36]. Surprisingly, with the same experimental apparatus, red cells irradiated with 50 Gy (X rays) and stored up to 4 weeks in CPD did not show any difference with the controls [21]. In this last study, the authors did not find variations of mean cell volume (MCV) during storage. On the contrary, in the studies with MAP, MCV decreased progressively during storage. Presumably, this happened partly because of the hypertonicity of MAP, and partly because of the potassium leakage (see below). We consider it probable that this kind of deformability measurement be mainly a function of MCV. An alternative explanation for the difference between the results with CPD and with MAP is the presence of plasma in the first. A study already quoted above showed that plasma protects the red cells against the oxidative damage [32]. In any case, considered the results with MAP, which certainly preserves the erythrocytes better than CPD, we may conclude that this deformability test is not correlated with viability. Another kind of experimental apparatus, according to Barjas-Castro *et al.* [37], measures the elasticity of single erythrocytes. In fact, however, it is based on the deformation of cells dragged along the direction of flow. Up to 14 days of storage in citrate-phosphate-dextrose-adenine-1 (CPDA-1), there was no difference between red cells irradiated with 25 Gy and controls (not even in comparison to day 0). The differences appeared after 21 days and were very marked after 28 days. Despite the opinion of the authors, the results leave many doubts about the sensitivity of this test.

We studied the deformability of leucoreduced red cells, irradiated with 25 Gy and stored in saline-ad-

enine-glucose-mannitol (SAGM). Our technique measures the filterability through $3 \mu\text{m}$ pores and was designed to eliminate the influence of known disturbing factors: the red cell suspension is free of leucocytes, platelets and plasma; the test is performed at 37°C in a buffer at pH 7.4 and normal osmolarity [38]. With our technique, we evidenced differences of deformability already after a week of storage in several anticoagulant and nutrient solutions [39]. *Figure 2* shows the results obtained with irradiated red cells and controls (the same blood units were divided in two aliquots). On the day after irradiation the differences are not evident, but they appear already after a week and increase progressively in time (note that the data reported in *Figure 2* are logarithmically transformed). Judging from the graph (*Figure 2*), irradiated red cells present deformability values, after a week of storage, similar to non-irradiated red cells after 3 weeks. Altogether, erythrocyte deformability, as measured by our filterability technique, has a temporal behaviour corresponding to what is known about viability.

IN WHAT WAY IRRADIATION INFLUENCES DEFORMABILITY?

If deformability is really the factor responsible for the loss of red cell viability after irradiation, it is appropriate to look for the mechanism that connects the two. Obviously, none of the factors discussed above can be the missing link. In this part, we will examine the relationship between irradiation and some characteristics that may influence deformability, like MCV and vesiculation. Moreover, we will consider the leakage of potassium, which has a temporal behaviour much like deformability. First of all, however, we will discuss the primary effects of irradiation.

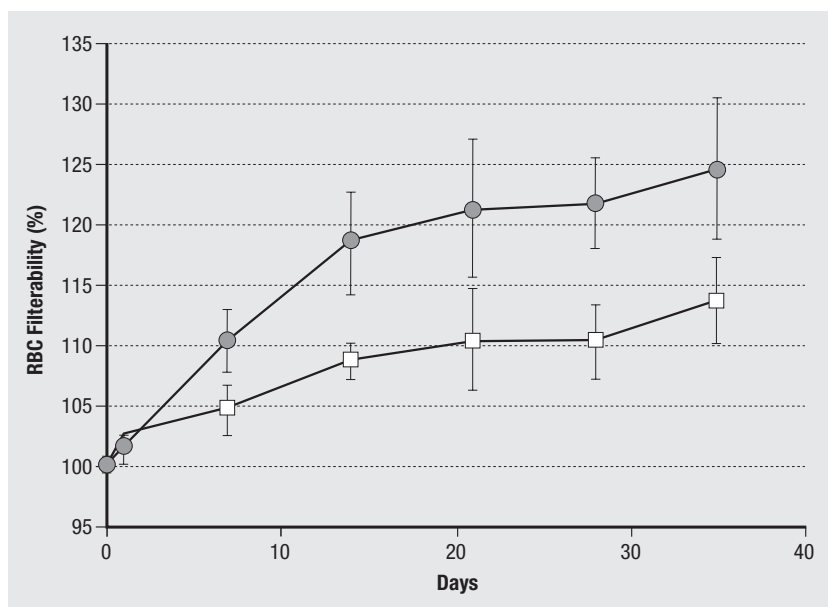


Fig. 2 | Red cell filterability (deformability) after irradiation with 25 Gy of gamma rays. Filterability is the time necessary for a 10ml volume of a dilute red cell suspension to pass through a $3\mu\text{m}$ pore filter. A higher value means a lower deformability. Raw data were logarithmically transformed and expressed as percentages with reference to the initial sample (day 0). Irradiation was performed on day 1. Data are means of 6-12 samples. Error bars represent 1 SD. (Closed circles: irradiated; open squares: non irradiated)

Primary effects of radiation on red cells

Mature erythrocytes are relatively radioresistant in comparison to other blood cells [27] and the type of damage is different: in nucleated cells, the main target of radiation is DNA. Therefore, leucocytes are exquisitely sensitive to alpha particles. Instead, red cells prevalently suffer an indirect damage, caused by water radiolysis that generates reactive oxygen species (ROS). For this reason, X or gamma rays are more effective [40]. Further indications that the damage is indirect are the inverse dose-rate effect [41], the protection provided by freezing or dehydration [42] and, *vice versa*, the enhancement due to the presence of oxygen [43]. An inverse dose-rate effect means that it is more damaging to administer the total dose in a longer time, rather than in a shorter. The explanation for this paradoxical phenomenon just lies in the generation of ROS: if ROS are produced in a low concentration, i.e. when the dose rate is low, they prevalently react with the surrounding protein or lipid molecules. In this way, they produce the radical chain reaction that leads to protein oxidation and lipid peroxidation [42]: e.g., up to 20 different amino acids can be damaged by a single ROS [44]. When the dose rate is higher, the concentration of ROS is greater and they tend to react with each other. In this way, the propagation of the radical chain reaction is limited and termination reactions are prevailing [41]. However, the relationship between total dose, dose-rate, time and biological effects is more complex: at the same total dose and dose rate, the administration in two parts, divided by 3.5 hours of interval, conferred a certain protection: 2.4 times less haemolysis, less metHb, less damage to membrane lipids, but the damage to proteins was not changed [45]. Freezing or dehydration very effectively protect biological molecules from the effects of irradiation so that, to obtain

the same injury, doses up to 100 times higher are needed [42]. In these conditions, ROS cannot freely diffuse and the radical chain reaction is blocked. Therefore, direct effects of radiation prevail [42]. On the contrary, the presence of oxygen enhances the effect of ROS 16 times in comparison to anaerobic conditions [46]. The radiolysis of water, i.e. the dissociation of its molecules, provokes the formation of several ROS: hydroxyl radicals ($\cdot\text{OH}$), hydrated electrons and hydrogen atoms [43]. In the presence of air, hydrated electrons and hydrogen atoms rapidly react with oxygen forming peroxide radicals. These last ones react more slowly and are easily inactivated in intact cells because of the presence of endogenous catalase [40]. Therefore, hydroxyl radicals are the main responsible for the indirect effects of irradiation. In anaerobic conditions, the dominating process induced on red cells by radiation is the aggregation of membrane proteins, caused by the formation of S-S bridges. In aerobic conditions, oxygen suppresses the cross-linking and catalyses an intense protein oxidation and lipid peroxidation [46]. In the presence of antioxidants, red cells are partially protected against lipid peroxidation and the decrease in the osmotic resistance [32]. However, the effects on potassium leakage are modest (-10% to -20%) [47] and data on red cell viability are lacking. Altogether, the primary effects of radiation do not offer an immediate explanation of the effects on deformability.

Red cell volume (MCV)

In the paragraph on rheologic parameters, we commented that some deformability tests are probably influenced by MCV. Presumably, our filterability test also is influenced by MCV or, at least, this is a plausible explanation for the sensitivity to pH (at acidic pH, red cells swell) and osmolarity changes

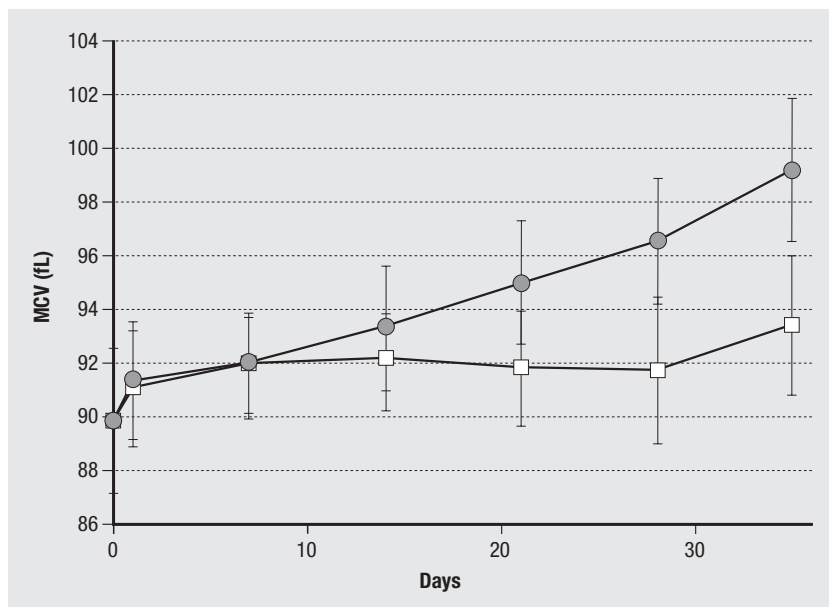


Fig. 3 | Mean cell volume (MCV) of red cells after irradiation with 25 Gy of gamma rays. Irradiation was performed on day 1. Data are means of 6-12 samples. Error bars represent 1 SD. (Closed circles: irradiated; open squares: non irradiated)

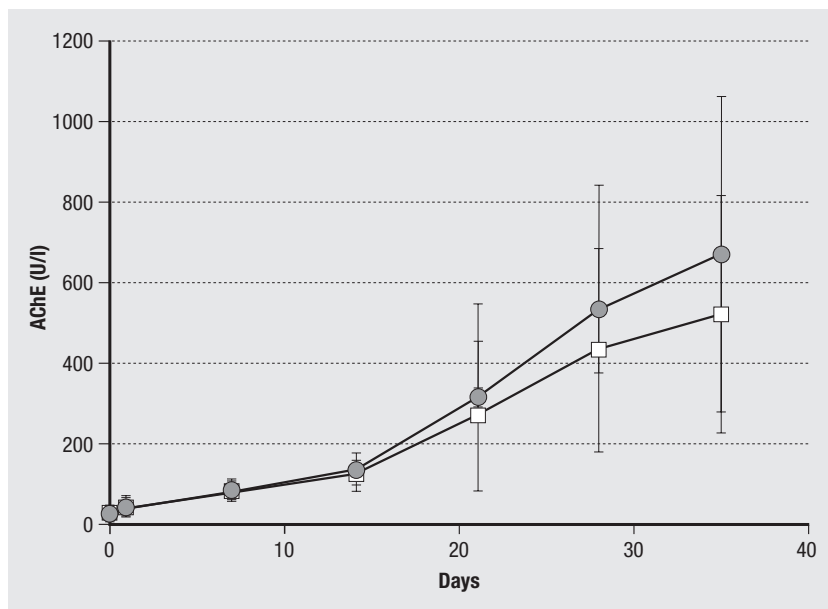


Fig. 4 | True acetylcholinesterase activity (vesiculation) in the supernatant after irradiation with 25 Gy of gamma rays. The true acetylcholinesterase activity is exclusively associated with cell membrane and therefore is an excellent marker of vesiculation. Irradiation was performed on day 1. Data are means of 6-12 samples. Error bars represent 1 SD. (Closed circles: irradiated; open squares: non irradiated)

(increasing the osmolarity of the medium, the erythrocytes decrease their volume) [38]. Data on MCV changes after irradiation are scanty and contradictory. Brugnara and Churchill [48] found that MCV increased and mean corpuscular haemoglobin concentration (MCHC) decreased during storage, as expected [20], but there were no differences between irradiated and control red cells. Suzuki *et al.* used red cells in CPD, as in the experiment cited above, but they did not observe any change, neither caused by storage, nor by irradiation [21]. The same group, using red cells in MAP, found significant differences between irradiated and control red cells since the first week of storage, but in these experiments MCV decreased and MCHC increased with time [35, 36]. Finally, we and others [23] observed significant differences between irradiated and control red cells, but in our case MCV increased during storage (Figure 3). Actually, the increase in the MCV during storage is a matter of fact [4], at least with the common storage solutions. However, according to some studies [49], the swelling is reversible and it masks a real decrease in the cell volume that appears when the erythrocytes are incubated at 37 °C for 24 hours in autologous plasma. These volume changes are blocked inhibiting the K-Cl cotransport, but not inhibiting the Na-K pump, nor the Na-K-Cl cotransport, nor the Ca-activated K channel [31]. These opposite changes in the cell volume according to the manipulation of the erythrocytes could explain the different results reported above. However, in the quoted articles [35, 36] there is no mention of any incubation at 37°C before the measurement of the red cell indices. In any case, in our experiments the differences between irradiated and control red cells appeared no sooner than after two weeks (Figure 3); therefore they were not so early as to explain the loss of deformability.

Vesiculation

During storage, erythrocytes lose their normal discocytic form and become echinocytes. These morphological changes are only partially reversible, because microvesicles are released from the extremity of the spicules [20]. These vesicles are rich of membrane but contain very little haemoglobin [50]. Since in this way the surface/volume ratio decreases, vesiculation could represent a plausible mechanism for the loss of deformability after irradiation. To our knowledge, there are no further data on this argument, apart from those collected by us (Figure 4). We measured the true acetylcholinesterase activity in plasma, which is exclusively associated with cell membranes and therefore is an excellent marker of vesiculation. The release of microvesicles is more pronounced in the irradiated samples, but the difference is small in comparison with the variability among the different subjects. Moreover, it appears too late (not less than 21 days) to be responsible for the loss of deformability.

Potassium leakage

The release of potassium into the supernatant is the only parameter we have studied to show differences between irradiated and control red cells as precocious as deformability (Figure 5). This phenomenon was described in the first studies on irradiation [6] and subsequently confirmed by all others. However, the leakage of potassium is not characteristic of irradiation, because it also appears during the storage of non-irradiated red cells. Brugnara and Churchill demonstrated that the Na-K pump is not damaged but only inactive, owing to the low temperature of storage [48]. Once incubated at 37 °C, the red cells recover intracellular potassium and at the same time the MCHC. The difference between irradiated and control red cells is already evident after a week and is probably due to an increase of the passive permeability of the

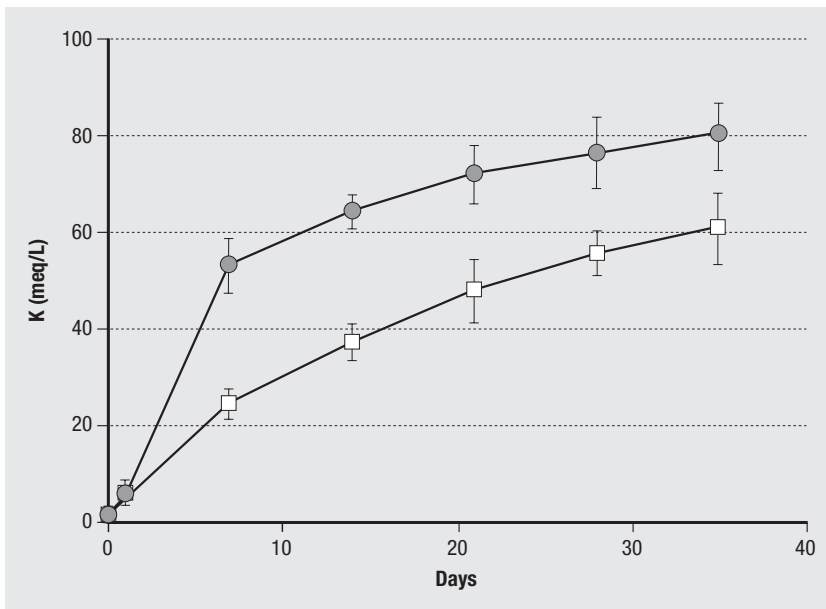


Fig. 5 | Extracellular potassium after irradiation with 25 Gy of gamma rays. Irradiation was performed on day 1. Data are means of 6-12 samples. Error bars represent 1 SD. (Closed circles: irradiated; open squares: non irradiated)

membrane [48]. It is interesting to note from *Figure 5* that the difference between irradiated and control cells reaches a maximum early (about 7 days) and, afterwards, it tends slowly to decrease. This behaviour was reported by others, too [36, 48], and clearly shows that potassium is not released because of haemolysis only (compare *Figure 1* and *Figure 5*). Despite some similarity, the curves of extracellular potassium (*Figure 5*) and deformability (*Figure 2*) are sufficiently different to suggest that there is no cause-effect relationship between the two. Moreover, there is no *prima facie* mechanism to link these two parameters.

CONCLUSIONS

The storage of red cells after irradiation decreases viability in a linear way, approximately 2% per week [16]. The mechanism by which irradiation influences viability is not clear, but deformability is the only known parameter related to viability that possesses all the characteristics of the culprit. Deformability is clearly impaired by irradiation but, again, we ignore by what mechanism. However, what we know about the effects of irradiation on viability suggests a number of practical measures:

- viability is not impaired immediately after irradiation, therefore the best practice is to irradiate just before transfusion;
- all known experimental data suggest that the ef-

fects of irradiation are not influenced by the prior storage of red cells. Accordingly, there is no point in limiting the permissible storage age before irradiation;

- red cells show the inverse dose-rate effect. Therefore, the total dose should be reached as fast as possible to limit the damage to red cells. In general, more attention should be paid to the intensity (the duration) of the irradiation, besides the total dose: e.g., the total dose is usually delivered in a few minutes using a ^{137}Ce source, but may require more than 60 minutes with a teletherapy unit. However, to increase the dose-rate further, it would be necessary to use a high-energy source or to replace it earlier than customary;
- at the same dose, alpha particles should be more damaging to white cells and less to red cells, than gamma or X rays. Unfortunately, alpha particles have such a low penetration that their use in our context is not practical.

In any case, we need a much greater understanding of the mechanisms activated by the primary effects of radiation on red cells. It is not improbable that those mechanisms are the same involved in the loss of viability after storage. If this is the case, irradiation could be viewed as inducing a sort of accelerated aging.

Submitted on invitation.

Accepted on 3 April 2007.

References

1. Moroff G, Luban NLC. The influence of gamma irradiation on red cell and platelet properties. *Transfus Sci* 1994;15:141-8.
2. Anderson K. Broadening the spectrum of patient groups at risk for transfusion-associated GVHD: implications for universal irradiation of cellular blood components. *Transfusion* 2003;43:1652-4.
3. Moroff G, Luban NLC. The irradiation of blood and blood components to prevent graft-versus-host disease: technical issues and guidelines. *Transfus Med Rev* 1997;11:15-26.
4. Mollison PL, Engelfriet CP, Contreras M. *Blood transfusion in clinical medicine*. Oxford: Blackwell Science; 1997.
5. Schiffer LM, Atkins HL, Chanana AD, Cronkite EP, Greenberg

- ML, Johnson HA, Robertson JS, Stryckmans PA. Extracorporeal irradiation of the blood in humans: effects upon erythrocyte survival. *Blood* 1966;27:831-43.
6. Button LN, DeWolf WC, Newburger PE, Jacobson MS, Keyv SV. The effects of irradiation on blood components. *Transfusion* 1981;21:419-26.
 7. Moroff G, Holme S, Heaton A, AuBuchon J. Effect of gamma irradiation on viability of AS-1 red cells. *Transfusion* 1992;32(S):70S.
 8. Moroff G, Holme S, AuBuchon JP, Heaton WA, Sweeney JD, Friedman LI. Viability and *in vitro* properties of AS-1 red cells after gamma irradiation. *Transfusion* 1999;39:128-34.
 9. Friedman KD, McDonough WC, Cimino DF. The effect of pre-storage gamma irradiation on post-transfusion red blood cell recovery. *Transfusion* 1991;31(S):50S.
 10. Davey RJ, McCoy NC, Yu M, Sullivan JA, Spiegel DM, Leitman SF. The effect of prestorage irradiation on post-transfusion red cell survival. *Transfusion* 1992;32:525-8.
 11. Mintz PD, Anderson G. Effect of gamma irradiation on the *in vivo* recovery of stored red blood cells. *Ann Clin Lab Sci* 1993;23:216-20.
 12. Suda BA, Leitman SF, Davey RJ. Characteristics of red cells irradiated and subsequently frozen for long-term storage. *Transfusion* 1993;33:389-92.
 13. Miraglia CC, Anderson G, Mintz PD. Effect of freezing on the *in vivo* recovery of irradiated red cells. *Transfusion* 1994;34:775-8.
 14. Valeri CR, Pivacek LE, Cassidy GP, Ragno G. *In vitro* and *in vivo* measurements of gamma-irradiated, frozen, glycerolized RBCs. *Transfusion* 2001;41:545-9.
 15. Davey RJ, Stec NM, Lee JL, Leitman SF. The effect of prestorage leukocyte reduction on the irradiation-induced red cell storage lesion. *Transfusion* 1995;35(S):55S.
 16. Heaton A. Blood component irradiation and prevention of Graft-Versus-Host Disease. *Transfus Sci* 1995; 16:121-3.
 17. Holme S. Current issues related to the quality of stored RBCs *Transfus Apheresis Sci* 2005;33:55-61.
 18. Council of Europe. *Guidelines to the preparation, use and quality assurance of blood components*. Strasbourg: Council of Europe Publishing; 2006.
 19. Italia. Decreto 3 Marzo 2005. Caratteristiche e modalità per la donazione del sangue e di emocomponenti. *Gazzetta Ufficiale – Serie Generale* n. 85, 13 Aprile 2005.
 20. Högman CF, Meryman HT. Storage parameters affecting red blood cell survival and function after transfusion. *Transfus Med Rev* 1999;13:275-96.
 21. Suzuki Y, Seiyama A, Tateishi N, Yamanishi S, Maeda N. Rheological evaluation of X-Ray irradiated blood. *Vox Sang* 1993;64:139-44.
 22. Jin YS, Anderson G, Mintz PD. Effects of gamma irradiation on red cells from donors with sickle cell trait. *Transfusion* 1997;37:804-8.
 23. Baumler H, Radtke H, Haas T, Latza R, Kiesewetter H. Influence of 30 Gy gamma irradiation on the quality of red blood cell concentrates in several storage media. *Infus Ther Transfusionsmed* 1999;26:212-21.
 24. Moore GL, Ledford ME. Effects of 4000 rad irradiation on the *in vitro* storage properties of packed red cells. *Transfusion* 1985;25:583-5.
 25. Leitner GC, Neuhauser M, Weigel G, Kurze S, Fischer MB, Höcker P. Altered intracellular purine nucleotides in gamma-irradiated red blood cell concentrates. *Vox Sang* 2001; 81:113-8.
 26. Hillyer CD, Tiegerman KO, Berkman EM. Evaluation of the red cell storage lesion after irradiation in filtered packed red cell units. *Transfusion* 1991;31:497-9.
 27. Jacobs GP. A review on the effects of ionizing radiation on blood and blood components. *Radiat Phys Chem* 1998;53:511-23.
 28. Schlenke P, Müller-Steinhardt M, Kirchner H. Effects of γ -irradiation on WBC-depleted RBC units. *Transfus Med Hemother* 2003;30(S):41-2.
 29. Dern RJ, Brewer GJ, Wiorkowski JJ. Studies on the preservation of human blood. II. The relationship of erythrocyte adenosine triphosphate levels and other *in vitro* measures to red cell storageability. *J Lab Clin Med* 1967;69:968-78.
 30. Beutler E, Kuhl W, West C. The osmotic fragility of erythrocytes after prolonged liquid storage and after reinfusion. *Blood* 1982;59:1141-7.
 31. Olivieri O, de Franceschi L, de Gironcoli M, Girelli D, Corrocher R. Potassium loss and cellular dehydration of stored erythrocytes following incubation in autologous plasma: role of the KCl cotransport system. *Vox Sang* 1993;65:95-102.
 32. Sharifi S, Dzik WH, Sadzadeh SMH. Human plasma and tirilazad mesylate protect stored human erythrocytes against the oxidative damage of gamma-irradiation. *Transfus Med* 2000;10:125-30.
 33. Haradin AR, Weed RI, Reed CF. Changes in physical properties of stored erythrocytes. *Transfusion* 1969;9:229-37.
 34. Card RT, Mohandas N, Mollison PL. Relationship of post-transfusion viability to deformability of stored red cells. *Br J Haematol* 1983;53:237-40.
 35. Suzuki Y, Tateishi N, Cicha M, Shiba M, Muraoka M, Tadokoro K, Maeda N. Decreased deformability of the X-ray-irradiated red blood cells stored in mannitol-adenine-phosphate medium. *Clin Hemorheol Microcirc* 2000;22:131-41.
 36. Cicha I, Suzuki Y, Tateishi N, Shiba M, Maraoka M, Tadokoro K, Maeda N. Gamma-ray-irradiated red blood cells stored in mannitol-adenine-phosphate medium: rheological evaluation and susceptibility to oxidative stress. *Vox Sang* 2000; 79:75-82.
 37. Barjas-Castro ML, Brandão MM, Fontes A, Costa FF, Cesar CL, Saad STO. Elastic properties of irradiated RBCs measured by optical tweezers. *Transfusion* 2002;42:1196-9.
 38. Reverberi R., Govoni M., Menini C. Measuring erythrocyte filterability: factors influencing sensitivity and reproducibility. *La Trasfusione del Sangue* 1991;36:582-6.
 39. Reverberi R., Govoni M., Menini C.: Filterability, vesiculation and ATP concentration during red blood cell storage *in vitro*. *La Trasfusione del Sangue* 1991;36:587-92.
 40. Puchala M, Szweda-Lewandowska Z, Kiefer J. The influence of radiation quality on radiation-induced hemolysis and hemoglobin oxidation of human erythrocytes. *J Radiat Res* 2004;45:275-9.
 41. Krokosz A, Koziczak R, Gonciarz M, Szweda-Lewandowska Z. Study of the effect of dose-rate on radiation-induced damage to human erythrocytes. *Radiat Phys Chem* 2006;75:98-105.
 42. Hitschke K, Bühler R, Apell HJ, Stark G. Inactivation of the Na, K-ATPase by radiation-induced free radicals. Evidence for a radical-chain mechanism. *FEBS Lett.* 1994;353:297-300.
 43. Gonciarz-Wach M, Szweda-Lewandowska Z. The influence of X-rays on human erythrocytes. Primary radicals. *Cell Mol Biol Lett* 2003;8:141-6.
 44. Neuzil J, Gebicki JM and Stocker R. Radical-induced chain oxidation of proteins and its inhibition by chainbreaking antioxidants. *Biochem J* 1993;293:601-6.

45. Koziczak R, Gonciarz M, Krokosz A, Szweda-Lewandowska Z. The influence of split doses of γ -radiation on human erythrocytes. *J Radiat Res* 2003;44:217-22.
46. Szweda-Lewandowska Z, Krokosz A, Gonciarz M, Zajczkowska W, Puchala M. Damage to human erythrocytes by radiation-generated HO• radicals: molecular changes in erythrocyte membranes. *Free Radic Res* 2003;37:1137-43.
47. Hirayama J, Abe H, Azuma H, Ikeda H. Leakage of potassium from red blood cells following gamma ray irradiation in the presence of dipyridamole, trolox, human plasma or mannitol. *Biol Pharm Bull* 2005;28:1318-20.
48. Brugnara C, Churchill WH. Effect of irradiation on red cell cation content and transport. *Transfusion* 1992;32:246-52.
49. Turner S, Williams AR, Rees JMH. The role of mean corpuscular haemoglobin concentration in limiting the storage life of human blood. *Vox Sang* 1987;52:177-81.
50. Lutz HU, Liu SC, Palek J. Release of spectrin-free vesicles from human erythrocytes during ATP depletion. *J Cell Biol* 1977;73:548-60.

A methodology to study the deformability of red blood cells flowing in microcapillaries *in vitro*

Giovanna Tomaiuolo^(a), Valentina Preziosi^(a), Marino Simeone^(a), Stefano Guido^(a), Rosanna Ciancia^(b), Vincenzo Martinelli^(b), Ciro Rinaldi^(b) and Bruno Rotoli^(b)

^(a)Dipartimento di Ingegneria Chimica; ^(b)Dipartimento di Biochimica e Biotecnologie Mediche, Sezione di Ematologia, Facoltà di Medicina e Chirurgia, Università degli Studi Federico II, Naples, Italy

Summary. The deformability of red blood cells flowing in microvessels is essential to maintain optimal blood circulation and to allow gas transfer between blood and tissues. Here, we report on an experimental methodology to investigate the deformability of RBCs flowing in microcapillaries having diameter close to the average cell size. The microcapillaries are placed in a rectangular flow cell, where a suspension of RBCs, properly diluted in albumin-added ACD, is fed through a syringe under the action of a liquid head in the physiological range. Video microscopy images of the flowing RBCs are acquired at high magnification and later processed by an automated image analysis macro. It was found that RBCs from healthy donors exhibit the classical parachute shape observed *in vivo*. Furthermore, all the data of healthy RBC velocity vs liquid head are well represented by the same linear regression, independently on the donor. Preliminary results on β -thalassemia RBCs are also presented and show, on the average, a reduced velocity compared to healthy samples.

Keywords: erythrocytes, capillaries, erythrocyte deformability, microfluidics, thalassemia.

Riassunto (*Una metodologia per lo studio in vitro della deformabilità di globuli rossi in flusso attraverso microcapillari*). La deformabilità dei globuli rossi circolanti nei vasi di piccolo calibro è una proprietà essenziale per mantenere un flusso ottimale e per consentire gli scambi gassosi fra sangue e tessuti. In questo contributo viene descritta una metodica sperimentale per lo studio della deformabilità di globuli rossi in flusso attraverso microcapillari artificiali di diametro paragonabile alla dimensione cellulare media. I microcapillari sono collocati in una cella di flusso rettangolare, in cui una sospensione di globuli rossi, opportunamente diluiti in ACD addizionato di albumina, viene inviata mediante una siringa sotto l'azione di un battente liquido nel range fisiologico. Le immagini di globuli rossi in flusso sono acquisite ad elevato ingrandimento mediante video microscopia ottica ed elaborate successivamente attraverso routine di analisi dell'immagine. I globuli rossi da donatori sani mostrano la classica forma a paracadute osservata *in vivo*. Tutti i dati di velocità eritrocitaria in funzione del battente liquido per donatori sani sono inoltre ben rappresentati dalla stessa regressione lineare, indipendentemente dal donatore. Risultati preliminari su globuli rossi da pazienti affetti da β -talassemia mostrano in media una riduzione di velocità rispetto ai campioni da donatori sani, in accordo con la ridotta deformabilità di membrana associata a questa patologia.

Parole chiave: eritrociti, capillari, deformabilità eritrocitaria, microfluidica, talassemia.

INTRODUCTION

The deformability of red blood cells (RBCs) flowing in microvessels is essential to maintain optimal blood circulation and to allow gas transfer between blood and tissues, and is implicated in several physiopathological processes. RBC deformability has been the subject of a number of investigations in the literature. One of the main research directions in this area has been the design of flow cells somehow mimicking the fluidodynamic conditions experienced by RBCs in the microcirculation *in vivo*. The experimental methods so far reported in the literature include

sedimentation velocity of centrifuged blood [1], filtration through membranes with different porosity [2, 3], the time spent by RBCs in passing through a single membrane pore [4], blood viscosity as a function of the deformation velocity [5, 1], the aspiration of a single RBC in a micropipette [6, 7], the diffraction of RBC suspensions undergoing shear flow in a Couette rheometer (ektacytometer) [8], the separation between two microspheres adherent to RBC surface using optical tweezers [9-11]. A measurement associated, though indirectly, to RBC deformability is that of blood viscosity, which depends both

on plasma composition and on the properties and concentration of the suspended cells [12]. It was indeed found that blood viscosity is higher if RBCs are made less deformable (for example, by crosslinking with glutaraldehyde [13]). From the haemorheological point of view, one of the most popular techniques is the measurement of apparent viscosity of whole blood or RBC suspensions at different concentrations in artificial capillaries, usually made of glass or silica [14]. These studies include the pioneering work of Fåhræus [15] on the variation of apparent blood viscosity with capillary diameter. Even though this rheological approach is still followed, direct measurements of deformability of RBCs flowing in microcapillaries with size smaller than cell body are scarce in the literature. In fact, observations of flowing RBCs by optical microscopy have been mainly described for capillary diameters larger than cell size [14]. Data of RBC deformability in case of pathological cells are even more limited.

The progress of the experimental techniques has been paralleled by the development of theoretical analyses to model the ability of RBC to deform and flow through channels smaller than the size of the cells at rest. The deformability, defined as the extension of the cell body under the steady state application of a fluidodynamic stress, is mainly function of three variables: internal viscosity, surface/volume ratio, and viscoelasticity of the membrane [16, 17]; The structure of RBC membrane has been modelled on a microscale as a network of elastic elements [18, 19]. The relation between deformability and morphology has been also studied, focusing on the change from the usual biconcave shape to the one observed for echinocytes and stomatocytes [20]. Notwithstanding the recent applications of numerical simulation techniques [21] the modelling of RBC fluidodynamic behavior and the comparison with experimental data are still at a preliminary stage, especially for pathological situations, and further investigations are at order.

In fact, in spite of the progress in experimental techniques, from the clinical standpoint RBC deformability is still measured by quite approximate methods, for example by measuring the time of perfusion through filters with pores of a given size. The main limits of this technique are the difficult standardization of the methodology, the intrinsic variability of pore size, the lack of information concerning single cell deformability, and the limited quantitative results that can be so obtained. Therefore, the setup of novel experimental systems *in vitro* appears as a relevant research goal towards a deeper understanding of the biological significance of RBC deformability, especially in a physiopathological perspective.

In this work, we describe an experimental methodology to investigate RBC deformability in microcapillaries having internal diameter close to cell size. Our approach is based on direct visualization of flowing RBCs by video-enhanced microscopy and automated image analysis procedures to meas-

ure cell velocity and deformation. The experimental variables investigated in this work include flow rate, size and length of microcapillaries. RBCs from healthy donors and from patients suffering from β -thalassemia have been investigated; preliminary results are presented and discussed.

MATERIALS AND METHODS

Blood samples

Fresh venous blood was drawn from both healthy and heterozygous β -thalassemic consenting volunteers into Vacutainer tubes. All blood samples were used within 4h of collection. RBC viability was checked before each experiment by observing cell morphology under static conditions at high magnification (100x objective). Approximately 1 mL of whole blood was diluted with 100 mL of anticoagulant ACD (0.6% citric acid, 1.1% dextrose anhydrous, 2.3% sodium citrate, 96% water), 5 mL of human albumin and 5 mL of PBS (phosphate-buffered saline). Such level of dilution ensured optimal performance of the flow cell. The viscosity of the suspending fluid was measured by a Ubbelohde glass viscometer immersed in a water bath at 37 °C, and was equal to 0.8 mPa·s. The presence of RBCs at the dilution used in the experiments did not change significantly the value of fluid viscosity.

Experimental apparatus

The microcapillaries used in this work were either made of silica (with 5 and 6.6 μm ID, Polymicro Technologies) or embedded in a gel matrix. In the latter case, a 2% w/w agarose solution at ca. 90 °C was cast in a rectangular mold enclosing a 5 micron diameter gold-plated tungsten wire. After gelation, the wire was gently removed from the agarose slab, thus leaving a 5 μm microcapillary. The diameter and the length of all the capillaries used in this work were carefully measured by video microscopy. The measurements were carried out by filling the capillaries with an isorefractive fluid to avoid optical distortions.

The flow cell (a schematic is shown in *Figure 1*) was made of two Plexiglass plates separated by a rubber spacer. A window was cut in the bottom plate to allow insertion of a coverslip slide for observations at high magnifications with oil immersion objectives. The RBC suspension was fed to the flow cell through an input hole by a flexible tubing connected to a syringe. The suspension coming out from the flow cell through an output hole was collected by a plastic tubing in a glass reservoir placed on a vertical translating stage. The distance between the liquid menisci in the feeding syringe and the exit reservoir was adjusted by the translating stage. Such liquid head was measured during the experiment by imaging both the syringe and the exit reservoir with a CCD video camera against a graph paper background. This allowed to monitor the pressure differential in the course of the experiment.

The flow cell was placed on the motorized x-y stage of an inverted microscope (Zeiss Axiovert 100) equipped

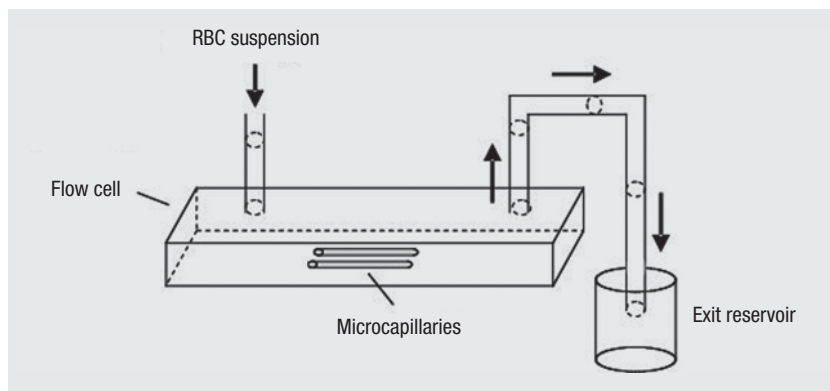


Fig. 1 | Schema of the flow cell.

with a motor assembly for focus control. Sample positioning was controlled by a custom LabView routine. In each experiment sample temperature was kept at 37 °C by enclosing the microscope and the flow cell assembly (including the feeding syringe and the exit reservoir) in a Plexiglass cage equipped with an air thermostating system based on a PID controller.

Images of the flowing RBCs were acquired by another CCD videocamera (Hitachi) and the whole experiment was recorded on video tape for reference (this recording was synchronized with that of the liquid head for later comparison). Real time image sequences (1000 images at a rate of 25 frames/s) were also digitized during the experiment by means of a frame grabber (National Instrument IMAQ PCI 1409) installed on a Pentium-based host PC and saved in computer memory for later analysis. The images were processed off-line by a macro calling standard image analysis routines from the library of a commercial package (Image Pro Plus 4.5). The fully automated macro operation allowed to isolate the subsets of images from each sequence where the passage of a cell could be identified and to determine the position of the flowing cell as a function of time. From these data RBC velocity was calculated as the slope of cell displacement vs time. Images of the flowing RBC were then saved in a database to evaluate the extent of cell deformation under the action of flow.

Images of RBCs at rest were also acquired to evaluate the cell size distribution. The measurements were carried out by pouring a drop of the dilute cell suspension between a microscope slide and a coverslip and acquiring images of several fields of view (the total number of counted cells was around 200). RBC size was measured by image analysis as the diameter of the cell body in the plane of observation (tilted cells were not considered in the measurements).

RESULTS

In a typical experiment, the pressure differential across the microcapillaries was regulated by adjusting the relative liquid levels in the syringe and the exit reservoir. The liquid head was initially set to 30 cm H₂O for about 5 minutes to fill the inlet and outlet tubings and the flow chamber. Then, the liquid head was brought

to 13 cm H₂O by lowering the position of the exit reservoir. The following decrease of the liquid head due to the emptying of the syringe and the filling of the exit reservoir was continuously recorded during the whole experiment by using the second CCD videocamera. From time to time, the syringe was refilled and the liquid head set back to 30 cm H₂O for about 10 minutes to prevent RBC sedimentation and the possible clogging of the outlet tubing around the exit hole.

As described in the previous section, real time image sequences were acquired throughout the experiment and processed off-line by the image analysis macro. The passage of an RBC through the microcapillary under observation was then associated to the current liquid head from the continuous recording of the distance between the two liquid levels in the syringe and the exit reservoir. A typical plot of cell displacement as a function of time in a silica microcapillary from a healthy donor sample is shown in *Figure 2a*, where the symbols refer to the data points and the solid line is the corresponding linear regression (the coefficients are also shown in the figure). Capillary length and diameter are 3.6 mm and 6.6 μm, respectively. It can be noticed that the data points follow quite closely a linear trend (the R² value of the regression is close to 1), thus showing that at the point of observation (which is located about halfway between the inlet and outlet microcapillary sections) RBC flow is under steady state conditions. The slope of the linear regression is the cell velocity, which is ca. 166 μm/s. An image of the flowing RBC is also shown in the inset of *Figure 2a*. The classical parachute shape, which is found *in vivo* [22], can be clearly observed in the image, and shows that the cells are indeed subjected to flow conditions similar to those experienced under physiological conditions. Similar shapes are also observed in the capillaries embedded in the agarose gels, as shown in *Figure 2b* (capillary ID is around 5 μm). It so appears that the parachute shape is due to the imposed fluidodynamics, and is essentially independent on the inner surface of the microcapillary.

The data analysis procedure illustrated in *Figure 2a* was systematically applied in a range of liquid heads from 1 to 10 mmHg. At each value of liquid head

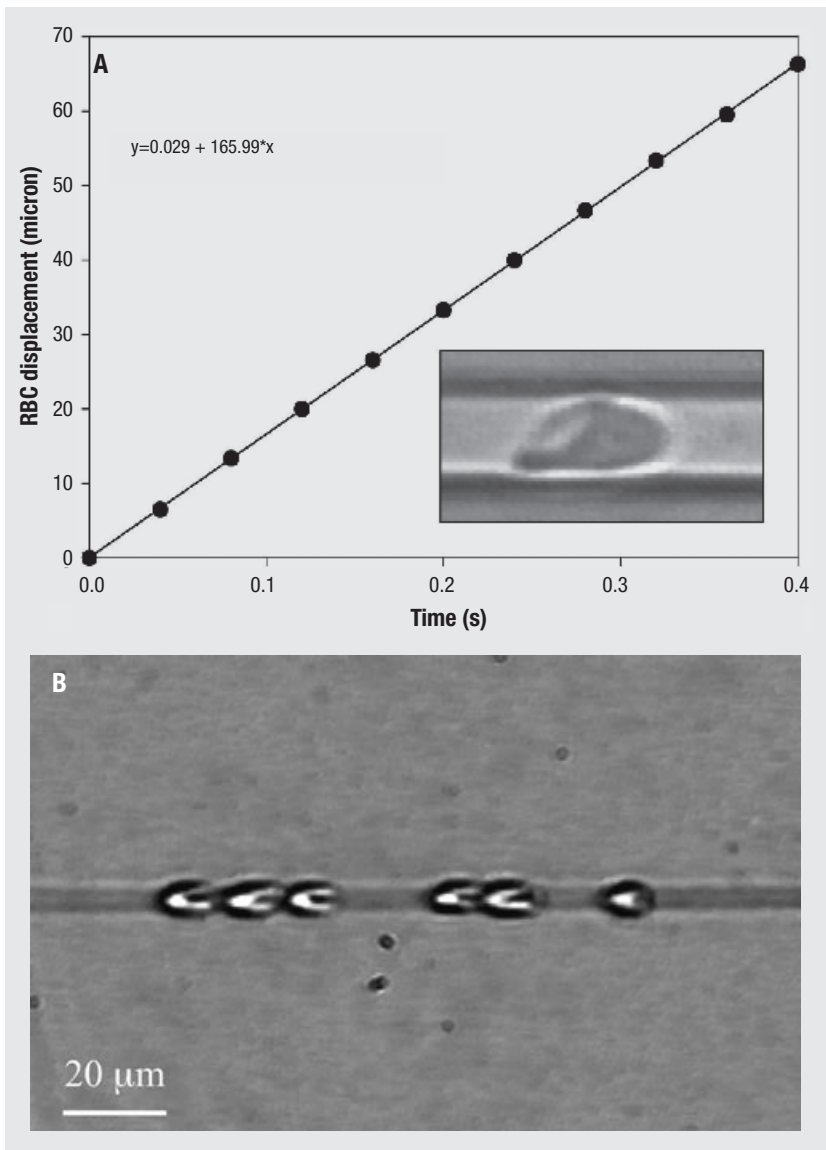


Fig. 2 | A) Cell displacement vs time in a microcapillary; B) images of RBCs flowing in a microcapillary embedded in agarose gel.

the velocity of 10-20 RBCs was measured. The results from three different healthy donors are plotted in *Figure 3a*. Each point in *Figure 3a* is the average value of RBC velocity from several measurements at the corresponding liquid head, and the error bars represent the standard deviation of the data. The three sets of points correspond to experimental runs from different donors with different capillary length from 3.6 to 4.9 mm, and the solid lines are linear fit to the data. All the data sets are well represented by the linear fit, and tend to zero at vanishing liquid head. This shows that the measured liquid head is dominated by the pressure drop between the ends of the microcapillaries, the other pressure losses (feeding and exit tubings, pressure drop due to converging flow to the capillary) being negligible.

In *Figure 3b* the same sets of data as in *Figure 3a* are scaled to the capillary length of 3.6 mm by assuming a direct proportionality between cell veloc-

ity and capillary length. It can be noticed that this scaling makes the three data sets superimpose each other, thus generating a “master curve” of healthy RBC velocity vs liquid head. In other words, the microcapillary flow behaviour of healthy RBCs does not depend on the donor, and it can be taken as a reference to be compared to pathological situations. The solid line shown in *Figure 3b* is the calculated value of the average fluid velocity $\langle v_z \rangle$ along the capillary axis z according to the classical equation

$$\langle v_z \rangle = \frac{\Delta P R^2}{8 \mu L} \quad (1)$$

where ΔP is the liquid head, R and L are capillary radius and length, respectively, and μ is the viscosity of the suspending liquid (which was measured by glass viscometry as described in the experimen-

tal section). The above equation is based on the assumption of well developed parabolic flow of a Newtonian fluid in a circular cross-section tube (Poiseuille flow), and does not contain any fitting parameters. The agreement between equation (1) and the experimental data of healthy RBC viscosity in *Figure 3b* is quite good. It shows that healthy RBCs move in a plug flow fashion inside microcapillaries of diameter comparable to cell size. The average RBC size at rest of the healthy samples was around $7 \mu\text{m}$ with a standard deviation of 0.5, as measured by optical microscopy and image analysis (see experimental section for details).

The measurements of RBC velocity vs liquid head from healthy donors were used as a control to evaluate the flow behavior of pathological blood samples. To exemplify the application of our methodology to pathological RBCs, we report preliminary data

from β -thalassemia blood samples. In *Figure 4*, the RBC velocity of four heterozygous β -thalassemia patients is plotted as a function of the liquid head. In the same figure, results from healthy RBCs are also shown for comparison. *Figure 4* shows that data from the β -thalassemia patients investigated in this work follow a linear trend passing through the origin. At variance with the healthy RBC results, however, β -thalassemia data do not superimpose on the same “master curve”, but rather exhibit different slopes, one being even coincident with the healthy case. The remaining three pathological data sets fall significantly below the velocity of healthy RBCs (the slopes are between 64% and 35% smaller), thus showing an increased hydrodynamic resistance in microcapillary flow. The lower panel in *Figure 4* shows representative images of flowing β -thalassemia RBCs from the four samples investi-

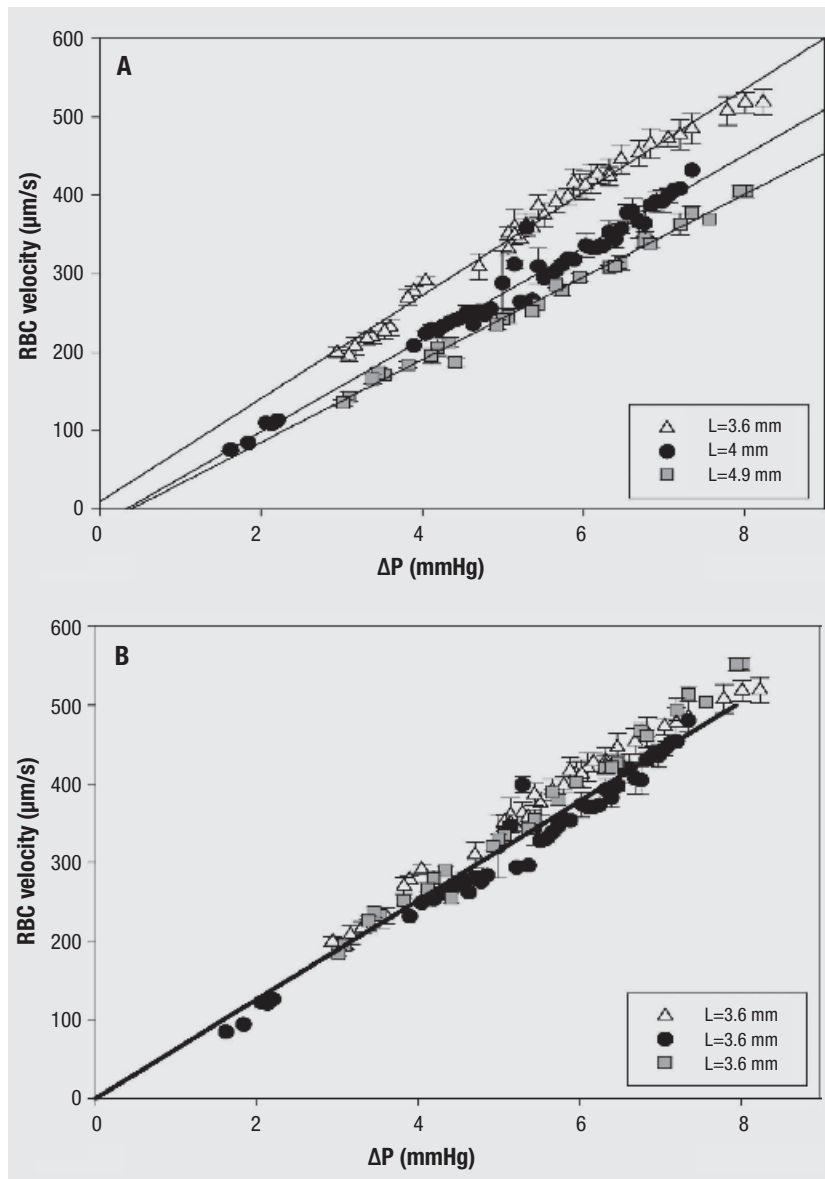


Fig. 3 | A) RBC velocity vs liquid head for three samples from healthy donors in microcapillaries of different lengths; B) same data as in A) rescaled to the same microcapillary length by assuming direct proportionality between RBC velocity and microcapillary length.

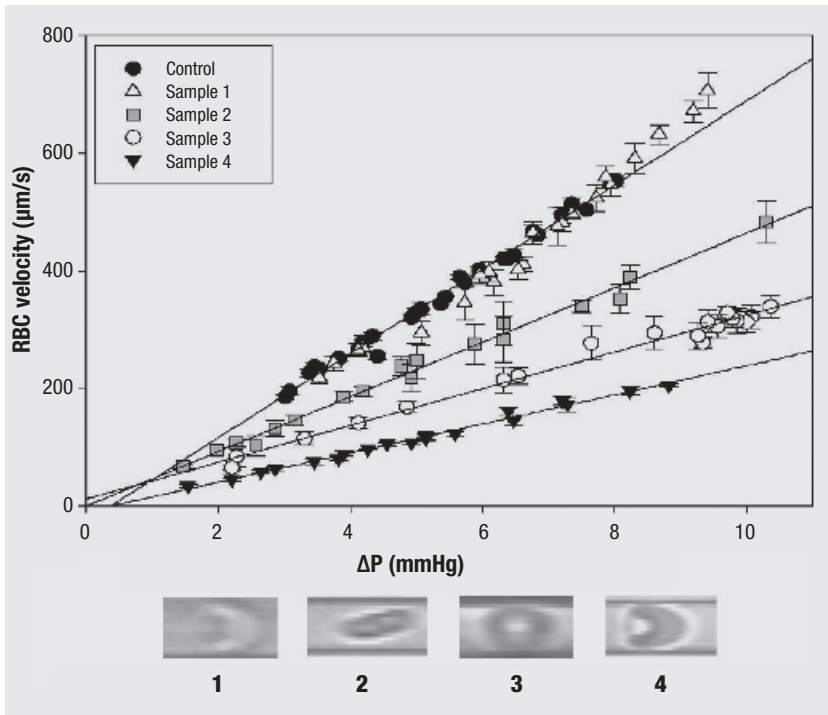


Fig. 4 | RBC velocity vs liquid head for four samples from β -thalassemia patients and one control from a healthy donor.

gated at a liquid head of ca. 6.5 mmHg. A parachute-like cell shape was observed in most images of the flowing RBCs, in analogy with the healthy samples. The RBC size distribution at rest was determined by video microscopy and image analysis for the β -thalassemia samples of Figure 4. The average size was slightly lower compared to the healthy case, going from 6.6 to 7.0. Some hematological data for the blood samples of Figure 4 are presented in Table 1. No simple correlation between RBC velocity and hematological parameters can be derived from Table 1. A systematic investigation to extend these preliminary results is currently in progress.

CONCLUSIONS

In this work, we describe an experimental methodology to investigate the flow behaviour of RBCs in microcapillaries of diameter comparable to cell size. Our approach is based on imaging deformed RBCs at high magnification by a video microscopy work-

station equipped with a motorized stage for precise positioning of the flow cell and a temperature control system. The acquired images are processed by image analysis techniques in an automated way to measure RBC velocity as a function of the imposed pressure differential. The performance of the apparatus was tested on blood samples from healthy donors, and it was found that RBC velocity is not dependent on the donor and is equal to the average fluid velocity in the microcapillary as calculated from the classical Poiseuille equation.

Preliminary results from heterozygous β -thalassemia patients are also reported, and show an average decrease of RBC velocity with respect to the healthy individuals. This is not unexpected, since it is well known that β -thalassemia is associated with an increased rigidity and a reduced mechanical stability of the cell membrane and cytoskeleton, leading to impaired RBC deformability [23]. Evidence of reduced deformability in β -thalassemia RBCs

Table 1 | Haematological data of the blood samples of Figure 4

Sample	Hb (g/dL)	HCT (%)	MCV (fL)	D* (\pm SD)
Control	13.2	42.1	85.6	6.9 (\pm 0.6)
1	15	47.7	75.5	6.3 (\pm 0.63)
2	8.8	30.1	65.6	6.5 (\pm 0.94)
3	13	40.8	60.1	7.0 (\pm 0.92)
4	13.9	43.8	72.2	6.4 (\pm 0.78)

D* is the RBC diameter in the plane of observation.
SD = standard deviation.

suspended in PBS viscosized with addition of dextran has been provided by laser diffractometry [24] in a flat glass cell. However, a direct visualization of RBC shape and velocity in a microcapillary of comparable size, such as in the present investigation, has not been reported so far to our knowledge. A further advantage of our approach is that it allows one to discriminate the flow deformability of RBCs from different patients and to give a quantitative evaluation of the difference with respect to the healthy case. A systematic work to elucidate the mi-

crocapillary flow behaviour of β -thalassemia RBCs and to correlate these results with clinically relevant parameters is currently in progress.

Acknowledgments

Financial support from the Italian Ministry of University under the Prin 2004 program is gratefully acknowledged.

Submitted on invitation.

Accepted on 3 April 2007.

References

1. Sirs JA. The measurement of the haematocrit and flexibility of erythrocytes with a centrifuge. *Biorheology* 1968;5:14.
2. Teitel P. Basic principles of the "filterability test" (FT) and analysis of the erythrocyte flow behavior. *Blood Cells* 1977;3:55-70.
3. Dormandy J, Flute P, Matrai A, Boger L, Mikita J. The new St. George's blood filterometer. *Clin Hemorheol* 1985;5:975-83.
4. Kiesewetter H, Mussler K, Teitel P, Dauer U, Schmid-Schonbein H, Sphor R. New methods for red cell deformability measurement. In: Lowe GDO, Barbenel JC, Forbes CD (Ed.). *Clinical aspects of blood viscosity and cell deformability*. Berlin: Springer-Verlag; 1981.
5. Dupin PA, Sirs JA. The relationship of plasma fibrinogen, erythrocyte flexibility and blood viscosity. *Thromb Haemost* 1977;38:660-7.
6. Evans EA. New membrane concept applied to the analysis of fluid shear – and micropipette-deformed red blood cells. *Biophys J* 1973;13:941-54.
7. Chien S. Principles and techniques for assessing erythrocyte deformability. *Blood Cells* 1977;3:71-99.
8. Bessis M, Mohandas N. A diffractometric method for the measurement of cellular deformability. *Blood Cells* 1975;1:307-13.
9. Ashkin AJ, Dziedzic M, Yamane T. Optical trapping and manipulation of single cells using infrared laser beams. *Nature* 1987;330:769-71.
10. Hénon S, Lenormand G, Richter A, Gallet F. A new determination of the shear modulus of the human erythrocyte membrane using optical tweezers. *Biophys J* 1999;76:1145-51.
11. Sleep J, Wilson D, Simmons R, Gratzer W. Elasticity of the red cell membrane and its relation to hemolytic disorders: an optical tweezers study. *Biophys J* 1999;77:3085-95.
12. Hoffman R, Benz EJ Jr, Shattil SJ, Furie B, Cohen HJ, Silberstein LE, Mc Glave P. *Hematology basic principles and practice*. Philadelphia: Churchill Livingstone; 2000.
13. Fung YC. *Biomechanics: Mechanical properties of living tissues*. New York: Springer Verlag; 1993.
14. Pries AR, Neuhaus D, Gaetgens P. Blood viscosity in tube flow: dependence on diameter and hematocrit. *Am J Physiol* 1992;263 (Heart Circ Physiol 32):H1770-8.
15. Fährræus R, Lindqvist T. The viscosity of the blood in narrow capillary tubes. *Am J Physiol* 1931;96:562-8.
16. Mohandas N, Chasis JA. Red blood cell deformability, membrane material properties and shape: regulation by transmembrane, skeletal and cytosolic proteins and lipids. *Semin Hematol* 1993;30:71-92.
17. Mohandas N, Evans E. Mechanical properties of the red cell membrane in relation to molecular structure and genetic defects. *Annu Rev Biophys Biomol Struct* 1994;23:787-818.
18. Boey SK, Boal DH, Discher DE. Simulations of the erythrocyte cytoskeleton at large deformation. I. Microscopic models. *Biophys J* 1998;75:1573-83.
19. Hansen JC, Skalak R, Chien S, Roger A. An elastic network based on the structure of the red blood cell membrane skeleton. *Biophys J* 1996;70:1466-6.
20. Kuzman D, Svetina S, Waugh RE, Zeks B. Elastic properties of the red blood cell membrane that determine echinocyte deformability. *Eur Biophys J* 2004;33:1-5.
21. Pozrikidis C. Numerical simulation of the flow-induced deformation of red blood cells. *Ann Biomed Eng* 2003;31:1194-205.
22. Tsukada K, Sekizuka E, Oshio C, Minamitani H. Direct measurement of erythrocyte deformability with a transparent microchannel capillary model and high-speed video camera system. *Microv Res* 2001;61:231-9.
23. Yuan, J, Bunyaratvej A, Fucharoen S, Fung C, Shinar E, Schrier SL. The instability of the membrane skeleton in thalassaemic red blood cells. *Blood* 1995;86:3945-50.
24. Bunyaratvej A, Butthep P, Sae-Ung N, Fucharoen S, Yuthavong Y. Reduced deformability of thalassaemic erythrocytes and erythrocytes with abnormal hemoglobins and relation with susceptibility to *Plasmodium falciparum* invasion. *Blood* 1992;79:2460-3